RADIOLYSE DES POLYMERES A BASE DE FLUORURE DE VINYLIDENE - ANALYSE DES RADICAUX.

INTRODUCTION

L'étude de la radiolyse des matériaux polymères est encore aujourd'hui associée à d'illustres noms tels que Chapiro, Charlesby et Pinner, qui se sont attachés à décrire, dès les années 60, l'évolution de la structure des chaines macromoléculaires lorsqu'elles sont soumises à un rayonnement ionisant. A partir de mesures macroscopiques, typiquement des fractions de gel, ils ont réussi à déterminer les rendements de scission et de réticulation de différentes matrices et ont ainsi posé les bases de la compréhension des mécanismes radicalaires mis en jeu pendant l'irradiation des polymères. Néanmoins, si l'on souhaite sonder et caractériser les évènements induits dans la matrice et notamment les coupures de liaisons, d'autres techniques d'analyses sont nécessaires. La Résonance Paramagnétique Electronique (RPE) devient alors une technique de choix puisqu'elle permet d'analyser les électrons non appariés des radicaux. L'aspect quantitatif de la méthode la rend très attractive ; on peut par exemple déterminer la quantité de radicaux disponibles pour amorcer une réaction de greffage suivant une chimie radicalaire. De plus, l'allure du signal RPE étant directement liée à la structure du radical (atomes présents en position α et β), il est également possible d'identifier la structure chimique des espèces radicalaires formées lors de l'irradiation ainsi que leurs proportions respectives. On comprend alors que l'utilisation de cette technique constitue une base solide et incontournable pour la compréhension des mécanismes mis en jeu lors du processus d'irradiation. Néanmoins, la démarche associée nécessite de connaitre les espèces radicalaires susceptibles d'être formées ainsi que leur signaux RPE respectifs.

Dans cette partie, une première section est consacrée à l'établissement d'un modèle de simulation de spectres RPE des radicaux formés lors de l'irradiation du PVDF sous atmosphère inerte. Celui-ci permet, entre autres, de déterminer la concentration de chaque espèce radicalaire. La véracité et la robustesse du modèle seront discutées à travers l'étude de l'influence d'un recuit sur la proportion des radicaux (Partie I). Fort de ce modèle, la section suivante sera consacrée à l'étude de l'évolution de la concentration de chaque espèce radicalaire en fonction de différents paramètres expérimentaux, liés à l'étape d'irradiation (tel que la dose d'irradiation) ou post-irradiation (tel que le temps de recuit). Les tendances observées seront mise en relation avec la réactivité de chaque espèce ainsi qu'avec la formation et la densification d'un réseau induites par la recombinaison des radicaux (Partie II). Enfin, le modèle de simulation sera étendu au cas du copolymère p(VDF-co-HFP) au cours de la dernière section. Nous montrerons son utilité ainsi que ses limites (Partie III).

I. Electron Spin Resonance Quantitative Monitoring of Five different Radicals in γ-Irradiated Polyvinylidene Fluoride.

The complex superimposition of electron spin resonance (ESR) signals of the five different radicals generated on PVDF upon γ-rays exposure are fully simulated for the first time, including g factors as well as a_α and a_β hyperfine splitting constants of proton or fluorine in α or β positions from the radical. The starting parameters were selected based on a thorough literature survey on their better-known fluorocarbons and perhydrogenated radical analogues and discussed in terms of correspondence with radicals in PVDF. Particularly, the electronegativity difference between F and H atoms is taken into account since it directly affects the electron delocalization in the radical. The finally obtained ESR parameters are consistent with the spectroscopic characteristics and the chemical stability of the radicals. Since radical absolute concentration for each radical is accessible, the simulation was also applied to monitor their stability upon annealing for different exposure times at 373K. The resulting trend is in full adequacy with the expected relation between electron delocalization, mobility and stability.

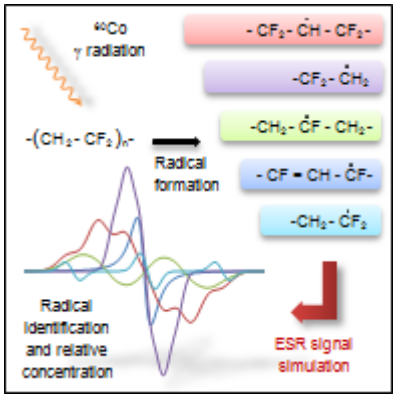

INTRODUCTION

Exposition to high γ-irradiation doses is most of the case lethal to living systems and creates also more or less reversible damages to inert matter during nuclear accidents, uncontrolled transportation of radionuclide or merely to containers designed for ionizing radiation protection.[1] Such most often damages appear as radicals that chemists or biochemists may also used in a positive way for quality control and even more interesting to modify materials. In all the cases, identification and quantization of these radicals are mandatory to further develop environment friendly applications. Indeed, irradiation is already a well-developed technique to modify surface or bulk properties, eventually a cost-effective way for sterilization of materials dedicated to food or bio-medical fields, and has been an interesting alternative for chemical modifications of polymeric materials through irradiation-induced grafting strategies.[2] Polymers radiolysis mechanisms are relatively well known[3] and lead to the formation of free radicals through the cleavage of covalent bonds and chemical rearrangement. As a consequence, irradiation causes crosslinking, chain scission, rearrangement, etc... Although most of these events are quite fast, in semi-crystalline polymers, transients such as radicals can survive for hours. Moreover, even for very simple chemical structure, irradiation of polymers leads to multiple radical species which the relative concentration depends on experimental parameters such as dose, thermal history or environment.[3] Electron spin resonance (ESR), also known as EPR (electron paramagnetic resonance) is a powerful characterization technique providing not only information on the chemical structure of the radicals but also spin concentration, *i.e.*, quantization.[4] However, s and p type radicals are restrained in a narrow range of spectral response that leads to the superimposition of all the signals and each of them are most often made of several peaks. The signals are so complex that it is difficult to fully interpret without simulating the overall ESR response. Nonetheless, reasonable solution cannot be found without a *priori* knowledge of each radical ESR parameters such as the symmetry of the g tensor and the hyperfine tensor.

Because of their intrinsic properties such as chemical inertness in a wide range of solvents, stabilities at high temperature, piezo-and pyroelectric properties and so forth, poly(vinylidene fluoride) PVDF is an interesting polymer which applications lay from medical suture wires, filtration membranes, separators for lithium-ion batteries etc…[5] However, to perfectly meet the requirements of a given application, mechanical or surface properties have to be adapted and enhanced. Irradiation-induced chemical changes have lately been a relevant strategy for that purpose as it can be applied after the polymer has been processed.

According to simple energetic considerations, each covalent bond of the VDF repeating unit can be broken when the material is exposed to ionizing radiations. C-F, C-H and C-C bond energies

are respectively 4.42, 4.28 and 3.44 eV,[6] which values are very weak compared to gamma photon energies lying in the keV order of magnitude. A random bond scission results [7] and leads to five different types of free radicals as suggested by Makuuchi [8] in the early 70s.

$-(CF=CH)_n-\dot{C}F-$ (I) ; $-CF_2-\dot{C}H-CF_2-$ (II) ; $-CH_2-\dot{C}F-CH_2-$ (III) ;

$-CF_2-\dot{C}H_2$ (IV) ; $-CH_2-\dot{C}F_2$ (V).

Figure 1. List of radicals generated in irradiated PVDF according to ref. 8

So far, there is no study yet which presents a full ESR signal simulation comprising these five species and monitoring their intensity depending on conditions of irradiation. Indeed, radicals (I) and (II) are the best documented species with generally accepted ESR parameters. On the contrary, there are obvious discrepancies regarding the ESR parameters of radicals (III), (IV) and (V). Because of the complexity of each signal and their superimposition in the same spectral range, it is important to start the simulation with reasonable g and A tensor and verify that a given set of parameters applies to a variety of irradiation and post treatment conditions. Educated guess on these parameters can conveniently rely on analogue species generated in other polymers. This is the approach applied here to simulate the ESR spectrum of γ-irradiated PVDF at a radiation dose of 150 kGy. The fit was obtained using starting parameters based on values taken from data collected on irradiated fluorinated species, polytetrafluoroethylene (PTFE) [9-12] and perfluoroalkanes [13-15] as well as on hydrogenated species, polyolefin [16-18] and ethylene/tetrafluoroethylene copolymers (ETFE).[19]

I.1. Experimental Methods

Samples of commercially available K741 PVDF (Arkema, France) with $\overline{M_n}$ = 110 000 g/mol as determined by GPC in DMF were used. Powder was compacted and introduced into 5mm Suprasil quartz ESR tubes mounted with a glass valve. Samples were vacuumed at room temperature, intermittently purged with argon and finally kept under argon atmosphere. The mounted tubes were placed into another vacuum bell under argon to prevent from any oxygen contamination. Irradiations were carried out using an industrial ^{60}Co gamma source at room temperature (300K) with dose rate of 0.7 kGy.h^{-1}. Irradiated samples were then kept at 255K until they were studied to prevent any radical decay. ESR spectra were recorded on a Bruker ELEXSYS E500 spectrometer operating in the X band microwave frequency range with a liquid nitrogen temperature controller. All spectra were acquired at 255K using a modulation amplitude of 0.1 mT, an optimum microwave power of 1.013 mW, a center field of 335 mT, and a sweep width of 40 mT.

Residual quartz signal was removed by a simple subtraction. Radical concentrations were calculated from the double integration of the first absorption derivative spectrum, using a calibration curve built up from a series of chloroform solutions of diphenylpicrylhydrazine (DPPH) with known concentrations. A freeware ESR simulator, i.e. WinSIM 2002 program [38] was used to correlate experimental and simulated spectrum taking into account hyperfine splitting constants, g values, signal lineshape and signal linewidth. The simulated ESR spectrum is optimized using the downhill simplex algorithm of WinSIM program.

Sol-gel analyses were performed in DMF. About 1 g of sample was used. Sample weight was determined accurately (w_i) and a large excess of solvent (60 mL) was added. The solution was heated at 353K for 48 h to allow the complete extraction of the soluble component. Swollen gels were weighted at 353K (w_g). The swollen samples had been carefully wiped with a tissue before any weighing. The solvent was then evaporated under vacuum for 24 h at 373K to determine the weight of dried gel (w_{dg}). The gel content (*% gel*) was calculated using the following equation:

$$\%_{gel} = \frac{w_{dg}}{w_i} \times 100$$

I.2. Results And Discussion

I.2.1. Initial statement.

It is well known that the hyperfine splitting constant (HSC), a, is proportional to the gyromagnetic ratio, γ_N, of the nucleus and the spin density, ρ_S, on this nucleus.[20] Considering that γ_H and γ_F for hydrogen and fluorine are very close one to another, 2.67 10^8 and 2.518 10^8 rad.T^{-1}.s^{-1} respectively, the ratio of the coupling constants is equal to the ratio of spin density within an approximation of 6%.

$$\frac{a_H}{a_F} = \frac{\rho_H}{\rho_F}$$

Though precise prediction of spin density may require theoretical calculation, an empirical approached based on the electronegativity of the elements is likely to be sufficient as it is for chemical shift evaluation in Nuclear Magnetic Resonance spectroscopy. Indeed, the latter relies on the de-shielding effect of the electrons around the nucleus. This is closely related to electron displacement under bond polarization therefore, driven by electronegativity differences. Such a type of calculation routinely used for NMR is based on a mere additive effect of each first and second neighbors around the observed nucleus as far as s or p atoms are concerned as it is for polymers. Here, we apply the same approach to estimate the trace of the tensor a (contact term) to the unknown

polymer containing both proton and fluorine using perfluorinated or hydrogenated analogues as references for a given local structure. In addition, the relationship provided above between the HSC values of H and F atoms is taken into account.

The second important simplification relies on use of only five radicals as suggested by Makuuchi (*vide supra*) assuming no polymerization defects (Figure 1).[8] Indeed, PVDF usually presents some head-to-head or tail-to-tail defects, which can be quantified by ^{19}F NMR and ^{1}H-NMR. In the PVDF sample used in this work, the total rate of defects is lower than 6%. Moreover, the number of radicals generated in the present irradiation conditions is 5.21 10^{18} spin.g^{-1}.i.e., 1 radical per 1800 repetition units. The probability for a radical to be on a chain defect with two subsequent CF_2 or CH_2 groups, is of the order of magnitude 1 over 10 000 at most and cannot be detected among the other signals.

I.2.2. Discussion on each radical expected ESR characteristics.

The first species to be considered in the model is the polyenyl radical (I). This radical has already been studied by many authors [21-25] in the case of irradiated polymer matrices as presented in Table 1.

Table 1. Electron spin resonance parameters of the polyenyl radical (I).

Polymers[a]	Multiplicity	Lineshape	Linewidth mT	g factor	Additional information	Ref
PVC	singlet	Gaussian	1.7	-	γ-irradiated in vacuum	22
PE	singlet	Gaussian	1.7	-	heated after electron-beam irradiation	22
PVDF	singlet	-	-	-	γ-irradiated in vacuum	21
p(VDF-co-TrFE)	doublet	Lorentzian	0.7[b]	2.0175	electron-beam irradiation stocked under air. Doublet splitting of 1.4 mT	24
PVDF	singlet	Lorentzian	-	1.9998	swift heavy ion irradiation under air. Thermally treated. ΔHpp = 1.40 to 1.20 mT	25
PVDF	singlet	Gaussian	2.0	> g_e[c]	-	26
PE	singlet	-	1.45	-	photo and thermal treatment	27

[a] PVC = Polyvinyl chloride, PE = Polyethylene, PVDF = Polyvinylidene fluoride and p(VDF-co-TrFE) = Poly(vinylidene fluoride-co-trifluoroethylene); [b] the apparent linewidth is obtained by adding the doublet splitting (1.4 mT) to the intrinsic linewidth (0.7 mT), *i.e.*, 2.1 mT; [c] g_e = 2.0036 (free electron ESR resonance)

The number of conjugated unsaturations defines the signal shape. For high order polyenyl radicals (n > 2) the delocalization of the unpaired electron is high, and consequently the number of hyperfine lines becomes large and the HSC small. As a result, the hyperfine structure is most often unresolved and the signal appears as a broad singlet. Not surprisingly, a good deal of discrepancy is found in the literature regarding the shape and the linewidth for this particular radical. In PE and PVC, a Gaussian linewidth of *ca.* 1.7 mT was first proposed for polyenyl radicals.[22] Latter, Helbert et al.[21] attributed such a type of singlet in irradiated PVDF to polyenyl radical without precising the lineshape. In perfluorinated polymers, Betz et al.[25, 26] proposed two different sets of values for a similar singlet also assigned to polyenyl radicals. One of the interpretations was recently confirmed by Goslar et al.[24] In both studies, they used the same type of lineshape (Lorentzian) though assuming a different spectral structure (a doublet instead of a singlet). Lately, Kasser et al.[27] attributed also such a kind of singlet with a linewidth of 1.45 mT to the polyenyl radicals in polyethylene (PE) photo and thermally treated. They explained a possible sharpening of the signal when radicals are exposed to air or via a photon process to form a polyenyl radical with a higher degree of unsaturation. It is worth noting that the number of conjugated unsaturations in the polyenyl sequence is expected to vary depending on the type of irradiation (γ, UV, etc.) up to the point that the hyperfine resolution is lost to yield a pseudo singlet more or less broadened as shown by Ohnishi et al.[22]

Despite some divergences, the sets of data coming from Ohnishi et al.[22] and Helbert et al.[21] appears more appropriate since they rely on a larger number of polymers (fluorinated or not). Though Helbert et al. did not explicitly provide any linewidth, we were able to retrieve the value from their spectra using a Lorentzian line, with the help of Engauge Digitizer 4.1 software. Hence, the parameters used to simulate the polyenyl radical (I) were a Lorentzian function with a corresponding linewidth of 1.7 mT and a value for *g* not well defined ranging from 1.9998 to 2.0175.

Considering the mid-chain methyne radical (II) recent and precise data were reported for PVDF and for a poly(vinylidene-co-trifluoroethylene) copolymer irradiated by fast electrons.[24, 28] Consistently with the radical structure, the ESR signal exhibits a double quintet with hyperfine splitting constants of ca. $a_{\alpha 1H}$ = 2.3 mT and $a_{\beta 4F}$ = 4.3 mT, respectively. The spectrum is centered at g = 2.004 and simulated with a Gaussian lineshape and a peak to peak linewidth ΔH_{pp} of 3.3 mT. Based on this work, ESR spectrum of radical (II) is simulated using a Gaussian function with a linewidth of 1.7 mT as for (I). Hyperfine coupling constants are kept the same and the *g* value is around 2.004.

In the case of radical (III), the signal should be a doublet of quintuplet. The only reports on this radical in γ-irradiated PVDF were assigned by Aymes-Chodur et al.[29, 30] to a single doublet with a HSC of 18 mT corresponding to fluorine in α position. The β-hydrogen coupling was not resolved

and implicitly taken into account in the linewidth of the signal. To guess what would be the HSC for such position in (III), the following perfluorinated (VI) or perhydrogenated (VII) analogues were used as references:

$$-CF_2-\dot{C}F-CF_2- \quad \text{(VI)} \; ; \qquad -CH_2-\dot{C}H-CH_2- \quad \text{(VII)}$$

The radical (VI) hyperfine splitting constants are 9.0 ± 0.5 and 3.3 ± 0.3 mT with one α-fluorine and four β-fluorine, respectively. The g values are ranging from 2.0021 to 2.0045.[9, 10, 12, 31, 32] Moreover, the ESR signal can be fitted using a Gaussian lineshape.[12] The radical (VII) exhibits a hyperfine splitting constant of $a_{\alpha 1H}$ ~ 1.4 to 2.2 mT and $a_{\beta 4H}$ ~ 3.3 mT.[27] Alternatively, the HSC is assigned to 5 equivalent hydrogen atoms in α and β position with a_{5H} ~ 3.0 mT.[22, 33] Considering radical (III), as fluorine is far more electronegative than hydrogen, the electron density will drastically be increased on carbon linked to fluorine and on the α position. Accordingly, replacing all four β-fluorine of radical (VI) by four hydrogen atoms would lead to an increase of the electron density on the α-fluorine leading to a higher HSC (a_F > 9 mT) to the expense of the localization on β-proton HSC (a_H < 3.3 mT). To be consistent with the idea that the line broadening is a function of mobility and could be considered as similar for all mid-chain radicals considered here, the linewidth of both mid-chain radicals (II) and (III) were approximated as equal and kept constant to the value chosen for radicals (I) *i.e*, 1.7 mT.

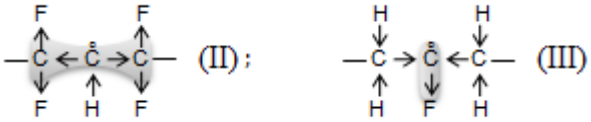

Figure 2. Schematized electron displacement by inductive effect exemplified on free radicals (II) and (III) containing both fluorine and hydrogen nuclei.

With regard to end-chain radicals (IV) and (V), the ESR signal should appear as a triplet of triplet. Again because of a lack of resolution for a_β, it is most often reported as a broad triplet.[34] Fortunately, in few instances such as for perhydrogenated or perfluorinated analogues (VIII and IX), both a_α and a_β are known and the same approach as above can be applied to feed the simulation program (Table 2).[9, 10, 12, 13, 19, 24, 28, 31, 34, 35]

$$-CH_2-\dot{C}H_2 \quad \text{(VIII)} \quad ; \quad -CF_2-\dot{C}F_2 \quad \text{(IX)}$$

Table 2. Hyperfine splitting parameters for perhydrogenated (among them VIII) and perfluoro (among them IX) end-chain radicals.

Radical	Polymer/ molecule[a]	α-HSC (nb[b],is[c]) mT	β-HSC (nb)	g factor	Mode of production and conditions	Ref
$-\dot{C}H_2$	n-heptane	3.1 (2,is)	-	-	air-free	13
$-\dot{C}H_2$	PVDF, p(VDF-co-TrFE)	1.6 (2,is)	-	2.009	e-beam irradiation & stocked under air	24, 28
$-CH_2-\dot{C}H_2$	CTE	3.2, 2.2, 1.2 (an)	2.5 (2,is)	2.003	decomposition of a fluoroperoxy radical	19
$-CF_2-\dot{O}$	PTFE	1.4 (2,is)	-	-	γ-irradiation in vacuum - reacted with O_2	10
$-\dot{C}F_2$	p(TFE-co-HFP)	1.6 (2,is)	-	-	γ-irradiation under vacuum - reacted or not with O_2	31, 36
$-\dot{C}F_2$	p(TFE-co-HFP)	1.7 – 1.8 (2,is)	-	2.0041	UV irradiation in vacuum combined with an O_2 plasma	35
$-\dot{C}F_2$	p(TFE-co-HFP)	1.7 (2,is)	-	2.0029	γ-irradiation under vacuum	34
$-CF_2-\dot{C}F_2$	PTFE	6.9 (1,an) 8.1 (1,an) 10.5 (2,is)	1.43 (2,is)	2.0053	plasma-irradiation under argon	12
$-CF_2-\dot{C}F_2$	PTFE	7.4 to 11.0 (2,is)	1.0 to 1.7 (2,is)	-	γ-irradiation under vacuum, exposed to air and UV irradiation after reevacuation	37

[a] p(VDF-co-TrFE) = Poly(vinylidene fluoride-co-trifluoroethylene); CTE = poly(tetrafluoroethylene-co-ethylene), p(TFE-co-HFP) = poly(tetrafluoroethylene-co-hexafluoropropylene); [b] *nb* is the number of equivalent nuclei; [c] "is" stands for isotropy, "an" for anisotropy

For radical (IX) in irradiated PTFE, the wings of the signal exhibit peak intensities that follow the Pascal's triangle rule facilitating its assignment as a triplet of triplet simulated by Kuzuya et al. for 2F in α and 2F in β positions, respectively.[12] More precisely, Toriyama et al.[37] solved the HSC angle dependence in an oriented film produced by mere mechanical stretching. Allayarov et al.[19] were also able to obtain a full fit of radical (VIII) in irradiated CTE (Table 2). Misleading triplets are often observed in aerobic conditions and due to oxidized radical such as the oxyfluorocarbon radical characterized by small HSC of 1.4 mT that should be discarded here.[10, 33] Replacing two β-hydrogen nuclei by two fluorine nuclei on radical (VIII) which would lead to radical (IV), would decrease $a_{\alpha H}$ below 2.2 mT and increase $a_{\beta F}$ above 2.5 mT according to the literature.[12, 19] Along the same reasoning obtaining (IV) from radical (IX) would lead to a larger domain and is not discussed here. Conversely starting from (IX) is more relevant to get the

parameter ranges for radical (V) as the domain is more restrained: $a_{\alpha F}$ (> 10.5 mT) and $a_{\beta H}$ (< 1.43 mT) (Table 2). Most of the cases, Gaussian lineshapes were used to simulate radicals. Only, Kuzuya et al.[12] used instead a pure Lorentzian lineshape for end-chain radicals but in their case the anisotropic component was taken into consideration contrary to the other researchers. Since anisotropy is ignored here, Gaussian lineshape was preferred. The linewidth of the end chain-radicals such as radicals (IV), (V), (VIII) and (IX) should be smaller than those of mid-chain radicals (I), (II) and (III) (< 1.7 mT) because of their higher mobility and the averaging effect on each conformational positions.[20]

I.2.3. SIGNAL SIMULATION

According to this survey, the starting parameters fed into the simulation of the overall spectrum are reported in Table 3. When a parameter was submitted to automatic adjustment the starting value is provided on its side in parenthesis. Note that the linewidths were kept constant for mid-chain radicals (I), (II) and (III) and only adjusted for end-chain radicals (IV) and (V). A very good fit quality obtained from the Spearman's rank correlation coefficient, ρ = 0.99914, was reached adjusting all the other parameters. The g factors were started with all the same value 2.004 and undergone very little change as expected for S= ½ s-p type of radicals.

Table 3. Parameters used to fit the ESR signal of irradiated PVDF. The values used as starting variables as discussed in the text are provided in parenthesis.

Radical	Lineshape[a]	Linewidth mT	α-HSC[b] mT	β-HSC[b] mT	g factor	Intensity %
(I)	L	1.7	-	-	2.0046 (2.003)	7.4 (20)
(II)	G	1.7	2.3 (2.3)	4.25 (4.3)	2.0048 (2.004)	51.8 (20)
(III)	G	1.7	10.9 (10.0)	2.5 (2.0)	2.0036 (2.004)	14.9 (20)
(IV)	G	1.0 (1.2)	1.45 (1.5)	2.3 (2.0)	2.0037 (2.004)	24.1 (20)
(V)	G	1.0 (1.2)	10.7 (10.5)	0.5 (1.0)	2.0018 (2.004)	1.8 (20)

[a] L stands for Lorentzian and G for Gaussian; [b] Values for equivalent nuclei in same position.

Figure 3 shows the result of the best fit assuming the approximations on linewidths and ignoring the effect on the γ-positions that are implicitly included in the apparent linewidth and expected negligible. The simulation residue has been estimated and is smaller than 5% (Figure S1). Taking into account coupling constants in γ-position or considering Lorentzian lines instead of Gaussian ones for radicals (II) (III) (IV) and (V), did not lead to any improvement on the simulation spectrum (in terms of correlation coefficient/ data not shown).

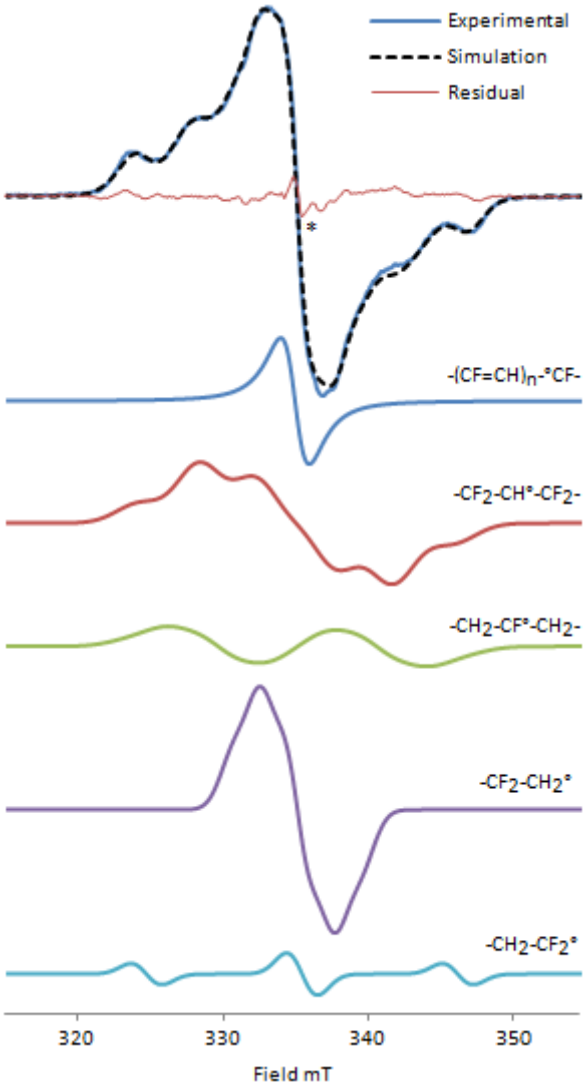

Figure 3. Experimental, simulated and residual spectra of γ-irradiated PVDF powder; each ESR contribution of (I), (II), (III), (IV) and (V) are provided with the intensity corresponding to the fit and from above to bottom, respectively. The position of the radical associated to the irradiated ESR quartz tube is indicated by a star (Figure S2).

Each of the five simulated signals is presented on Figure 3 The first remark is that a successful fit was achieved using the same linewidth for mid-chain radical (I) (II) and (III) as proposed above. The parameters obtained for (II) matches well those reported previously,[24, 28] setting a landmark for the present approach. The simulation of radical (III) with the same linewidth of 1.7

mT fixed for (I) and (II) allows us to estimate both a_α(F) = 10.9 mT and a_β(H) = 2.5 mT for the first time. The value for a_α(F), which is clearly smaller than the previous estimation (18 mT) that neglects a_β(H) [29, 30] appears more reasonable according to the discussion based on comparison with perfluorinated and perhydrogenated analogues. The simulation also confirms that the linewidth of end-chain radicals (IV) and (V) are reasonably approximated as being equal and found smaller (1 mT) than for mid-chain radicals which is consistent with the argumentation on dynamics and narrowing effect. Again, all the HSC and g values of the fit remain in the range discussed above in comparison with their F and H analogues. All these results strongly support the physical meaning of the actual simulation. Another point to discuss may be the g-factor of species (V) that appears smaller compared to the other ones. This may not be real and may result from an artifact of simulation with regard to the small contribution of this signal (1.9 %) and the low accuracy on this value (Indeed, the quality factor remains excellent by fixing g =2.004 for this species (ρ = 0.998). Finally, the residue may contain signals that were not fitted. Looking at the little features centered in the spectrum one may find six lines split by 6 to 7 mT that could account for dienyl radical, i.e., $-(CF=CH)_2-\dot{C}F-$. Though this is a reasonable possibility, including this species in the fit would be questionable with regard to the intensity of such a signal in comparison with the residue.

I.2.4. Model Consistency

The consistency of the model can also be verified with regards to the relative concentration of each radical that reflects their chemical stability. The rational is a higher stability for a higher delocalization of the electron along the carbon chain. A second source of stabilization is a lower statistic of recombination due to the radical localization. Indeed, it is well known that PVDF mainly suffers crosslinking compared to chain scission upon irradiation.[6] In our conditions, the gel content, obtained by sol-gel analysis with DMF, is 70 wt%. This value is the same range as others reported for comparable irradiation dose, as this parameter is known to drastically affect the gel content.[6] As a consequence, radicals embedded in polymer segments between two crosslinks such as mid-chain radicals are less mobile and provide lower statistics of recombination, therefore a higher stability, than end chain ones. Moreover, radicals centered on fluorinated carbon are less stable than their analogues centered on hydrogenated carbon. This is verified by a higher concentration of (II) versus (III) and also of (IV) versus (V) for mid-chain and end-chain radicals, respectively. Again comparing end-chain radicals versus mid-chain radicals, a higher concentration of (II) versus (IV) and of (III) versus (V) is obtained, consistently with the mobility effect. As a consequence the two dominating species are (II) and (IV) accounting for 75 % of the overall species. Interestingly, the polyenyl radicals which are known to be the most stable species because of the mesomeric effect represents

less than 10 % of the radical population after irradiation. This can be explained by the irradiation dose used here (150 kGy) in comparison with the dose needed to generate high concentration of polyenyl radicals (>500 kGy).[21]

The robustness of the simulation is tested on an irradiated PVDF sample on which annealing was applied for different times at a given temperature, and its effect on each radical concentration was monitored using ESR measurements operated in similar conditions as above. This produces samples with different relative radical concentrations due to their different chemical reactivity. Here the selected temperature was 373K, well below the melting temperature of the PVDF, and the ESR spectra were recorded up to 120 min. The simulation was performed with the same ESR parameters as reported in Table 3 while only intensities were allowed to vary. Fits with good quality were obtained, providing the evolution of each radical (Figure 4). As a first observation, the total radical concentration decreases down to an apparent threshold value of ca. 15 % of the initial concentration. Since such a threshold seems to be temperature dependent according to a value of 25% previously reported for a lower annealing temperature of 333K,[30] it is likely related to the internal dynamics of the chains within the polymer where recombination is somehow limited. Moreover, it is apparently not related to the level of crystallinity but likely due to the crosslinking level. Second, the dominant species remains the mid-chain radical (II) centered on H-bearing carbon even after reaching the threshold conditions (43% of the overall radical concentration against 29 % for radical (I)). Note that radical (IV) which concentration decays relatively fast still accounts for about 26 % of total concentration from 30 min and longer. If one assumes exponential concentration decay, the concentration profile can be fitted taking into account a threshold value for each species. The resulting thresholds are 2.3 ± 0.2 , 5.3 ± 0.5, 0.5 ± 0.2 , 3.7 ± 0.3 and 0.08 ± 0.08% for (I), (II), (III), (IV) and (V), respectively, for a total value of 12.6 ± 2.0 % close to the value already obtained at 30 min from Figure 4 (see calculation in SI and Figure S4). The half-life time for each species at 373K was computed and the values are gathered in Table 4.

Table 4. Calculated half-life time for each radical.

Radical	(I)	(II)	(III)	(IV)	(V)
Half-life time (min)	17 ± 3.4	5.4 ± 0.9	3.8 ± 1.9	4.5 ± 1.9	4.9 ± 2.8

As expected, it is confirmed that the polyenyl species (I) are very stable radicals as their half-life time is the largest one. Note that $t_{1/2}$ for (V) is not accurate enough to be considered as larger than the ones for (III) or even (IV). Apart radical (I) that is a secondary product formed by HF elimination from radicals (II) and (III), the stability order follows the relative concentration observed

before annealing. Another interesting point of this study relies on the definitively smaller stability and concentration of (V) compared to (IV) which at first sight can be surprising as these radicals are formed by a homolytic scission of the CH_2-CF_2 bond and thus should present an identical concentration. This indicates that radical (V) reacts, probably rapidly, not only with its cutting counterpart (IV) (which would lead to an increase in the mean molecular weight of the chain) but also with radical (III) and (II), which corresponds to a crosslinking reaction. The consecutive possibility to increase the gel content of PVDF upon annealing will be presented in a forthcoming report. The higher reactivity of the F-bearing mid-chain radical (III) when compared to its H-bearing counterpart (II), as demonstrated by a much lower concentration of the former at any moment of the process might explain the relatively high concentration of radicals (IV) remaining after the fast decay down to a threshold value of 3.7 ± 0.3 % (26% of total remaining radicals at 373K).

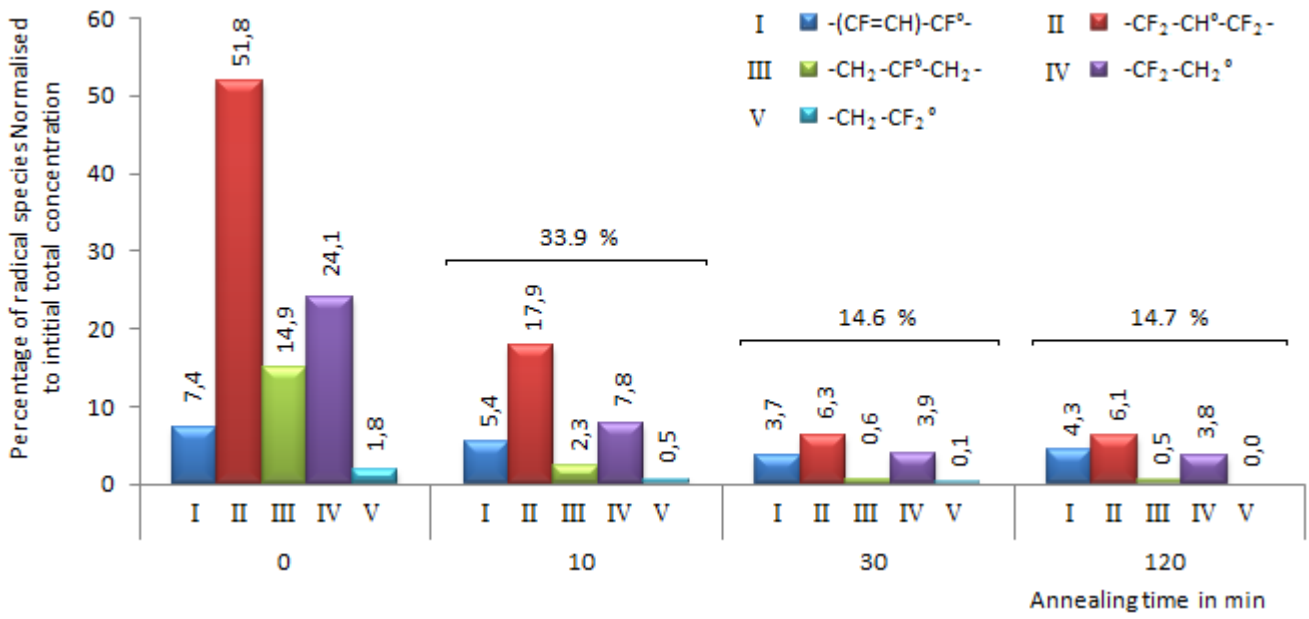

Figure 4. Evolution of each radical species in γ-irradiated PVDF upon annealing at T = 373K as a function of time. Proportions are normalized by the initial amount of radicals (at t = 0) and given as label for each species.

CONCLUSION

The ESR simulation proposed here was based on a thorough literature survey including the five most important radicals expected in irradiated PVDF. Despite the complexity of the signal, a minimal number of parameters have been validated leading to a robust model that is consistent not only with the physical spectroscopic parameters but also with the chemical stability of each species. A better description of the ESR parameters was proposed including the hyperfine splitting constants nuclei in β position of mid chain (III) and end-chain radicals (IV) and (V) which were not reported yet in the literature. In addition, the present model provides the possibility to monitor the evolution of each radical concentration upon a chemical process as illustrated here with a study of annealing at 373K that allows the determination of their individual half-life time, which are comprised between 17 and 4 minutes. The present methodology can be applied to many other studies such as irradiation dose effect, post synthesis polymer chemical modifications on many other polymers and copolymers or their mixtures.

REFERENCES

1. Alpen, E. A. *Radiation Biophysics*, 2nd ed.; Academic Press, 1997.
2. IAEA. *Advances in radiation chemistry of polymers, Proceedings of a technical meeting of IAEA, Notre-Dame Indiana, 13-17 Sept. 2003;* IAEA Ed.: Vienne, 2004.
3. Dawes, K.; Glover, L.; Vroom, D. The Effects of Electron Beam and γ-Irradiation on Polymeric Materials. In *Physical Properties of Polymers Handbook;* Mark, J. E., Ed.; Springer: New York, 2007; pp 867-887.
4. Schilck, S., Ed. *Advanced ESR methods in polymer research;* John Wiley & Sons: Hoboken, New Jersey, 2006.
5. Ameduri, B. From Vinylidene Fluoride (VDF) to the Applications of VDF-Containing Polymers and Copolymers: Recent Developments and Future Trends. *Chem. Rev.* **2009,** *109* (12), 6632-6686.
6. Lyons, B. J. Radiation Crosslinking of Fluoropolymers – A Review. *Radiat. Phys. Chem* **1995,** *45* (2), 159-174.
7. Rosenberg, Y.; Siegmann, A.; Narkis, M.; Shkolnik, S. Low Dose γ-Irradiation of some Fluoropolymers: Effect of Polymer Chemical Structure. *J. Appl. Polym. Sci.* **1992,** *45* (5), 783-795.
8. Makuuchi, K.; Masaharu, A.; Toshihiko, A. Effect of Evolved Hydrogen Fluoride on Radiation-Induced Crosslinking and Dehydrofluorination of Poly(vinylidene Fluoride). *J. Polym. Sci. Pol. Chem.* **1976,** *14* (3), 617-625.
9. Siegel, S.; Hedgpeth, H. Chemistry of Irradiation Induced Polytetrafluoroethylene Radicals: I. Re-examination of the EPR Spectra. *J. Chem. Phys.* **1967,** *46* (10), 3904-3912.
10. Matsugashita, T.; Shinohara, K. Electron Spin Resonance Studies of Radicals Formed in Irradiated Polytetrafluoroethylene. *J. Chem. Phys.* **1961,** *35* (5), 1652-1656.
11. Allayarov, S. R.; Mikhailov, A. I.; Barkalov, I. M. Analysis of the ESR Spectra of the ~CF_2CFCF_2~ Macroradical Trapped in a y-Irradiated Polytetrafluoroethylene Matrix at 77 K. *High Energ. Chem.* **2000,** *34* (3), 141-144.
12. Kuzuya, M.; Ito, H.; Kondo, S. I.; Noda, N.; Noguchi, A. Electron Spin Resonance Study of the Special Features of Plasma-Induced Radicals and Their Corresponding Peroxy Radicals in Polytetrafluoroethylene. *Macromolecules* **1991,** *24* (25), 6612-6617.

13. Allayarov, S. R.; Gordon, D. A.; Kim, I. P. Radiolysis of n-perfluoroalkanes and polytetrafluoroethylene. *J. Fluorine Chem.* **1999,** *96* (1), 61-64.
14. Allayarov, S. R.; Konovalikhin, S. V.; Olkhov, Y. A.; Jackson, V. E.; Kispert, L. D.; Dixon, D. A.; Ila, D.; Lappan, U. Degradation of y-irradiated linear perfluoroalkanes at high dosage. *J. Fluorine Chem.* **2007,** *128* (6), 575-586.
15. Shiotani, M.; Persson, P.; Lunell, S.; Lund, A.; Williams, F. Structures of Tetrafluorocyclopropene, Hexafluorocyclobutene, Octafluorocyclopentene and Related Perfluoroalkene Radical Anions Revealed by Electron Spin Resonance Spectroscopic and Computational Studies. *J. Phys. Chem. A* **2006,** *110* (19), 6307-6323.
16. Klimova, M.; Tino, J.; Borsig, E.; Ambrovic, P. The Effect of Crosslinking on the Reactivity of Free Radicals in Isotactic Polypropylene. *J.Polym. Sci. Pol. Phys.* **1985,** *23* (1), 105-111.
17. Kuzuya, M.; Yamashiro, T.; Kondo, S. I.; Sugito, M.; Mouri, M. Plasma-induced surface radicals of low-density polyethylene studied by electron spin resonance. *Macromolecules* **1998,** *31* (10), 3225-3229.
18. Zhou, W.; Zhu, S. ESR Study of Peroxide-Induced Cross-Linking of High Density Polyethylene. *Macromolecules* **1998,** *31* (13), 4335-4341.
19. Allayarov, S. R.; Konovalova, T. A.; Waterfield, A.; Focsan, A. L.; Jackson, V.; Cracium, R.; Kispert, L. D.; Thrasher, J. S.; Dixon, D. A. Low-temperature fluorination of fluoro-containing polymers EPR studies of polyvinylidenefluoride and the copolymer of tetrafluoroethylene with ethylene. *J. Fluorine Chem.* **2006,** *127,* 1294–1301.
20. Gerson, F.; Huber, W. *Electron Spin Resonance Spectroscopy of Organic Radicals;* WILEY-VCH Verlag GmbH & Co. KGaA: Weinheim, 2003.
21. Helbert, J. N.; Wagner, B. E.; Poindexter, E. H.; Kevan, L. Matrix ENDOR of polyenyl radicals in polymers. *J.Polym. Sci. Pol. Phys.* **1975,** *13* (14), 825–834.
22. Ohnishi, S. I.; Ikeda, Y.; Sugimoto, S. I.; Nitta, I. On the ESR Singlet Spectra Frequently Observed in Irradiated Polymers at a Large Dose. *J. Polym. Sci.* **1960,** *47* (149), 503-507.
23. Seguchi, T.; Tamura, N. Electron Spin Resonance Studies on Radiation Graft Copolymerization. I. Grafting Iniated by Alkyl Radicals Trapped in Irradiated Polyethylene. *J. Polym. Sci. Pol. Chem.* **1974,** *12* (18), 1671-1682.
24. Goslar, J.; Hilczer, B.; Smogor, H. Radiation-Induced Modification of P(VDF/TrFe) Copolymers Studied by ESR and Vibrational Spectroscopy. *Appl. Magn. Reson.* **2008,** *34* (1-2), 37-45.
25. Betz, N.; Petersohn, E.; Le Moël, A. Free Radicals In Swift Heavy ion Irradiated Fluoropolymers: An Elelectron Spin Resonance Study. *Radiat. Phys. Chem.* **1996,** *47* (3), 411-414.
26. Betz, N.; Petersohn, E.; Le Moël, A. Swift heavy ions effect in fluoropolymers: radicals and crosslinking. *Nucl. Instrum. Meth. B* **1996,** *116* (1-4), 207-211.
27. Kasser, M. J.; Silverman, J.; Al-Sheikhly, M. EPR Simulation of Polyenyl Radicals in Ultrahigh Molecular Weight Polyethylene. *Macromolecules* **2010,** *43* (21), 8862-8867.
28. Goslar, J.; Hilczer, B.; Smogor, H. ESR Studies of Fast Electron Irradiated Ferroelectric Poly(Vinylidene Fluoride). *Acta Phys. Pol. A* **2005,** *108* (1), 89-94.
29. Aymes-Chodur, C.; Betz, N.; Porte Durrieu, M. C.; Baquey, C.; Le Moël, A. A FTIR and SEM Study of PS radiation grafted fluoropolymers : influence of the nature of the ionizing radiation on the film structure. *Nucl. Instrum.Meth. B* **1999,** *151,* 377-385.
30. Aymes-Chodur, C.; Esnouf, S.; Le Moël, A. ESR Studies in y-irradiated and PS-Radiation-Grafted Poly(vinyldene fluoride). *J.Polym. Sci. Pol. Phys.* **2001,** *39,* 1437-1448.
31. Iwasaki, M.; Toriyama, K.; Sawaki, T.; Inoue, M. Electron Spin Resonance of y-Irradiated Tetrafluoroethylene-Hexafluoropropylene Copolymers. *J. Chem. Phys.* **1967,** *47* (2), 554-559.
32. Dargaville, T. R.; Hill, D. J. T.; Whittaker, A. K. An ESR study of irradiated poly(tertrafluoroethylene-co-perfluoropropyl vinyl ether) (PFA). *Radiat. Phys. Chem.* **2001,** *62* (1), 25-31.
33. Zhao, Y.; Wang, M.; Tang, Z.; Wu, G. ESR study of free radicals in UHMW-PE fiber irradiated by gamma rays. *Radiat. Phys. Chem.* **2010,** *79* (4), 429-433.
34. Hill, D. J. T.; Mohajerani, S.; Pomerya, P. J.; Whittaker, A. K. An ESR study of the radiation chemistry of poly(tetrafluoroethylene-co-hexafluoropropylene) at 77 and 300 K. *Radiat. Phys. Chem.* **2000,** *59* (3), 295-302.

35. Rasoul, F. A.; Hill, D. J. T.; George, G. A.; O'Donnell, J. H. A study of a simulated low earth environment on the degradation of fep polymer. *Polym. Advan. Technol.* **1998,** *9* (1), 24-30.
36. Iwasaki, M.; Toriyama, K. Photoinduced and Thermal Radical Conversions in y-Irradiated Copolymers of Tetrafluoroethylene and Hexafluoropropylene as Studied by Electron Spin Resonance. *J. Chem. Phys.* **1967,** *47* (2), 559-563.
37. Toriyama, K.; Iwasaki, M. Change with Temperature of the Electron Spin Resonance Spectra of ~CF_2-CF_2° Trapped in Irradiated Polytetrafluoroethylene. *J. Phys. Chem.* **1969,** *73* (9), 2919-2924.
38. Duling, D. R. Simulation of Multiple Isotropic Spin Trap EPR Spectra. *Journal of Magnetic Resonance, Series B* **1994,** *104* (2), 105-110.
39. Duling, D. R. Simulation of Multiple Isotropic Spin Trap EPR Spectra. *J. Magn. Reso. Ser. B* **1994,** *104* (2), 105-110.

SUPPORTING INFORMATION

ESR generality

According to Gerson et al.,[1] the isotropic hyperfine splitting constant *a* is given by:

$$a = \frac{2}{3}\mu_0\mu_N g_N \rho_N$$

With μ_o the permeability of vacuum, μ_N the nuclear magneton, g_N the g factor of nucleus and ρ_N the spin density. Nuclear magneton can be defined as follow:

$$\mu_N = \frac{h\gamma_N}{2\pi g_N}$$

Where *h* is the Planck constant and γ_N the gyromagnetic ratio of nucleus.

Hyperfine splitting constants can be expressed as a function of gyromagnetic ratio and spin density.

$$a = cte.\gamma_N \rho_N$$

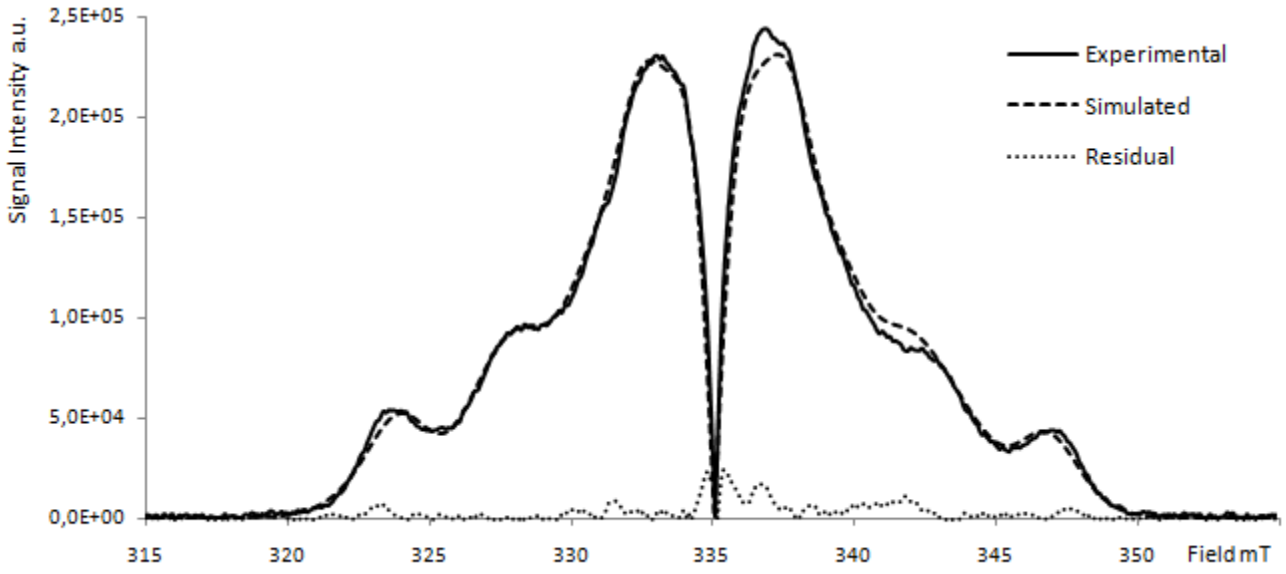

Figure S1. Absolute value of the experimental, simulated and residual spectra used to estimate the residual weight compare to the overall signal. This calculation provides a value of 5 % that is overestimated according to this method of evaluation. (The double integration of the residual was not a satisfying approach since a baseline correction was too delicate to apply).

The signal of irradiated tube in quartz is represented on Figure S2. Correction on the experimental spectrum is obtained by a simple algebraic subtraction of irradiated quartz signal from experimental datum.

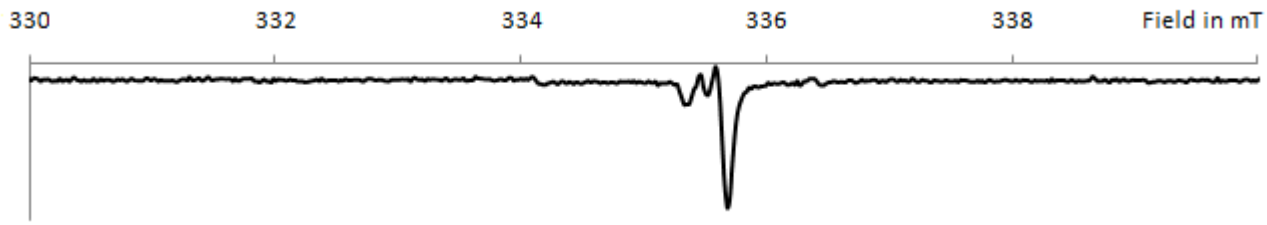

Figure S2. ESR signal of irradiated tube in quartz without the polymer.

Signal integration is performed on experimental data after correction of quartz signal. A baseline correction using an arctangent curve is applied to have a correct integral as shown in Figure S3.

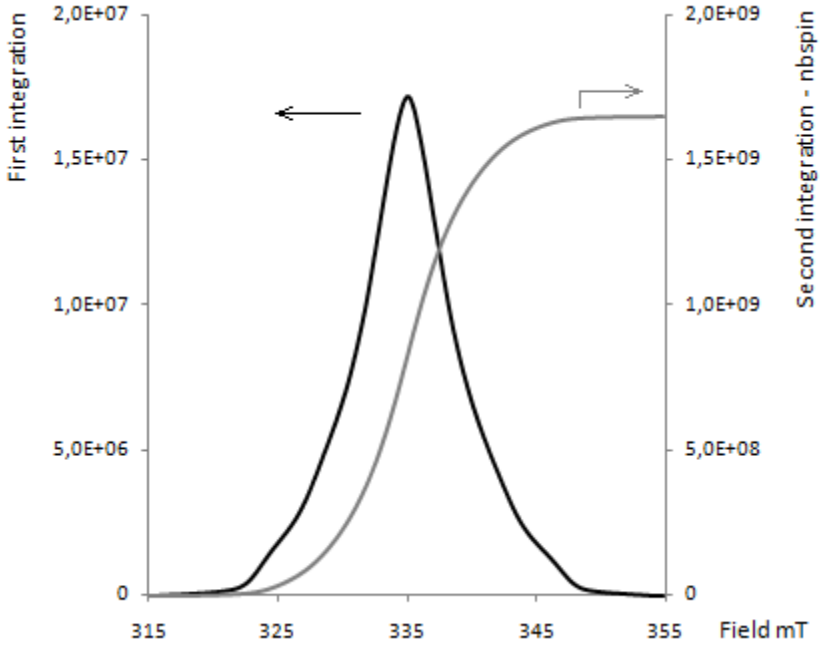

Figure S3. First and second integration of the experimental ESR signal.

Concentration decay estimation:

Knowing that there is a part of the radicals that is stable for rather long time (several hours) even under annealing at 373K, the rate of decay was estimated only for species undergoing fast decay below 30 minutes. Therefore, the data were reported as the difference of concentration at time t, [R(i)], minus the concentration at time longer than 30 minutes $[R(i)]_f$. The concentration of long lasting species $[R(i)]_f$ was obtained by trial and error method, trying to get a linear curve of the plot of $\ln([R(i)]-[R(i)]_f)$ versus time for each species R(i) (Figure S4).

The mathematical fit for the linearization on the three first points was good enough and taking into account the concentration after 120 minutes led to inconsistencies:

$$Ln\left([R(i)] - [R(i)]_f\right) = \frac{-t}{\tau} + Ln\left([R(i)]_i - [R(i)]_f\right)$$

$t_{1/2} = \tau.\ln(2)$

with the initial radical concentration at time 0, $[R(i)]_i$, the mean-life time decay τ and the half-life time $t_{1/2}$

Table S1. Results of the fit obtained with the 3 first experimental points:

Radical	$1/\tau$ min^{-1}	$[R(i)]_i$-$[R(i)]_f$	R(quality)	$[R(i)]_f$ %	$t_{1/2}$ min
(I)	0.0409	1.6182	0.9997	2.2	17
(II)	0.1278	3.8283	0.9997	5.3	5.4
(III)	0.1807	2.5569	0.9999	0.5	3.8
(IV)	0.1537	2.9886	0.9999	3.7	4.5
(V)	0.1411	0.5479	0.9999	0.08	4.9

Accuracy was obtained using both extreme values of the accuracy range on the radical concentration determined from the simulation.

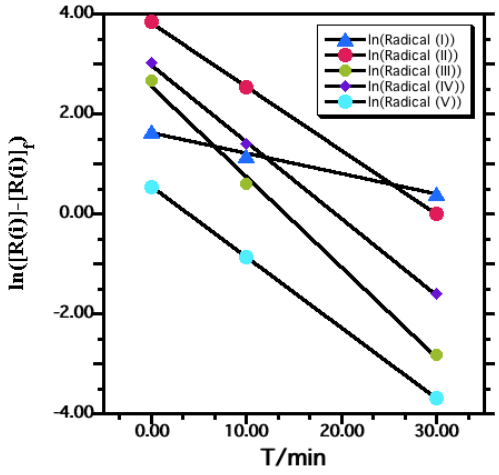

Figure S4. Variation of $\ln([R(i)]-[R(i)]_f)$ as a function of time. (see SI text for assumption and calculation)

References

1. Gerson, F.; Huber, W. *Electron Spin Resonance Spectroscopy of Organic Radicals;* WILEY-VCH Verlag GmbH & Co. KGaA: Weinheim, 2003

II. Effect of dose and subsequent annealing on radicals distribution in γ-irradiated PVDF as quantitatively monitored by ESR: correlation between network features and radical type.

A simulation model which takes into account the molecular structure, the localization and the chemical environment of radicals is used to quantitatively monitor the five radical species generated on PVDF upon γ-irradiation at different dose ranging from 100 to 500 kGy. While from 150 kGy to upper dose the overall concentration of radicals is similar, the distribution differs due to their chemical structure and localization (mid-chain versus end-chain). The changes obtained with an annealing at 373K on the total amount of radicals and in the relative proportions of each species are presented. The observed differences are not only related to intrinsic reactivity of radicals but also to the characteristics of the network (gel fraction, crosslinking density) obtained along radiation, as the mobility of polymeric segments is all the more reduced with increasing dose.

Introduction

For several years, extensive work has been devoted to the radiolysis of fluoropolymers.[1,2] Initially focused on perfluorinated polymers such as poly(tetrafluoroethylene) (PTFE), studies have rapidly been expanded to the entire family of fluoropolymers due to the large scope of applications they can cover. The radiolysis mechanisms are therefore well known: they involve the formation of radical species during the irradiation as a result of bond scissions. Once formed, these transients can follow different chemical paths such as crosslinking, internal rearrangements etc… The ratio between crosslinking and scission efficiencies reflects the ability of the polymer to form a network or otherwise to deteriorate mainly as a result of a decrease in molecular weight. PVDF is one of fluoropolymers that principally leads to a network when submitted to γ-radiation.[1] This ability to crosslink upon irradiation without the use of any reactants or solvent represents an interesting alternative for the modification of pristine materials when considering some specific applications, for which for example, excellent physicochemical affinity with a given liquid medium as well as a preservation of the dimensional integrity is required.

However, both the gel fraction and the cross-linking density resulting from irradiating PVDF depend on experimental conditions such as irradiation dose and dose rate, thermal history and environment. A conjunction of many reasons can be put forward to explain these results, such as concentration of radicals able to favor cross-linking, diffusion or mobility effects etc… At the same time, the global concentration of radicals generated onto PVDF also depends on these parameters. It is actually difficult to precisely study all the reactions involved, as the free radical mechanisms that occur during radiolysis of polymers are complex. Indeed, the generated radicals are numerous, even for simple polymer such as polyethylene, which makes the direct and detailed study of the future of all radicals challenging.

Although most of the reactions consuming radicals are quite fast, transients can survive for hours in semi-crystalline polymers such as PVDF which makes it possible to probe free radicals by electron spin resonance (ESR): in addition to a quantitative determination of the generated radicals, it allows determining the contribution of each species if their respective ESR parameters are known. Experimental ESR spectra of several paramagnetic species are superimposed and the most common way to interpret these complex spectra is to simulate them. However, this approach needs a *priori* knowledge of simulation parameters for all the involved species, which are generally not or only partly known. In the case of PVDF, several authors tried to attribute ESR spectrum to one given radical by varying the experimental conditions (radiation sources or others). According to simple energetic considerations[1,3], each bond of the VDF repeating unit can be broken when the polymer is exposed to γ-radiation. Bond scission can lead to five different free radicals as suggested by Makuuchi [4] but no study on the irradiation of PVDF has simultaneously presented the ESR signals of these five species.

$-(CF=CH)_n-\dot{C}F-$ (I) ; $-CF_2-\dot{C}H-CF_2-$ (II) ; $-CH_2-\dot{C}F-CH_2-$ (III) ; $-CF_2-\dot{C}H_2$ (IV) ; $-CH_2-\dot{C}F_2$ (V).

In a previous work[5], we have reported an ESR simulation model of free radicals in γ-irradiated high molecular weight PVDF. Simulation parameters of radicals (I)[6-10] and (II)[9,11] were directly retrieved from reported data, while for radicals (III) to (V), they were derived from a thorough literature studies of the parameters used to simulate ESR signal of fluorocarbon and perhydrogenocarbon radicals. This model takes into account the molecular structure, the localization and the chemical environment of each radical, that is to say the atoms present on the α and β positions of the radical. These parameters principally came from studies conducted on irradiated PTFE [12-15] or on perfluoroalkanes[16-19], or on ethylene/tetrafluoroethylene copolymers (ETFE).[20] This model was applied to the quantitative monitoring of radicals remaining on a PVDF sample exposed

to 150 kGy and subsequently annealed at high temperature for different time. The spectroscopic parameters based on the electron displacement under bond polarization driven by electronegativity differences strongly support the physical meaning of the simulation. Once these parameters settled, the quantitative monitoring of each generated species is rendered possible, and the values obtained actually reflects their chemical stability based on the delocalization of the single electron (inductive and mesomeric effects) and the mobility of the radical (mid-chain versus end-chain radical). This allowed us ordering the different radicals according to their reactivity through the determination of their half-life time. Using our model, it is now possible to quantitatively monitor the different radical species as a function of any experimental parameter, such as the irradiation dose. Moreover we looked at the distribution of radicals priory generated with exposure to different doses and subsequently annealed at high temperature. The distribution of radicals turns out to be different even when the concentration of radicals was initially identical. This is related to the network characteristics, investigated by sol-gel analyses.

II.1.EXPERIMENTAL SECTION

II.1.1. MATERIALS

Commercially available PVDF sample (reference K741) with molecular weight of 110 $kg.mol^{-1}$ was provided by Arkema, France. 2,2-Diphenyl-1-picrylhydrazyl (DPPH) from Aldrich was dissolved in chloroform to build a calibration curve for ESR.

II.1.2. METHODS

Powdered PVDF was introduced into 5mm Suprasil quartz ESR tubes mounted with a glass valve. Samples were vacuumed at ambient temperature, intermittently purged with argon and finally kept under argon atmosphere. The mounted tubes were placed into another vacuum bell under argon to prevent from any oxygen contamination. Irradiations were carried out using an industrial ^{60}Co gamma source at room temperature (300 K) with dose rate of 0.7 $kGy.h^{-1}$. Irradiated samples were then kept at 255 K until they were rapidly studied to prevent a radical decay. Films of PVDF used for UV-vis analysis were made by extrusion process.

ESR spectra were recorded on a Bruker ELEXSYS E500 spectrometer operating in the X band microwave frequency range with a liquid nitrogen temperature controller. All spectra were acquired at 255 K using a modulation of amplitude of 0.1 mT, a frequency modulation of 100 kHz, an optimum microwave power of 1.013 mW, a received gain of 60 dB, a center field of 335 mT, a

sweep width of 40 mT, a conversion time of 655.36 ms, a corresponding time constant of 81.92 ms to avoid distortion of signal, and a resolution of 2048 points. In these conditions, only one scan was sufficient to have a good signal to noise ratio. Residual quartz signal was removed by a simple subtraction. For this, a reference tube free of PVDF was irradiated in the same conditions of atmosphere and dose, and the ESR signal was recorded. In order to investigate the effect of annealing on the overall radical concentration and the evolution of the ESR spectra, samples were heated during different times at 373 K. Radical concentrations were calculated from the double integration of the first absorption derivative spectrum.

UV-visible measurements were made using a PerkinElmer Lambda 35 UV/VIS spectrometer between 190 to 900 nm. A window frame was made in aluminum to hold the polymer film. Each sample was first analyzed before irradiation to make its own background. UV-Vis samples were introduced with their aluminum frame into Schlenk flask and stocked under argon for the irradiation process.

Sol-gel analyses were performed with DMF. Around 1 g was taken from dumbbell specimen and introduced in a closeable flask. Sample weight was determined accurately (wi) and a large excess of solvent (60 mL) was introduced. Samples were heated at 353K during 48 h to allow the complete extraction of the soluble component. Swollen gels were carefully wiped with a tissue then weighted (w_g). The solvent was then evaporated under vacuum for 24 h at 373K to determine the weight of dried gel (w_{dg}). The gel content (% gel) and the solvent uptake (% sol) were calculated using the following equations:

$$\%\, gel = \frac{w_{dg}}{w_i} \times 100 \qquad \text{and} \qquad \%\, sol = \frac{w_g - w_{dg}}{w_{dg}} \times 100$$

II. 2. Results and discussion

II.2.1. Effect of irradiation dose.

The influence of the radiation dose ranging from 100 to 500 kGy was first evaluated. The progressive change of ESR spectra for γ-irradiated PVDF with irradiation dose is depicted in Figure 1a. Normalized intensities are presented for a better comparison. The first relevant information is the modification of the global shape of the signal as the dose increases. This progressive evolution reflects a change in the distribution of the radical species formed during the radiation process. Furthermore, it can be seen that the normalized intensity is also affected by the radiation dose. The evolution of the total concentration of free radicals is highlighted in Figure 1b. The radical concentration first increases with the radiation dose until it reaches a constant level. This result has

previously been reported by several authors and for different irradiation techniques.[17, 21-24] The concentrations of radicals in PVDF irradiated at different dose are actually in good agreement with the data available in the literature.[11, 21]

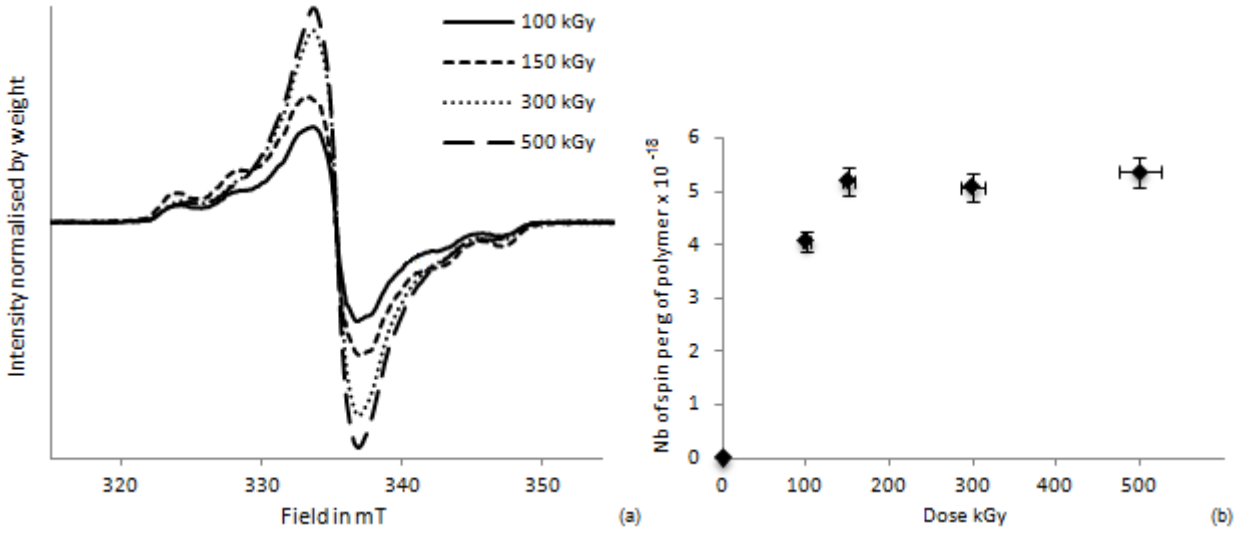

Figure 1. (a) Normalized ESR spectra of γ-irradiated high molecular weight PVDF and (b) Total concentration of spins per gram of polymer as a function of the dose (anaerobic conditions).

The threshold value is about 5.2 $.10^{18}$ spin.g^{-1}. Considering the molecular weight of the VDF unit (64 g.mol^{-1}), this means that statistically one residual radical species stands every 1800 repeating units. This maximum radical concentration is reached in our case at nearly 150 kGy and is known to depend on the experimental conditions, especially the temperature at which irradiation is carried out [25] as it is directly related to macromolecular mobility.

The change in concentration is a consequence of the balance between the generation of radicals (which depends on the inherent radiation chemical yield from PVDF and corresponds to the initiation step of a classical radical mechanism) on the one hand and the termination reactions occurring all along the irradiation process on the other hand. This balance has been related to the distance between radicals.[29] Radicals are generated randomly in the material, and they can move in a given volume for a short period of time. For those which are close enough, radicals can recombine when two volumes interpenetrate; for low doses, the concentration of radicals is low and the distance between radicals is statistically high. At a given dose value, the radicals are getting closer and consequently a quasi-steady state for radical concentration is reached. This is all the more facilitated that PVDF readily cross-links upon irradiation.[1]

Having in mind that five different radicals are generated upon irradiation, different termination reactions involving these species can occur, which extent will depend on the corresponding termination rate constant, on the concentration of radicals, on their mobility etc. Therefore, it appears as very interesting to point out the distribution of the radicals for different doses. The assumptions used to define the fitting parameters were recently presented in details.[5] The relative percentages of

each species were the only authorized adjustment variables, while keeping the spectroscopic fitting parameters constant.

The model was thus applied to fit the ESR spectra of PVDF samples exposed to different doses, and the residuals, as the subtraction between the experimental and the fitting curves, were also determined (Figure S1). Some small deviations can be observed at the center of the spectra, with a higher residual when compared to signal intensity, while the simulation curves correlate well with experimental data on the wings. The imperfect subtraction of the signal from irradiated quartz tube and the high signal intensity on this spectral range explain the deviations. Residual signal cannot be fitted meaning that no more species is hidden in this signal. By the way, the part of the signal which is not considered in the fit, through quantization by integration of the residual in absolute value, remains low. The values are 4.8%, 5%, 5.1 % and 6.2 % for radiation dose of 100 kGy, 150kGy, 300 kGy and 500 kGy respectively. At the same time, the Spearman's correlation rank coefficient for all considered simulations are greater than 0.99. Refining the spectroscopic parameters (such as hyperfine coupling constants, linewidth, lineshape or g-position variables) by the WinSim program[26] do not lead to any improvement, neither a lowering of the residual nor a significant increase of the correlation parameter. Actually, decrease of the linewidth of polyenyl radicals (I) signal can be observed as the conjugation degrees of unsaturation increases, as previously reported by Ohnishi et al. in several polymers.[7] In our case, as can be seen on the UV spectra measured for PVDF films irradiated at 150 and 500 kGy (Figure S2) not only an increase of the absorbance occurs but a bathochromic shift is also observed, both information pointing out that the number and the degree of unsaturation increase. This effect is also evidenced by a darkening of the samples which become brown-yellow when exposed to high radiation dose. The wavelengths of the observed maxima are in good agreement with the values reported in the literature, for dienes (227 nm) and trienes (272 nm) observed for fluoropolymer radicals. Moreover, a small bump can be distinguished at 350 nm, which might correspond to an even higher polyene structure, as it was observed for unsaturations generated in polyethylene.[27] High order unsaturated structures are actually more stable than diene and trienes and their formation is favored by successive dehydrofluorination processes.[4] Back to the ESR model, it is reasonable to consider that fitting all the unsaturated species (dienes, trienes and so on) with a broad singlet will not affect the concentration given by the model.

The relative composition of radical species (expressed in percent) for different investigated dose is detailed in Figure 2. It highlights the increase of the part of stable species as the dose increases. The progressive changes of the absolute concentration of radicals per gram of PVDF are also provided on the same graph.

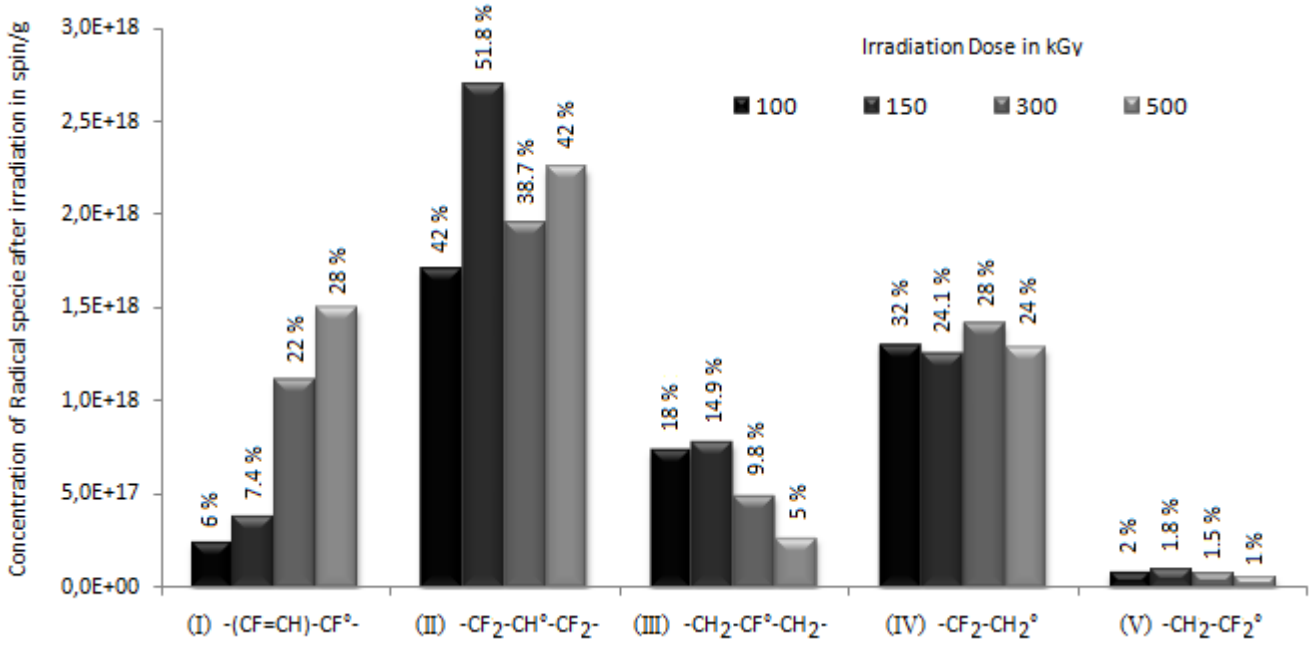

Figure 2. Evolution of the concentration of each radical species as a function of the radiation dose. (Concentration expressed as the number of spin per gram of polymer). The relative percentage of each species for a given dose is labeled.

Polyenyl radical (I) evolution is the most noticeable. The singlet signal of this species dominates the overall shape of the ESR spectra, with a significant increase of the signal intensity at the center of the field associated with the decrease of the intensity of the wings (Figure 1). This radical is not formed directly from irradiation of the pristine matrix, i.e. by a homolytic scission of a σ-bond. It results from successive dehydrofluorination of mid-chain radicals (II) and (III), a process which is favored by a more labile species in the β-position of a double bond. It can also be formed from a second phase of radical formation on the β-position of an unsaturated structure as it was presented by Kuzuya et al.[24] in the case of ethylene-tetrafluoroethylene copolymer, or in the case of PVC by Costa et al.[28]

The increase in proportion is principally due to the high stability of this species as explained by the mesomeric effect[16] which is all the more important that the degree of conjugation increases. An increase of the absolute concentration is also noticeable. Indeed, polyenyl radicals are known to preferentially be formed at high radiation dose.[29] This increase is still observed even when the threshold in the overall concentration of radical species is reached i.e. at 150 kGy in our experimental conditions (Figure 1b). These radicals are thus formed at the expense of more reactive radicals and particularly at the one of the mid-chain radical (III) which absolute concentration decreases once the threshold is reached. It is complex to distinguish exactly which species are responsible for this increase, and how much they affect the proportion of the polyenyl radicals as possible reactions are numerous.

Methyne centered radical (II) represents the major component whatever the dose, with a relative proportion around 40% and more. This is explained by the structure of this radical. First, it is a mid-chain radical, which means that its mobility is lower than the one of an end-chain radical. Secondly, the radical is surrounded by two highly electron-accepting fluoromethylene groups. As a consequence, this radical represents the most stabilized species that can be directly formed upon the radiation process. By the way, the proportion of species (II) increases until the maximum overall concentration is reached. For higher irradiation dose, the proportion of this species is lower but remains constant around 40%. This difference observed between 150 and 300 kGy could be the result of a higher crosslinking efficiency, with the increase of gel fraction and crosslinking density (*vide infra*). The latter phenomenon necessarily implies the consumption of mid-chain radicals, and could statistically implies the ones which are readily available (comparatively to radicals (III)) and reactive (comparatively to radicals (I)).

Part of radical (III) gradually decreases with the increase in the radiation dose. Compared to radical (II), it is reasonable to consider that their mobility are the same, but the electronegative stabilization is in this case inverted. Radical is highly centered on the fluoromethyne group and there is no compensation from the hydrogens in the β position as in the case of perfluoroalkyl radical.[5] As a result, radical (III) is very reactive and will then evolve, either through reaction all along the irradiation process (leading to crosslinking or branching), or through conversion into polyenyl radical, and thus much more easily than species (II).

Studies of end chain radicals show the influence of the chemical structure and the chain mobility as reported by Klimova et al.[30] By comparing radical (IV) to radical (II) on the one hand, and radical (V) to radical (III), on the other hand, the global concentration of end chain radicals is much lower than the one of resembling mid-chain species. Moreover, the difluoromethylene radical (V) is very reactive as shown by its low proportion and low concentration whatever the dose. The absolute concentration of end-chain radical (IV) is relatively constant and represents approximately 25 % of the overall species when the threshold is reached. It means that it has reached a quasi-steady state whatever the dose. Focusing on end-chain radicals, the proportion of radical bearing hydrogen in α-positions (radical IV) is higher than the one of radical bearing fluorine (radical V), proving that the former presents a higher stabilization and thus a lower reactivity. This can explain the large difference in concentrations for radicals (IV) and (V), while one could expect an identical concentration as these radicals are formed by a homolytic scission of the CH_2-CF_2 bond. Moreover, radical (V) follows the same trend than radical (III), that is to say a progressive decrease of its relative proportion such that it represents only 1 % of the spectrum for high radiation dose, pointing out again its high reactivity.

II.2.2. Effect of annealing for PVDF initially irradiated at different dose.

As discussed in the first part, the total concentration of radicals generated in γ-irradiated PVDF increases with the dose (due to a favored step of initiation when compared to termination reactions) before a steady-state is reached, as proved by a constant concentration of radicals for a threshold value of 150 kGy. However, applying the fitting model at different doses showed that the proportion of radicals was different, due to mobility and reactivity constraints. Then, as the change in radical proportion upon annealing might also depend on the initial stage of the sample, the effect of annealing at 373 K has been studied independently for different radiation doses. This temperature was selected as it is sufficiently low regarding crystallization of high molecular weight PVDF and obviously melting temperatures, such that no significant modification in the degree of crystallinity is observed on this dose range. For any dose, the evolution of the ESR signals with the annealing time follows the same trend as the one previously reported for 150 kGy:[5] the concentration of radicals rapidly decreases until 60 minutes, and then tends to a plateau. Moreover, the shape of the ESR signals is also affected until 60 minutes, and the spectra being then superimposed: a redistribution of radical species is thus anticipated along the first regime, as a relative greater decay of signal wings than centered signal is observed.

The results obtained after 60 minutes of annealing can be compared, firstly in terms of ESR shape (Figure 3a). As can be seen, two groups which resemble in shape and area, can be distinguished, the one for 100 and 150 kGy on the one hand, and for 300 kGy and 500 kGy on the other hand. Corresponding concentrations of radicals are depicted in Figure 3b. An increase is first noticed, and then the concentration levels off. At first sight, the differences observed between 150 kGy and 300 kGy appear all the more surprising than the concentrations before annealing were similar. If one compares the rate of residual radicals, while only 15% of radicals remain after annealing at 373K for a dose of 150 kGy, 30% of the radicals are still present in the sample for higher doses.

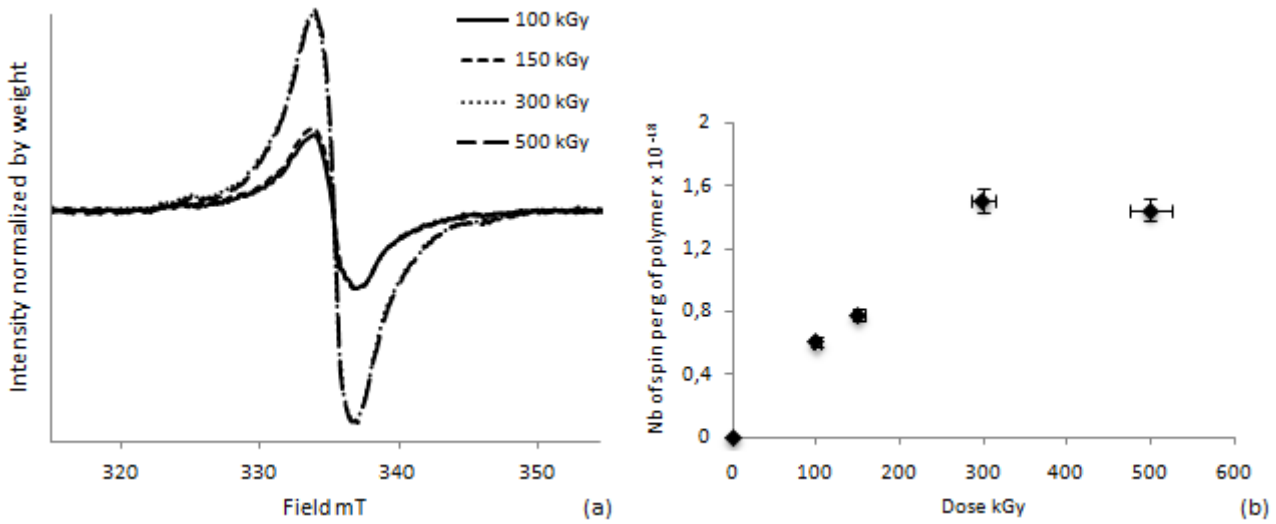

Figure 3. (a) Comparison of the first-derivative ESR spectra for PVDF samples irradiated at different dose followed by an annealing at 373K for 60 min– Intensity normalized by sample weight. (b) Total concentration of spins per gram of polymer as a function of the dose after an annealing time of 60 min.

These results cannot be explained only by the differences in the radical distribution before any annealing, and can rather be related to the difference in crosslinking density with the dose. The results of sol-gel analyses conducted in DMF are presented (Figure 4). These tests were performed in order to determine the gel content, and swelling tests were conducted to indirectly qualify the degree of crosslinking through volume expansion. Before comparing samples together, we first verified that the macroscopic behavior as evaluated by sol-gel analyses are not affected by annealing (Figure S3); the gel fraction and the solvent uptake were actually constant and equal to the ones before annealing. This confirms that crosslinking mainly occurs during the irradiation: annealing might contribute to the crosslinking of the polymer, but the impact of this stabilizing process on the features of the crosslinked material is scarce. From these results, it is reasonable to consider that the extent of crosslinking determined after annealing is an image of what was obtained before annealing.

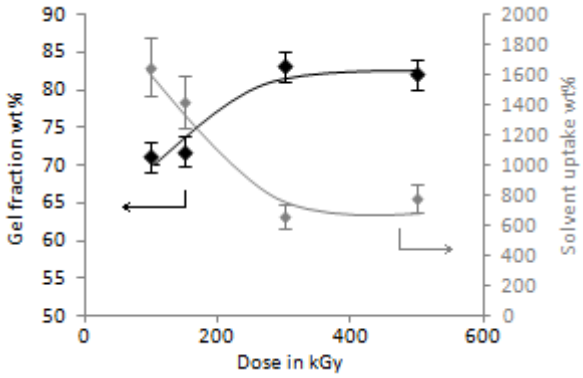

Figure 4. Gel fraction and solvent uptake obtained in DMF as a function of radiation dose.

The sol-gel results are presented in Figure 4. As can be seen, the gel fraction increases with the dose until 300 kGy and then levels off; at the same time the solvent uptake of the gel decreases until 300 kGy, due to a tighter network, and then remains constant. This indicates that more polymer chains are crosslinked concomitantly with a higher crosslinking density. Moreover, the increase of network density observed between two doses necessarily involves the consumption of mid-chain radicals, together with either another mid-chain radical (to form a so-called X-type crosslink) or with an end-type radical (to form a Y-type crosslink). As an indirect consequence, it also implies a reduction of mobility of polymer segments between two crosslinks, reducing the probability for radicals to meet. The large difference observed in solvent uptake at 150 kGy and 300 kGy (and higher dose) proves that a critical step has been overcome in this range. While the network is becoming somehow tighter, the reduction of mobility of polymer segments hampers the radicals from coupling, even if their intrinsic reactivity is high. This leads to a higher concentration of remaining radicals. This is actually in good agreement with the theory of the alkyl radical decay, for which it is usually assumed that limitation of alkyl radical recombination is caused by radical diffusion constraints in polymer matrix.[29] Furthermore, the loss of mobility is rather due to the chemical crosslinks than physical crosslinks (such as crystalline domains) since irradiation-induced crystallization is unlikely to occur in the range of dose investigated: actually, the crystallinity rate slightly increases with the dose up to 300 kGy but then dramatically decreases for higher values, as the damages caused in the crystalline part are too important.[31, 32]

By using our fitting model, it is possible to quantify each radical species after annealing. Integration of the residual in absolute value are slightly higher for annealed samples than for non-annealed samples, mainly because the signal-to-noise ratio decreases significantly as the concentration of radicals lowers down. However, the simulated spectra are correctly fitting the experimental curves, as confirmed by Spearman's rank correlation parameters that are always greater than 0.98. (Integration of residual in absolute value is currently comprised between 7% and

10% and the fitted spectra are presented in Figure S4). The distribution of radicals remaining after 60 minutes of annealing at 373 K is given in Figure 5. Before comparing the distributions together, we can first point out that the part of polyenyl radicals has dramatically increased when compared to un-annealed sample (Figure 2). This confirms our previous statement that polyenyl radicals (I) are very stable species. For the other radicals, the distribution verifies the order based on reactivity and localization, as developed in the first part. Indeed, the parts of α-hydrogen radicals (II) and (IV) are higher than their respective α-fluoro counterparts (III) and (V).

When comparing the distributions of radicals for different initial irradiation dose, the results obtained for 150 kGy somehow distinguish themselves from the others, in particular in the part of radicals (II). This reflects the initial distribution and overall concentration of radicals on the one hand, and the crosslinking density on the other hand. From 100 kGy to 150 kGy, the concentration of radicals increases as the network is relatively loose. At 150 kGy, while the overall concentration reaches the threshold value, the part of radicals (II) is already much higher than for any other dose before annealing, and so will it be after annealing. Actually, this type of radicals is the less reactive one directly generated upon irradiation: they will not react until the network is becoming tighter, as observed from 300 kGy.

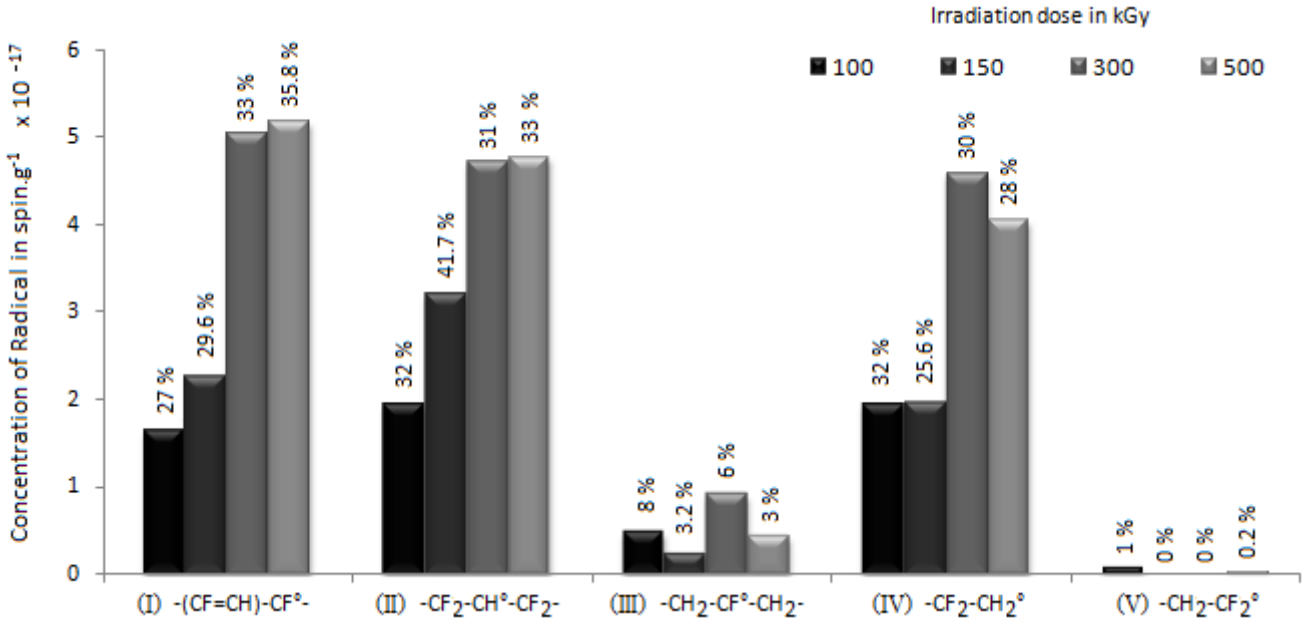

Figure 5. Evolution of the concentration of each radical remaining in PVDF irradiated at different doses and annealed at 373K for 60 min. The relative percentage of each species for a given dose is labeled.

This work points out the relationship between chemical structure of radicals and the network features obtained during irradiation, regarding the accessibility and future of radicals for a subsequent chemical process. Another possibility is to use the remaining radicals as initiating sites for polymerizing vinylic monomer through radical grafting. This corresponds to the so-called "pre-irradiation" strategy which consists in adding a vinylic monomer after the polymer has been irradiated. It is generally employed when the "simultaneous irradiation" strategy cannot be envisaged, mainly due to the high sensitivity of the given monomer with respect to irradiation. However, as many radical species with different stability and thus reactivity are generated, it is very important to estimate the proper irradiation conditions in order to generate the maximum concentration of efficient radicals which can subsequently initiate the desired reaction. However, because the cross-linking rate of the material evolves, the respective composition of the radicals also varies when the plateau for total radical concentration is reached. Then, looking at the grafting efficiency finally obtained on samples which were priory exposed to different irradiation conditions lead to different results, and thus different properties can be expected even if the concentration of radicals was initially the same. This work gathers fundamental insights in this context, and the results will be presented in a forthcoming paper.

CONCLUSION

The ESR simulation previously reported was applied to the quantitative monitoring of the five radicals generated in high molecular weight PVDF submitted to γ-irradiation with dose ranging from 100 kGy to 500 kGy. While the overall concentration increases until 150 kGy and then level offs, the distribution of the radical species is different. The part of mid-chain radicals (polyenyl (I), methyne (II) or fluoromethyne (III)) is the major contribution when compared to end-chain radicals (methylene (IV) and fluoromethylene (V)), pointing out that the mobility of the radical-bearing segment is crucial. In addition, a chemical structure effect is also demonstrated as α-hydrogen bearing radicals (II and IV) are more numerous than their α-fluoro-bearing counterparts (III and V), as the latter are intrinsically more reactive due to an inductive effect of the highly electronegative fluorine atoms. By the way, a significant increase of polyenyl radicals is observed with the dose, as confirmed by UV spectroscopic measurements. Among different possibilities, the radicals are involved in coupling reactions, as the degree of cross-linking increases with the dose.

Effect of annealing samples priory irradiated at different doses was further investigated. The annealing conditions were selected such that the crystalline part was not affected and the radical concentration reached equilibrated values.

Concentration of remaining radicals strongly depends on the gel content and crosslinking density, as determined by sol-gel analyses conducted in DMF. The distribution of radicals was also resolved: while the part of polyenyl radicals is increased with prior increasing dose, the part between the other radicals is an image of the distribution observed before annealing, proving that the reduced mobility due to higher cross-linking prevails again reactivity concerns. The simulation model has demonstrated its efficiency, and will be extended to the identification of radicals generated onto PVDF-based copolymers in order to gain deeper insights into the radiolysis of fluoropolymers. This work will be presented in a forthcoming paper.

REFERENCES

1. Lyons, B. J. Radiation Crosslinking of Fluoropolymers – A Review. *Radiation Physics and Chemistry* **1995,** *45* (2), 159-174.
2. Dawes, K.; Glover, L. C.; Vroom, D. A. *The Effects of Electron Beam and γ-Irradiation on Polymeric Materials. in Physical Properties of Polymers Handbook*, 2nd ed.; Springer: New York, 2007.
3. Rosenberg, Y.; Siegmann, A.; Narkis, M.; Shkolnik, S. Low Dose γ-Irradiation of some Fluoropolymers: Effect of Polymer Chemical Structure. *Journal of Applied Polymer Science* **1992,** *45* (5), 783-795.
4. Makuuchi, K.; Masaharu, A.; Toshihiko, A. Effect of Evolved Hydrogen Fluoride on Radiation-Induced Crosslinking and Dehydrofluorination of Poly(vinylidene Fluoride). *Journal of Polymer Science. Polym Chemistry Edition* **1976,** *14* (3), 617-625.
5. Dumas, L.; Albela, B.; Bonneviot, L.; Portinha, D.; Fleury, E. Electron Spin Resonance Quantitative Monitoring of Five different Radicals in γ-Irradiated Polyvinylidene Fluoride. *Submitted*.
6. Helbert, J. N.; Wagner, B. E.; Poindexter, E. H.; Kevan, L. Matrix ENDOR of polyenyl radicals in polymers. *Journal of Polymer Science: Polymer Physics Edition* **1975,** *13* (14), 825–834.
7. Ohnishi, S. I.; Ikeda, Y.; Sugimoto, S. I.; Nitta, I. On the ESR Singlet Spectra Frequently Observed in Irradiated Polymers at a Large Dose. *Journal of Polymer Science* **1960,** *47* (149), 503-507.
8. Seguchi, T.; Tamura, N. Electron Spin Resonance Studies on Radiation Graft Copolymerization. I. Grafting Iniated by Alkyl Radicals Trapped in Irradiated Polyethylene. *Journal of Polymer Science : Polymer Chemistry Edition* **1974,** *12* (18), 1671-1682.
9. Goslar, J.; Hilczer, B.; Smogor, H. Radiation-Induced Modification of P(VDF/TrFe) Copolymers Studied by ESR and Vibrational Spectroscopy. *Applied Magnetic Resonance* **2008,** *34* (1-2), 37-45.
10. Kasser, M. J.; Silverman, J.; Al-Sheikhly, M. EPR Simulation of Polyenyl Radicals in Ultrahigh Molecular Weight Polyethylene. *Macromolecules* **2010,** *43* (21), 8862-8867.
11. Goslar, J.; Hilczer, B.; Smogor, H. ESR Studies of Fast Electron Irradiated Ferroelectric Poly(Vinylidene Fluoride). *Acta Physica Polonica A* **2005,** *108* (1), 89-94.
12. Siegel, S.; Hedgpeth, H. Chemistry of Irradiation Induced Polytetrafluoroethylene Radicals: I. Re-examination of the EPR Spectra. *The Journal of Chemical Physics* **1967,** *46* (10), 3904-3912.
13. Matsugashita, T.; Shinohara, K. Electron Spin Resonance Studies of Radicals Formed in Irradiated Polytetrafluoroethylene. *The Journal Of Chemical Physics* **1961,** *35* (5), 1652-1656.
14. Allayarov, S. R.; Mikhailov, A. I.; Barkalov, I. M. Analysis of the ESR Spectra of the ~CF_2CFCF_2~ Macroradical Trapped in a γ-Irradiated Polytetrafluoroethylene Matrix at 77 K. *High Energy Chemistry* **2000,** *34* (3), 141-144.
15. Kuzuya, M.; Ito, H.; Kondo, S. I.; Noda, N.; Noguchi, A. Electron Spin Resonance Study of the Special Features of Plasma-Induced Radicals and Their Corresponding Peroxy Radicals in Polytetrafluoroethylene. *Macromolecules* **1991,** *24* (25), 6612-6617.
16. Allayarov, S. R.; Gordon, D. A.; Kim, I. P. Radiolysis of n-perfluoroalkanes and polytetrafluoroethylene. *Journal of Fluorine Chemistry* **1999,** *96* (1), 61-64.

17. Allayarov, S. R.; Konovalikhin, S. V.; Olkhov, Y. A.; Jackson, V. E.; Kispert, L. D.; Dixon, D. A.; Ila, D.; Lappan, U. Degradation of γ-irradiated linear perfluoroalkanes at high dosage. *Journal of Fluorine Chemistry* **2007,** *128* (6), 575-586.
18. Shiotani, M.; Persson, P.; Lunell, S.; Lund, A.; Williams, F. Structures of Tetrafluorocyclopropene, Hexafluorocyclobutene, Octafluorocyclopentene and Related Perfluoroalkene Radical Anions Revealed by Electron Spin Resonance Spectroscopic and Computational Studies. *The Journal of Physical Chemistry A* **2006,** *110* (19), 6307-6323.
19. Klimova, M.; Tino, J.; Borsig, E.; Ambrovic, P. The Effect of Crosslinking on the Reactivity of Free Radicals in Isotactic Polypropylene. *Journal of Polymer Science: Polymer Physics Edition* **1985,** *23* (1), 105-111.
20. Allayarov, S. R.; Konovalova, T. A.; Waterfield, A.; Focsan, A. L.; Jackson, V.; Cracium, R.; Kispert, L. D.; Thrasher, J. S.; Dixon, D. A. Low-temperature fluorination of fluoro-containing polymers EPR studies of polyvinylidenefluoride and the copolymer of tetrafluoroethylene with ethylene. *Journal of Fluorine Chemistry* **2006,** *127,* 1294–1301.
21. Mitov, S.; Hübner, G.; Brack, H. P.; Scherer, G. G.; Roduner, E. In situ Electron Spin Resonance Study of Styrene Grafting of Electron Irradiated Fluoropolymer Films for Fuel Cell Membranes. *Journal of Polymer Science: Part B: Polymer Physics* **2006,** *44,* 3323-3336.
22. Li, J.; Sato, K.; Ichiduri, S.; Asano, S.; Ikeda, S.; Iida, M.; Oshima, A.; Tabata, Y.; Washio, M. Pre-irradiation induced grafting of styrene into crosslinked and non-crosslinked polytetrafluoroethylene films for polymer electrolyte fuel cell applications. I: Influence of styrene grafting conditions. *European polymer journal A.* **2004,** *40* (4), 775-783.
23. Palacio, O.; Aliev, R.; Burillo, G. Radiation Graft Copolymerization of Acrylic Acid and N-Isopropylacrylamide from binary mixtures onto Polytetrafluoroethylene. *Polymer Bulletin A.* **2003,** *51* (3), 191-197.
24. Kuzuya, M.; Niwa, J.; Noguchi, T. Electron spin resonance study on plasma-induced surface radicals of ethylene-tetrafluoroethylene copolymer. *Polymer Journal A.* **1995,** *27* (3), 251-255.
25. Dargaville, T. R.; Hill, D. J. T.; Whittaker, A. K. An ESR study of irradiated poly(tertrafluoroethylene-co-perfluoropropyl vinyl ether) (PFA). *Radiation Physics and Chemistry* **2001,** *62* (1), 25-31.
26. Duling, D. R. Simulation of Multiple Isotropic Spin Trap EPR Spectra. *Journal of Magnetic Resonance, Series B* **1994,** *104* (2), 105-110.
27. Waterman, D. C.; Dole, M. Ultraviolet and infrared studies of free radicals in irradiated polyethylene. *Journal of Physical Chemistry A.* **1970,** *74* (9), 1906-1912.
28. Costa, L.; Brunella, V.; Paganini, M. C.; Baccaro, S.; Cecilia, A. Radical formation induced by y radiation in poly(vinyl chloride) powder. *Nuclear Instruments and Methods in Physics Research B* **2004,** *215* (3-4), 471-478.
29. Aymes-Chodur, C.; Esnouf, S.; Le Moël, A. ESR Studies in γ-irradiated and PS-Radiation-Grafted Poly(vinyldene fluoride). *Journal of Polymer Science: Part B: Polymer Physics* **2001,** *39,* 1437-1448.
30. Klimova, M.; Szöcs, F.; Bartos, J.; Vacek, K.; Pallanova, M. ESR and DSC Study of the Radiation Crosslinking Effect on Macroradical Decay in Poly(Vinylidene Fluoride). *Journal of Applied Polymer Science* **1989,** *37* (12), 3349-3458.
31. Zhudi, Z.; Wenxue, Y.; Xinfang, C. Study on increase in crystallinity in γ-irradiated poly(vinylidene fluoride). *Radiation Physics and Chemistry* **2002,** *65* (2), 173–176.
32. Dargaville, T. R.; Celina, M.; Clough, R. L. Evaluation of vinylidene fluoride polymers for use in space environments : Comparison of radiation sensitivities. *Radiation Physics and Chemistry* **2006,** *75* (3), 432-442.

SUPPORTING INFORMATION

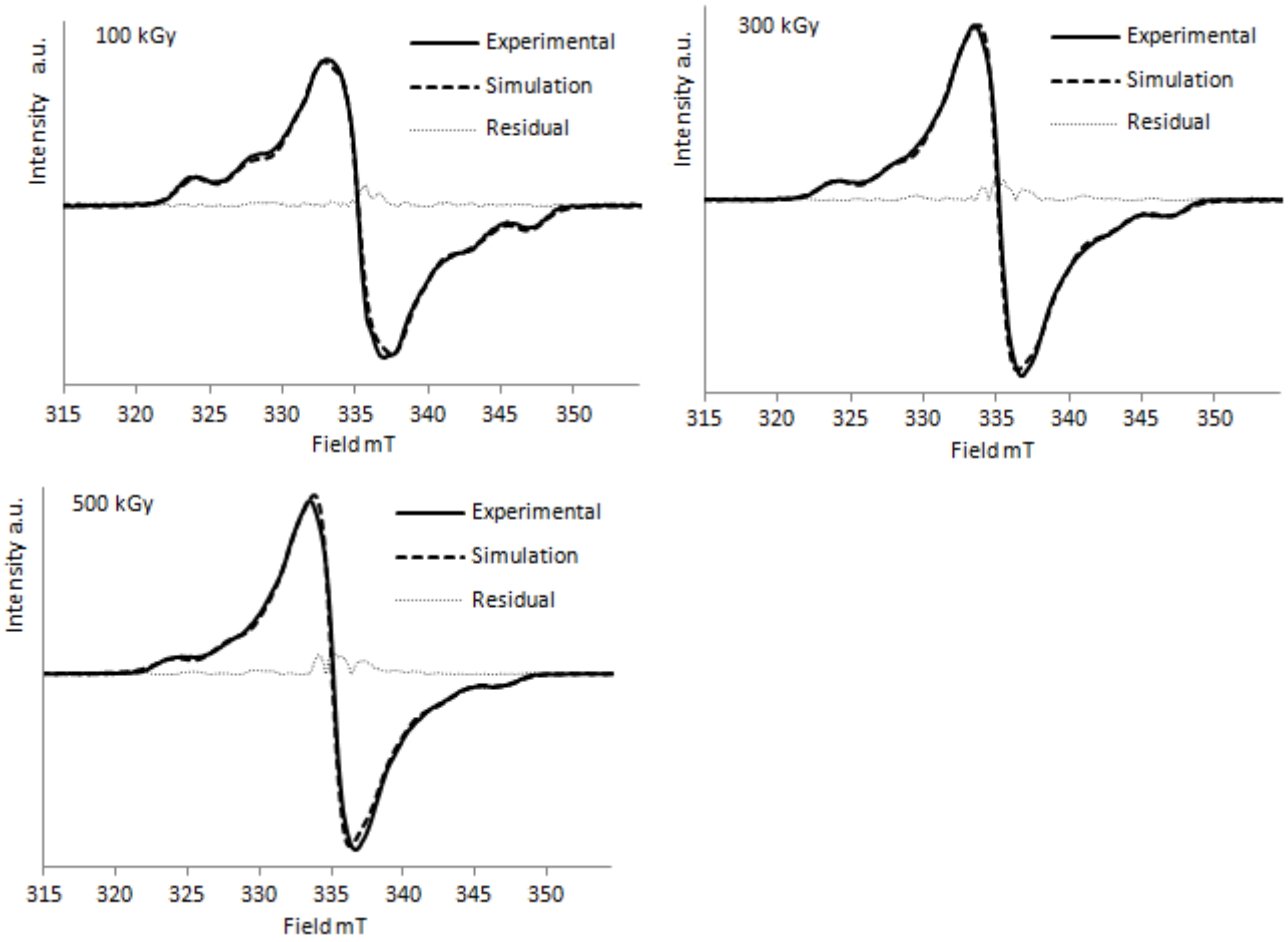

Figure S1. Experimental and simulated spectra of γ-irradiated PVDF at 100, 300 and 500 kGy in anaerobic conditions. Residual is presented in absolute value.

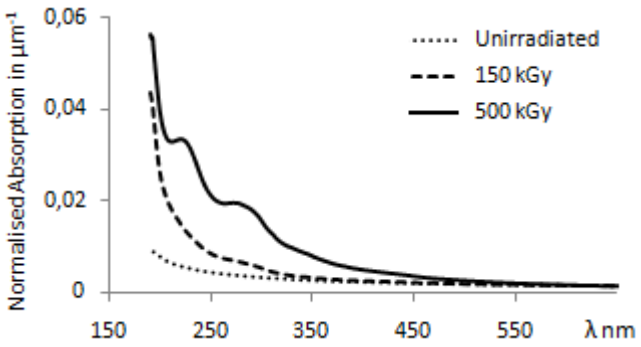

Figure S2. UV spectra of irradiated films of PVDF after an anneal of 1 h at 100°. Control film of unirradiated PVDF is given as reference. Absorptions are normalized by samples thickness.

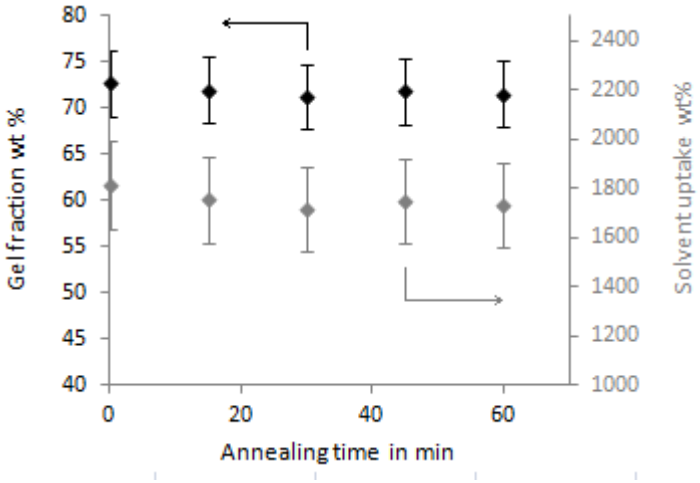

Figure S3. Gel fraction and solvent uptake obtained for different annealing times at 373 K. Solvent: DMF, Initial dose: 150 kGy.

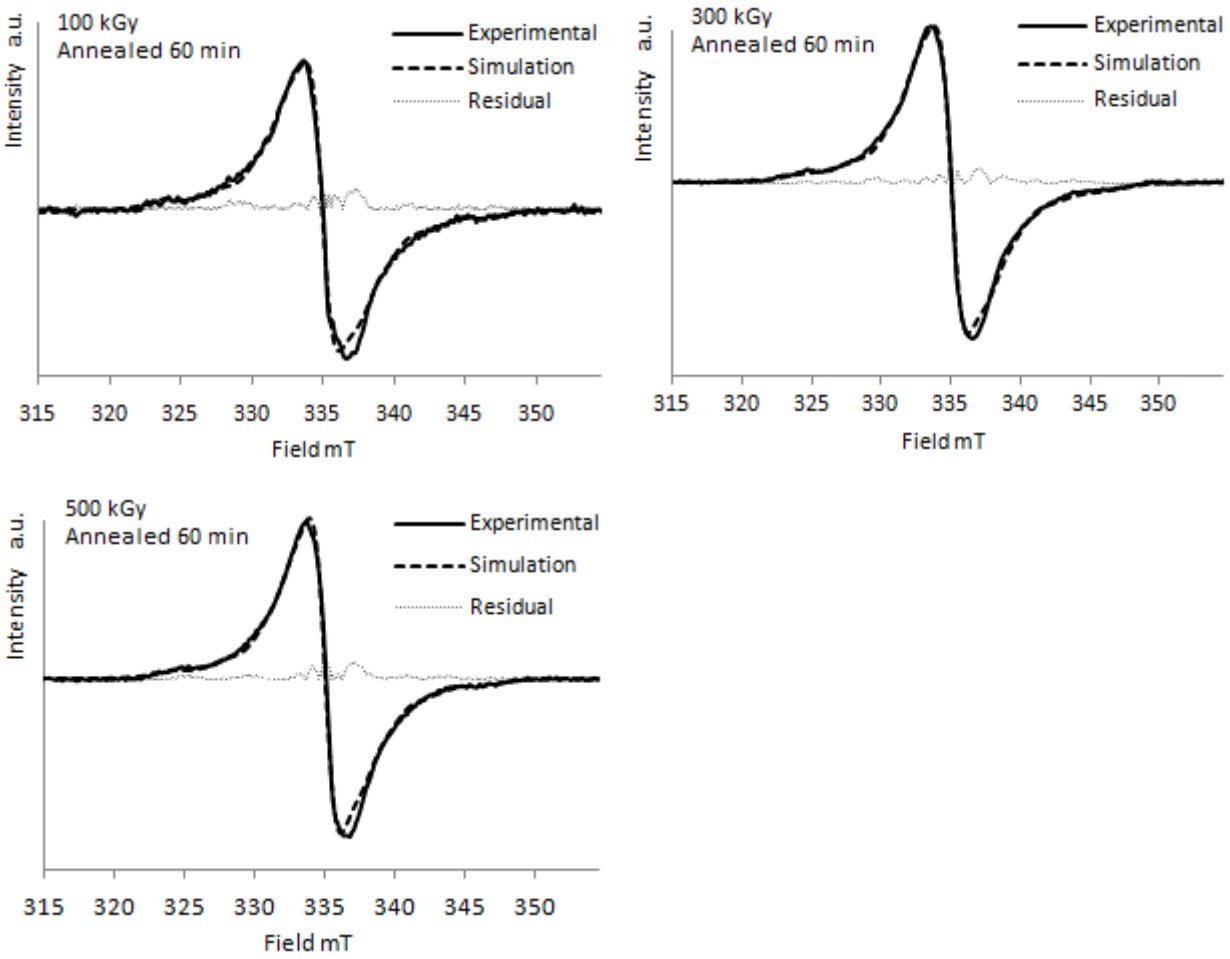

Figure S4. Experimental and simulated spectra of γ-irradiated PVDF at 100, 300 and 500 kGy annealed at 373 K during 60 min. Residual is presented in absolute value.

III. ESR INVESTIGATION OF RADICALS FORMED IN γ-IRRADIATED VINYLIDENE FLUORIDE BASED COPOLYMER.

Samples of copolymer based on vinylidene fluoride and hexafluoropropene p(VDF-co-HFP) were exposed to ^{60}Co emitting γ-radiation. Irradiation was performed under an inert atmosphere and led to the formation of radicals. The total amount of radicals has been quantified by electron spin resonance spectroscopy (ESR). An in-depth study of recorded ESR spectra allowed the identification of several types of radical species formed during radiolysis. Starting from an ESR simulation model established for irradiated PVDF, seven radical species have been identified in the case of p(VDF-co-HFP). Five of them are related to the VDF units while the two others are derived from the HFP unit. The establishment of the model used to simulate the EPR spectra is presented. The proportions of each species are discussed and associated to the amount of HFP units contained in the chain, and with the stability of each species depending on their local environment. Further, the evolution of radical density with radiation dose and the decay resulting from an annealing at a given temperature were analysed. Corresponding spectral evolution shows the progressive predominance of most stable species.

INTRODUCTION

Among fluoropolymers, PVDF presents exceptional properties such as physical and electrical ones, chemical inertness…[1] It is also typically 50-70% crystalline, which directly affects its processability. A possible way to adjust some of its properties is by copolymerization: actually, incorporating B units into a given polymer usually modulates both intra- and inter-molecular forces, affecting consequently crystallinity, thermal properties, stability, permeability, chemical reactivity and so on. In this context, VDF-based copolymers with additional unit of hexafluoropropylene p(VDF-co-HFP) have been widely studied and developed.[2] The presence of a CF_3 bulky side group along the polymer chain lowers the degree of crystallinity and the melting temperature while increasing molecular mobility, which confer to these copolymers a better processability compared to PVDF.[3] For low HFP units content (less than 15-19%), the resulting copolymers show thermoplastic properties while for higher contents, copolymers behaves like elastomers at room temperature due to the very low Tg. In any case, chemical resistance is maintained and the degradation temperatures remains still above 350°C. Consequently, p(VDF-co-HFP) copolymers found various applications in

hostile environment and are now highly prized for applications in the energy area (membranes for fuel cells, rechargeable lithium ion batteries, dye-sensitized solar cells).[2] However, their mechanical strength is lower than for PVDF but can be improved by crosslinking. Among the different possible strategies to crosslink VDF-based polymers, γ-radiation is in particular very attractive as it consumes only little energy and as no addition of cross-linker is mandatory to achieve high crosslinking rate.[4] It is known that p(VDF-co-HFP) copolymers present a better ability to crosslink than the PVDF homopolymer, concomitantly due to the lower degree of crystallization and the intrinsic radiosensitivity of HFP unit.[4] The mechanisms of radiolysis involve the formation of radical species as a result of bond scission.[5] Although most of the reactions consuming radicals are quite fast, transients can survive for hours in semi-crystalline polymers which makes it possible to probe free radicals by electron spin resonance (ESR): in addition to a quantitative determination of the generated radicals, it allows determining the contribution of each species if their respective ESR parameters are known. However, s and p type radicals such as the ones formed in polymers are restrained in a narrow range of spectral response that leads to the superimposition of all the signals, each of them being most often made of several peaks. Consequently, the most common way to quantize the part of each species is to simulate their ESR response. This approach needs a *priori* knowledge of all the involved species on the one hand, and their respective simulation parameters on the other hand, which are generally not or only partly known, even less for copolymers.[6] Indeed, in the latter case, the number and type of possible radicals not only depend on the intrinsic chemical structure of the repeating units but also on their distribution along the copolymer chain, namely the microstructure, as the neighboring groups of a given radical affect both the hyperfine splitting constants, the multiplicity and respective intensity of each peak. Consequently, the global ESR spectrum of a given copolymer is a combination of the spectra of each homopolymer plus some specific signals due to the sequencing of the repeating units in the polymer chain. This suggests that most of radical species formed during the radiolysis of the respective homopolymers must be found in the case of the copolymer and must be used as a starting point to simulate its ESR signal. Taking into account simple energetic considerations,[4,7] any bond of the VDF and HFP repeating unit can be broken when the copolymer is submitted to γ-radiation. In the case of PVDF, it is well admitted that five different types of free radicals are formed upon irradiation (radicals I to V).[8]

$-(CF=CH)_n-\dot{C}F-$ (I) ; $-CF_2-\dot{C}H-CF_2-$ (II) ; $-CH_2-\dot{C}F-CH_2-$ (III) ;

$-CF_2-\dot{C}H_2$ (IV) ; $-CH_2-\dot{C}F_2$ (V).

Scheme 1. Chemical structure of radicals generated in γ-irradiated PVDF.

In a previous work[9], we have reported an ESR simulation model of free radicals in γ-irradiated high molecular weight PVDF. Simulation parameters of radicals (I)[6,10-13] and (II)[13,14] were directly retrieved from reported data, while for radicals (III) to (V), they were derived from a thorough literature studies of the parameters used to simulate ESR signal of fluorocarbon and perhydrogenocarbon radicals. This model takes into account the molecular structure, the localization and the chemical environment of each radical, that is to say the atoms present on the α and β positions of the radical. It was used to quantitatively monitor each radical species generated in PVDF as a function of different experimental parameters such as initial radiation dose or subsequent annealing at high temperature.[15] It was shown that the distribution of radicals not only depend on the intrinsic stability of the radical but also on the gel content and crosslinking density of the irradiated polymer, proving that both effects have to be taken into account to fully interpret the behavior of a polymer when irradiated.

In our continuous work on the γ-irradiation of PVDF-based materials,[9,15,16] herein is presented a detailed study of the behavior of a commercially available semi-crystalline p(VDF-co-HFP) copolymer upon γ-radiation. First, the radical species resulting from the presence of the HFP units are suggested based on relative chemical stability and mobility concerns, and the spectroscopic parameters of their ESR response are derived from a thorough literature survey of comparable radical species as well as the electron displacement under bond polarization driven by electronegativity differences. By combining these values with the ones previously determined for PVDF, a complete simulation model of the ESR spectra of the copolymer is presented, which allows quantitatively monitoring each radical species. Second, this model is used to elucidate the distribution of radicals as a function of the initial irradiation dose, and subsequently annealed at high temperature. The changes are related to both respective chemical stability and extent of crosslinking, as measured by sol-gel analyses.

III.1. EXPERIMENTAL SECTION

III.1.1. MATERIALS.

p(VDF-co-HFP) (reference S2741) and PVDF (reference K741) under the form of powder were provided by Arkema, France. Their molecular weights were determined by SEC in DMF. For the copolymer, HFP content is around 6 wt%, M_n = 92 kg.mol^{-1} and degree of crystallinity is about 31%. For the homopolymer, M_n = 110 kg.mol^{-1} and degree of crystallinity is about 40 %. The degrees of crystallinity were calculated by normalizing the melting enthalpy of fusion, as determined

by DSC on the first heating ramp (v= 10 K/min), to the one of 100 % crystalline PVDF sample (which enthalpy is 104.7 $J.g^{-1}$). 2,2-Diphenyl-1-picrylhydrazyl (DPPH, Aldrich) was dissolved in chloroform to build a calibration curve for quantitative ESR analyses. Polymer films used for UV-vis analysis were made by extrusion process.

III.1.2. METHODS.

^{19}F NMR spectrum of the p(VDF-co-HFP) sample was recorded a ambient temperature on a Bruker Avance III 400 with a 5-mm QNP ($^{1}H/^{19}F/^{13}C/^{31}P$) operating at 376.5 MHz to probe ^{19}F nucleus and using deuterated acetone as the solvent. Chemical shift are given in ppm by calibrating the CF_2 of conventional sequence (head-to-tail) of VDF segments at -91.3 ppm. Spectra were recorded using the Bruker microprograms zgflqn30 with standard parameter sets and with 64 scans.
p(VDF-co-HFP) copolymer was introduced into 5mm Suprasil quartz ESR tubes mounted with a glass valve, then the tubes were vacuumed at room temperature, purged with argon several times and finally kept under argon atmosphere. The mounted tubes were placed into a vacuum bell under argon to avoid any oxygen contamination. Irradiations were carried out using an industrial ^{60}Co gamma source, at room temperature (300 K) with a constant dose rate of 0.7 $kGy.h^{-1}$. Irradiated samples were then kept at 255 K until they were studied to prevent any radical decay.

ESR spectra were recorded on a Bruker ELEXSYS E500 spectrometer operating in the X band microwave frequency range with a liquid nitrogen temperature controller. All spectra were acquired at 255K using a modulation amplitude of 0.1 mT, an optimum microwave power of 1.013 mW, a center field of 335 mT, and a sweep width of 40 mT. In these conditions, only one scan was sufficient to have representative spectrum with good signal-to-noise ratio. Residual quartz signal was removed by simple subtraction (Figure S1). To do so, a reference tube only (no copolymer) was irradiated in the same conditions of atmosphere and dose, and the ESR signal was recorded. Radical concentrations were calculated from the double integration of the first absorption derivative spectrum, using a calibration curve built up from a series of chloroform solutions of diphenylpicrylhydrazine (DPPH) with known concentrations (Figure S2). In order to investigate the effect of annealing on the overall radical concentration and the evolution of the ESR spectra, samples were heated during different times at 373 K, then their ESR response was recorded.

UV-visible experiments were performed using a PerkinElmer Lambda 35 UV/VIS spectrophotometer between 190 to 900 nm. A window frame was made in aluminum to hold the polymer film. Each sample was first analyzed before irradiation to make its own background. UV-Vis samples were introduced with their aluminum frame into Schlenk flask and stocked under argon for the irradiation process.

Sol-gel analyses were performed with DMF as a solvent. Around 1 g was taken from dumbbell specimens and introduced in a closeable flask. Sample weight was determined accurately (w_i) and a large excess of solvent (60 mL) was introduced. Samples were heated at 80 °C during 48 h to allow the complete extraction of the soluble component. Swollen gels were carefully wiped with a tissue then weighted (w_g). The solvent was then evaporated under vacuum for 24 h at 100 °C to determine the weight of dried gel (w_{dg}). The gel content (% gel) and the solvent uptake (% sol) were calculated using the following equations:

$$\%\, gel = \frac{w_{dg}}{w_i} \times 100 \qquad \text{and} \qquad \%\, sol = \frac{w_g - w_{dg}}{w_{dg}} \times 100$$

III.2. Results and discussion

III.2.1. Initial statement.

p(VDF-co-HFP) copolymers are usually prepared by emulsion or suspension polymerization,[3] and the polymer composition is tuned by the respective amounts of the monomers in the polymerization reactor. As HFP cannot homopolymerize in a free radical process, no HFP-HFP sequence is to be found and a random distribution of HFP along the polymer chains results from a continuous feeding of HFP along the polymerization.[2,17] Chain defects such as “head-to-head” or “tail-to-tail” additions are still possible between the two monomers, and can have a tremendous impact on the multiplicity and hyperfine splitting constants of a given radical, through the change in groups in β positions. However, during polymerization, the propagating radical is generally localized on the more substituted carbon atom which consequently favors a “head-to-tail” addition. The microstructure of VDF-based copolymers can be resolved by ^{19}F NMR, and the spectrum obtained for p(VDF-co-HFP) copolymer is presented in Figure 1.

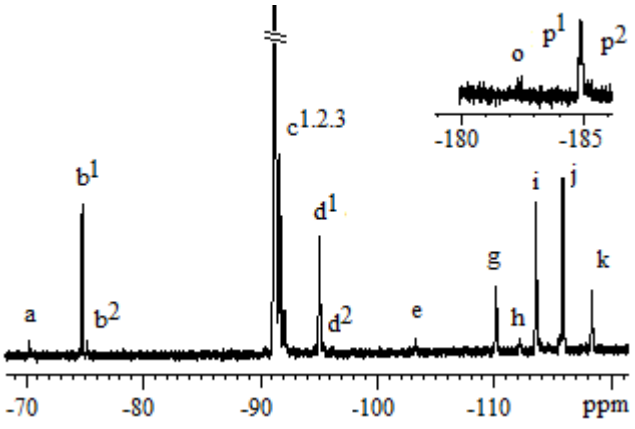

Figure 1. ^{19}F NMR spectrum of the pristine p(VDF-co-HFP) copolymer (in d_6-acetone).

Thanks to literature reports,[17-20] the complete assignment of the ^{19}F NMR spectrum is rendered possible. In particular, signals related to HFP units are the following: signals a (CH_2-CF_2-CF(*CF_3*)-CF_2, δ = -70.3 ppm), b^1 (CF_2-CF(*CF_3*)-CH_2-CF_2-, at δ = -74.3 ppm) and b^2 (CH_2-CF_2-CF_2-CF(*CF_3*)-CH_2-CF_2- CF_2-CF(CF_3), at δ =-75.2 ppm) correspond to the fluorine nuclei of the CF_3 group; signals e (CH_2-*CF_2*-CF(CF_3)-, at δ =-103.2 ppm) and k (-CF_2-*CF_2*-CF(CF_3)-, at δ =-119.5 ppm) to CF_2 and o (CF_2-*CF*(CF_3)-CF_2-, at δ = -182.3 ppm), p^1 (CF_2-*CF*(CF_3)-CH_2-, at δ = -185.0 ppm) and p^2 (CF_2-*CF*(CF_3)-CH_2-CF_2-CF_2-CF(CF_3), at δ = -185.2 ppm) to the CF group of the HFP repeating unit, respectively. Other signals correspond to the CF_2 groups of the VDF repeating unit in their different possible chain sequences, including "head-to-head", "tail-to-tail" links and also the proximity of the HFP repeating unit (see Table S1 for a complete assignment and Figure S3 for the integration values). As ^{19}F NMR is a quantitative analysis, the overall composition can be assessed and confirms around 6 wt% (2.65 mole%) HFP content in the copolymer. Moreover, the rate of -CF_2-CF(CF_3)-CF_2- sequence is determined to be less than 8 % in the overall sample. This result will be used in the following part dealing with the possible radical species resulting from the HFP units upon irradiation (*vide infra*).

III.2.2. ESR SPECTRUM OF P(VDF-CO-HFP) COPOLYMER; ESR MODEL.

The normalized ESR spectrum obtained for the p(VDF-co-HFP) copolymer γ-irradiated at a dose of 150 kGy is presented in Figure 2. As a matter of comparison, the one obtained for PVDF sample with a comparable molecular weight and irradiated in the same conditions is also provided. Few similarities exist between the two spectra: the spectra are centered in the same field range, characteristics of s and p types radicals, and some parts are superimposed, especially at the center field and at the side of wings. However, the two spectra are quite different at intermediate values for field. We initially tried to simulate the experimental spectrum obtained for p(VDF-co-HFP) copolymer with the simulation model previously reported for PVDF homopolymer[9] considering thus that radicals generated upon irradiation only concerned the major VDF content. The fit was not acceptable, proving that other species, certainly related to the comonomer and/or the HFP/VDF chainings have to be considered even for such low molar content of HFP in the copolymer. Another way to highlight the influence of HFP is to quantify the overall radical concentration from the double integration of the first absorption derivative spectrum, using a calibration curve built up from solutions of DPPH. For the p(VDF-co-HFP) copolymer, a concentration of 6.47 10^{18} spin.g^{-1} was found, which is 25% higher than the one obtained for PVDF.[9] To appreciate this difference, it corresponds to 1 radical every 1400 equivalent repeating units for the former, while on average 1 radical every 1800 repeating units is found for PVDF. While one could expect a lower concentration

of radicals for a (co)polymer which degree of crystallinity is reduced (due to inherent increased mobility of polymer chains which normally favors recombination of radicals), p(VDF-co-HFP) actually presents a higher radiosensitivy, and the resulting radicals are anticipated to be more stable than the one obtained from PVDF due to the attractive inductive effect of adjacent groups and dipolar effects. Thus, the impact of HFP content on the quantitative as well as qualitative aspects of the ESR response is confirmed by the previous statements.

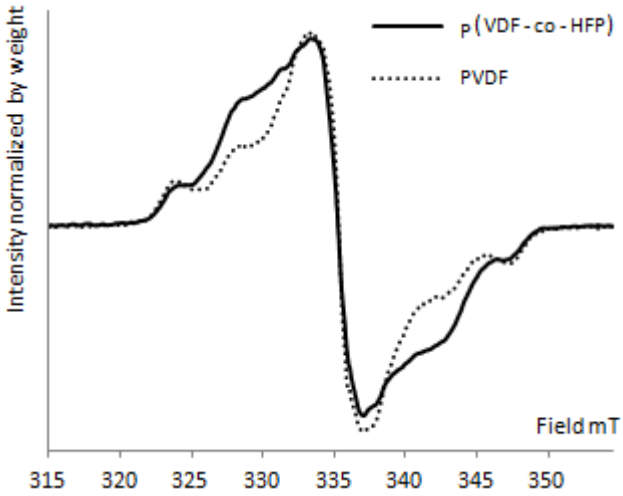

Figure 2. Normalized ESR spectra for PVDF and p(VDF-co-HFP) γ-irradiated at a dose of 150 kGy.

The major part of the work resides in *i)* the identification of the supplementary radicals which originate from HFP and *ii)* the simulation of their ESR response, through the determination of lineshape and linewidth of the signals, as well as g value and HSC due to neighboring atoms. Having in mind that γ-rays are energetic enough to break any bond of the p(VDF-co-HFP) copolymer, and taking into account all the possible addition sequences of the two comonomers, there is a plethora of possible new radical species ((a) to (j), scheme 2), in addition to the ones obtained from irradiated VDF units ((I) to (V), scheme 1).

$$-CF_2-\dot{C}F-CH_2- \quad (a); \qquad -CF_2-\dot{C}F-CF_2- \quad (b)$$

$$-CF_2-\dot{C}(CF_3)-CH_2- \quad (c); \qquad -CF_2-\dot{C}(CF_3)-CF_2- \quad (d)$$

$$-CF_2-CF(\dot{C}F_2)-CH_2- \quad (e); \qquad -CF_2-CF(\dot{C}F_2)-CF_2- \quad (f)$$

$$-CF_2-\dot{C}F-CF_3 \quad (g); \qquad -CH_2-\dot{C}F-CF_3 \quad (h)$$

$$-CF_2-CF(CF_3)-\dot{C}H_2 \quad (i); \qquad -CF_2-CF(CF_3)-\dot{C}F_2 \quad (j)$$

Scheme 2. Chemical structure of radicals possibly generated upon irradiation of p(VDF-co-HFP), due to either HFP units of VDF-HFP chaining.

The contribution of $\dot{C}F_3$ radical, as any gaseous species with low molecular weight, is neglected as its inner higher mobility and reactivity compared to macromolecular species would make it react rapidly. Moreover, such radical would present a signal with a HSC value of 14.6 mT corresponding to 3 α-fluorine[21] ; the corresponding signal would be a quadruplet, and its overall linewidth would be larger than 43.8 mT. This signal is absent from the spectrum. Moreover, as only 1 radical remains every 1400 units, the probability to find a radical localized on the end chain (initiator structure) is also low, and thus no other species will be considered. For the same reason, as the part of -CF_2-$CF(CF_3)$-CF_2- HFP-VDF addition sequence represents less than 8 % of the total sequences as determined by ^{19}F NMR, the probability for radicals (b), (d), (f) and (j) to be formed is relatively low and their contribution to the ESR response can reasonably be neglected as a first approximation.
The contribution of radical (i) may be also neglected as the probability to find an end chain radical $\dot{C}H_2$ beside a HFP unit is roughly equal to the probability to find an HFP unit in a polymer chain that is less than 2.65 %.

Furthermore, Iwasaki et al.[22,23] found that the tertiary-carbon radical (f) formed upon irradiation at low temperature (77K) is converted into radical (d) by a thermally process (Figure 3). They observed the same phenomenon for perhydrogenated radical.[24] We can consider that the same process occurs for radicals (c) and (e), such that only one species such as (c) can reasonably be accounted.

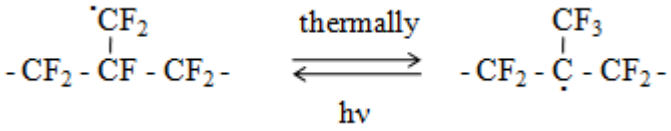

Figure 3. Thermal and photoconversion of fluorocarbon radical.[22]

At this stage, four radicals (a), (c), (g) and (h) still remain. A look on the stability of each radical can help to discriminate some of them. The electronic distribution of radical (a) and (h) is highly localized on the carbon bearing the radical, with the presence of hydrogen atoms on β position, when compared to other species (such as (g)) bearing fluorine in β position. Their reactivity is therefore anticipated to be more important, and as a starting point we will consider them as negligible. Thus, only species (c) and (g) will be first considered.
To determine the ESR parameters for species (c), we can refer to the pioneering work from Iwasaki and Toriyama[23] who pointed out the particular effect of the free rotating CF_3 group on their work on species (d). In our case, we neglected the contribution of the latter radical, based on the relative low part of the corresponding chain sequence as determined by ^{19}F NMR. They studied the formation of the tertiary carbon radical (d), bearing 3 F on β position on the fluoromethyl group and 4 F on β position along the backbone. They simulated its ESR spectrum, considering as a first approximation all the seven F nuclei as equivalent with a corresponding HSC of 2.85 mT. They refined the

simulation by taking into accounts the freely rotating CF_3 group, by considering a smaller β HSC. The reported values were $a_\beta(2F)$ = 3.3 mT for the CF_2 group and $a_\beta(3F)$ = 2.3 mT for the CF_3 one, respectively. The corresponding perhydrogenated radical, principally formed upon irradiation of polypropylene, was studied by Klimova et al.[25,26] A HSC for seven equivalent hydrogen atoms in β position was found to be 2.3 mT.

Back to radical (c), and based on our previous simplification to range HSC for radicals generated in PVDF,[9] we can expect an increase of both the β-coupling of fluorine nuclei at the expense of the β coupling of hydrogen. Moreover, β coupling of the two fluorine nuclei of the CF_2 group should be higher than the value of 4.3 mT which is the one obtained for radical (II).[9, 15] Thus, values for β coupling around 4.3 mT, 2.3 mT and 1.5 mT for CF_2, CF_3 and CH_2 groups respectively could be anticipated. Gaussian lineshape as well as a linewidth of 1.7 mT were considered as for any mid-chain radicals generated onto PVDF.[9] A lack of data subsists for the order of g value. This parameter will be left adjustable with the simulation, but a value close to the one obtained for fluoroalkyl radicals (around 2.003) is expected.

Regarding species (g), simulating parameters had not been reported in the literature, even if several works[21,27] with similar radicals were studied in the case of perfluoroalkanes. However, HSC values are not available for such a CF_3 group. Kispert et al.[28] gives the HSC for the CF_3-$\dot{C}F$-$CONH_2$ radical with 1 F on α position and 3 F atoms in β position. Even if the latter radical is quite different from the conventional fluorinated ones which are addressed in VDF-based copolymers, it is interesting to have the order of magnitude for such CF_3 group in β-position in terms of HSC. The given values were actually 7.4 mT for 1 F in α position and 2.23 mT for 3 F in β position, respectively. In the case of end-chain radical (g), the CF_2 neighboring group will more readily attract the free electron when compared to the $CONH_2$ one. A slight decrease of the HSC for CF and CF_3 group is anticipated while the HSC for the new fluoromethylene group should be in the range of tabulated value available in literature,[21,26-32] i.e. 3.0 mT. A Gaussian lineshape with a linewidth of 1.0 mT, as for end-chain radicals (IV) and (V), was used to start the simulation and no restriction was affected to g-value. As a conclusion, the five radicals obtained for PVDF homopolymer with the additional contribution of radicals (c) and (g) were considered for fitting the experimental ESR spectrum obtained in the case of p(VDF-co-HFP) copolymer. The starting parameters fed into the simulation using WinSim[33] simulating program are reported in Table 1. The values used for PVDF were the ones previously reported. When a parameter was submitted to automatic adjustment, the starting value is provided on its side in parenthesis. The proportion of each species was initially evenly distributed (initial value of 14.3 %).

Table 1. Parameters used to fit the ESR signal of p(VDF-co-HFP) γ-irradiated at 150 kGy. The values used as starting variables as discussed in the text are provided in parenthesis.

Radical	Lineshape[a]	LW mT	HSC[b] mT	g factor	Intensity %
(I)	L	1.7	-	2.0046	7.4 (14.3)
(II)	G	1.7	*α (1H)* 2.3 ; *β (4F)* 4.25	2.0048	51.8 (14.3)
(III)	G	1.7	*α (1F)* 10.9 ; *β (4H)* 2.5	2.0036	14.9 (14.3)
(IV)	G	1.0	*α (2H)* 1.45 ; *β (2F)* 2.3	2.0037	24.1 (14.3)
(V)	G	1.0	*α (2F)* 10.7 ; *β (2H)* 0.5	2.0018	1.8 (14.3)
(c)	G	1.7 (1.7)	*β (2F)* 4.6 (4.5) ; *β (3F)* 2.0 (2.3) ; *β (2H)* 1.5 (1.0)	2.0027 (2.003)	30.1 (14.3)
(g)	G	1.2 (1.0)	*α(1F)* 4.9 (6.0) ; *β (3F)* 2.1 (2.2) ; *β (2F)* 2.8 (3.0)	2.0038 (2.003)	13 (14.3)

[a] L stands for Lorentzian and G for Gaussian; [b] Values for equivalent nuclei in same position.

Simulated and experimental ESR spectra are presented in Figure 4a. A very good fit quality obtained from the Spearman's rank correlation coefficient, ρ = 0.991, was obtained through the automatic adjustment of the parameters. The simulation residue has been estimated and is smaller than 3% (also presented in Figure 3a), and this signal could not be fitted by any other added signal. It is noteworthy that the signal due to irradiated quartz is not integrally removed from the experimental spectrum, as can be seen around 335 mT, and some part of the simulated spectrum still present differences with respect to experimental data and cannot be correlated in a better way. However, as reported for PVDF, taking into account coupling constants in γ-position did not lead to any improvement on the simulation spectrum (in terms of correlation coefficient/ data not shown).

Other fits including species (a) and (h) using the same starting positions established for species (c) and (g) were attempted. An even better Spearman's rank correlation coefficient was obtained, but the new fit was accompanied with meaningless values in terms of HSC parameters for the four HFP-based radicals, and their g values were out of the range corresponding to fluorocarbon-based radicals. Thus, simulation performed with less number of species, namely (c) and (g) ones, led to better results which were in good agreement with both the experimental spectra and the physical meaning of the resulting values. Moreover, HSC values resulting from the fit for species (c) and (g) are in good agreement with electron displacement driven by electronegativity. The linewidth of

radical (g) has slightly increased, meaning that its mobility is relatively lower[34] than the one obtained for end-chain radicals (IV) and (V), probably due to the bulky CF_3 group.

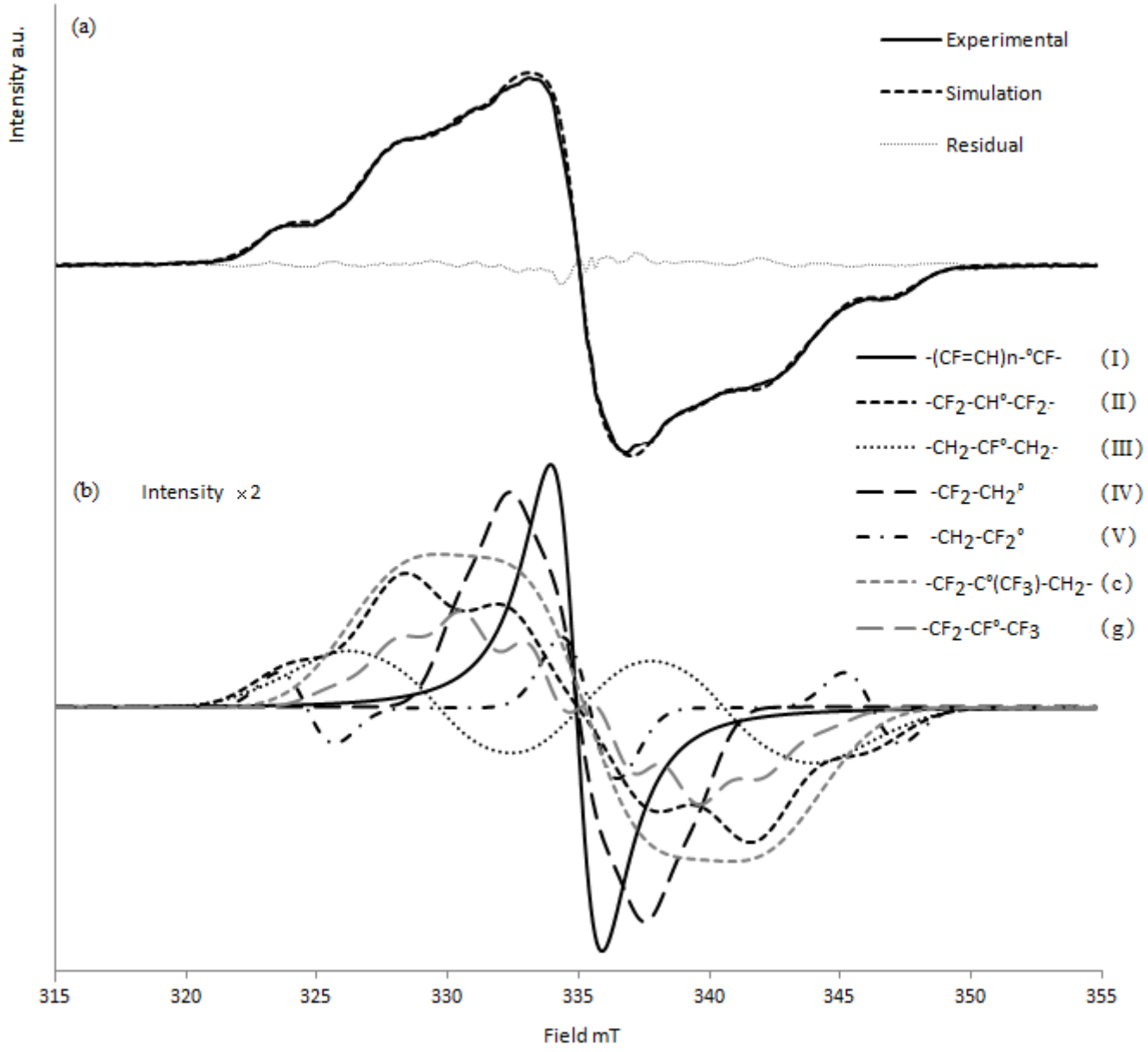

Figure 4. Experimental and simulated spectra of γ-irradiated p(VDF-co-HFP) powder (a). Species splitting (b); intensity is multiplied by a factor 2 and their proportions are given in percents.

The simulated signals obtained for each of the seven radicals are presented in Figure 3b. The consistency of the model can also be verified with regards to the relative concentration of each radical that reflects their chemical stability (values provided in Table 1). The rational is a higher stability for a higher delocalization of the electron along the carbon chain. A second source of stabilization is a lower statistic of recombination due to the radical localization (*i.e.* end-chain *vs* mid-chain). Indeed, it is well known that p(VDF-co-HFP), such as PVDF does, mainly suffers crosslinking compared to chain scission upon irradiation.[4]

Table 2. Sol-gel properties of PVDF and p(VDF-co-HFP) irradiated under argon.

	PVDF	p(VDF-co-HFP)			
Dose kGy	150	100	150	300	500
Gel content wt%	72	78	78	88	89
Solvent uptake wt%	1430	1170	980	520	490

In our conditions, the gel content, determined by sol-gel extraction with DMF, is higher than the one for PVDF irradiated in the same conditions (Table 2). This value is consistent with the higher mobility of the copolymer chains due to the lower degree of crystallinity.[1] Moreover, as determined by swelling measurements, the solvent uptake is lower for the p(VDF-co-HFP) copolymer, meaning that the crosslink is tighter than for PVDF. As a consequence, radicals embedded in polymer segments between two crosslinks such as mid-chain radicals are less mobile and provide lower statistics of recombination, therefore a higher stability, than end chain ones. These conclusions, which were settled for PVDF, also apply in the case of p(VDF-co-HFP) copolymer, as concentrations of radicals (II), (III) and (c) are higher than the ones for (IV), (V) and (g). Moreover, radicals centered on fluorinated carbon and resulting from VDF units are more reactive than their analogues centered on hydrogenated carbon. This is evidenced by a higher concentration of (II) versus (III) and also of (IV) versus (V) for mid-chain and end-chain radicals, respectively. Again comparing end-chain radicals versus mid-chain radicals, a higher concentration of (II) versus (IV), (III) versus (V) and (c) versus (g) is observed, consistently with their lower mobility. Regarding the radicals stemming from the HFP comonomer, the mid-chain radical (c) which is on a tertiary carbon surrounded by (CF_2) and (CF_3) electroattractive groups is highly stabilized and consequently less reactive. Moreover, the steric hindrance due to the trifluoromethyl group prevents the radical from any reaction, both reasons explaining the relatively high concentration of this species when compared to other (II) and (III) mid-chain radicals. For the same reasons, the end-chain radical (g) is also sterically and electronically more stabilized than species (IV) and (V), and its concentration is thus comparatively higher. Indeed, Forsythe et al.[5] qualified this species as a relatively non reactive-radical compared to traditional end-chain ones observed for fluorocarbons.

As a consequence the dominating species are mid-chain radicals (II) (IV) and (c), accounting for almost 70 % of the overall species. Interestingly, the polyenyl radicals which are considered as the most stable species because of the mesomeric effect represents less than 10 % of the overall radical species after irradiation. This can be explained by the irradiation dose used here (150 kGy) in comparison with the one needed to generate high concentration of polyenyl radicals (>500 kGy).[32]

While the HFP molar content is only 2.65 % for the given copolymer, HFP-based radicals stand for 43.1% of the overall radical concentration, confirming that they are much more stable than VDF-based radicals.

Following the example of Komaki et al.,[35] by assuming that radicals are regularly arranged in a cubic lattice of macromolecules and using an identical density of 1.78 $g.cm^{-3}$ for both PVDF and p(VDF-co-HFP), the radicals which remain after irradiation will occupy the volume of a cube which edge is 47.6 Å for PVDF and 44.3 Å for the copolymer. This means that the p(VDF-co-HFP) copolymer can accept a higher concentration of radicals than PVDF. In the case of poly(tetrafluoroethylene-co-hexafluoropropene) p(TFE-co-HFP), Hill et al.[36] suggested that the concentration of radicals increases while the composition of the copolymer is getting richer in HFP, due to the lower degree of crystallinity which implies a greater chain mobility and significantly limits cage recombination. From our results, not only the change in chain mobility impacts the respective concentrations of radicals but their relative stability is also an important parameter. Indeed, the percentage of HFP unit bearing a radical is about 1.16 % while for VDF units, this value falls down to 0.042 %. The latter value is slightly lower than the one obtained in pure PVDF, which is about 0.055 %. Noteworthy, the number of HFP units bearing a radical is 28 times greater than for VDF units, confirming that HFP-based radicals are much more stable.

The slight decrease of radicals generated in the VDF units in the copolymer is consistent with the gain in mobility, due to the presence of HFP units, thus inducing a lower degree of crystallinity. As a consequence, the gel content (78% *vs* 72%) and the solvent uptake (980% *vs* 1430%) as determined by sol-gel analyses prove that more polymer chains were cross-linked on the one hand, and that the crosslink is somehow tighter on the other hand in the case of p(VDF-co-HFP) copolymer. By the way, this is indirectly seen through the comparison of the concentrations of mid-chain radicals (II) and (III) between the two polymers, which are slightly lower in the case of the copolymer. These species are more likely to be involved in the crosslinking process as they are electronically less stabilized, and consequently slightly more reactive, than other mid-chains species such as (c).

Another comparison concerns polyenyl species (I), as their concentrations is not only determined through the ESR simulation model, but can also be indirectly probed by UV-visible spectroscopy.[6, 8, 37] Figure 5 presents the UV-vis spectra of both PVDF and p(VDF-co-HFP) polymers irradiated at 150 kGy. Two peaks, around 220 nm and 272 nm, can be seen which correspond to conjugated diene and triene structure.[8] Moreover, the peaks are slightly more intense for the copolymer than for PVDF, attesting for a higher concentration of conjugated species in the former polymer. This is in good agreement with the values resulting from the simulation of the experimental ESR spectra[6,8] (Respective concentration of polyenyl (I) radicals: 4.47 10^{17} $spin.g^{-1}$ for p(VDF-co-HFP) *vs* 3.86 10^{17} $spin.g^{-1}$ for PVDF).

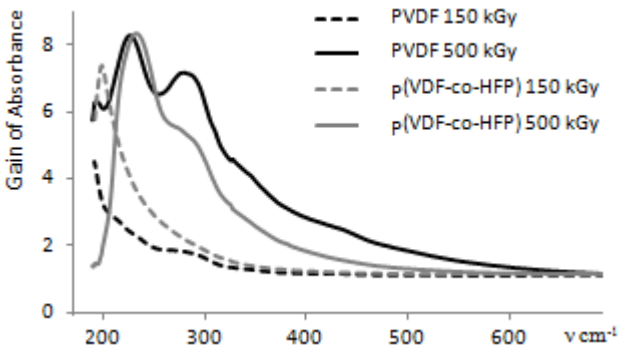

Figure 5. Gain of UV-visible absorbance of irradiated PVDF and p(VDF-co-HFP) for different radiation doses. Gains are calculated by the absorbance ratio of irradiated and unirradiated film samples.

III.2.3. Effect of irradiation dose.

The robustness of the simulation is tested on p(VDF-co-HFP) samples irradiated at different doses. As long as the radical species are identical, the experimental ESR spectra should be correctly fitted using the simulation model, and only the respective concentration of the species should vary. The influence of the radiation dose ranging from 100 to 500 kGy was first evaluated. The progressive change of ESR spectra is depicted in Figure 6a. (Normalized intensities are presented for a better comparison.) The first relevant information is the modification of the global shape of the signal as the dose increases. This progressive evolution reflects a change in the distribution of the radical species formed during the radiation process. The very center of the ESR spectra gradually increases at the expense of wings. The total concentration of free radicals as a function of dose is highlighted in Figure 6b. The radical concentration first increases with the radiation dose until it reaches a constant level. A threshold of highest radical concentration appears around 150 kGy. This result was previously reported by several authors.[21,38-41] The absolute value at the limit is slightly higher for p(VDF-co-HFP) compared to the PVDF homopolymer, reflecting again a higher stability of free radicals. The presence of a threshold limit has already been reported for many polymers, and is related to the balance between the generation of radicals and termination reactions occurring all along the irradiation process, which is all the more facilitated than the polymer continuously crosslinks upon irradiation.[15]

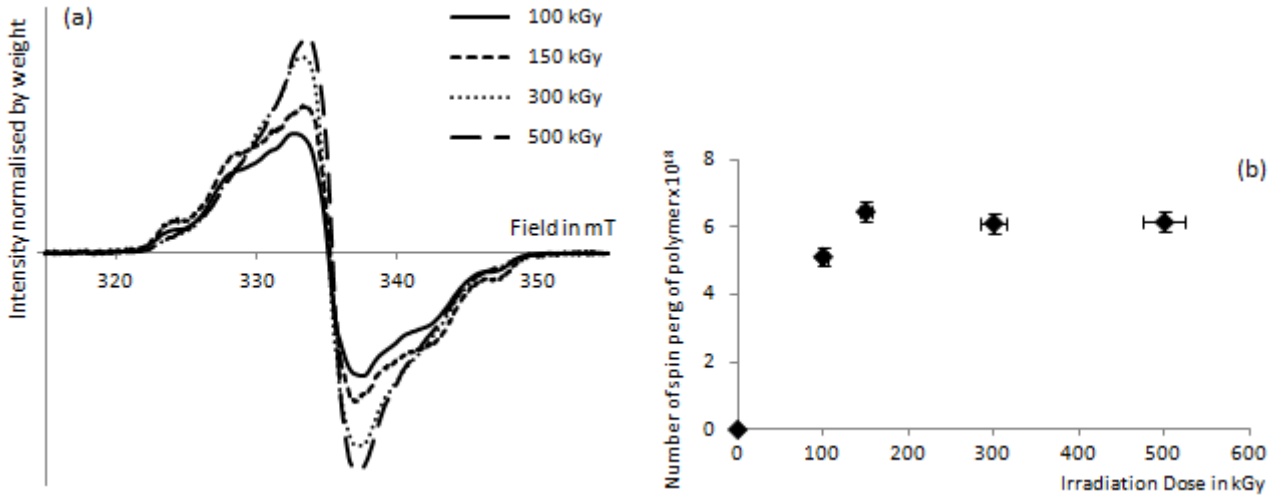

Figure 6. a) ESR spectra of γ-irradiated high molecular weight p(VDF-co-HFP) under anaerobic conditions for different doses – Intensity normalized by sample weight. (b) Concentration of radicals as a function of radiation dose.

The ESR simulation model was applied to the experimental ESR spectra obtained for different doses, and the only adjustable parameters were the relative percentages of each species. Simulations correlate very well the experimental data (Figure S4). Some small deviations are noticed at the center of the spectra, with a higher residual when compared to signal intensity, while the simulation curves correlate well with experimental data on the wings. The imperfect subtraction of the signal from irradiated quartz tube and the high signal intensity on this spectral range explain the deviations. Residual signal cannot be fitted meaning that no more species are hidden in this signal. By the way, the part of the signal which is not considered in the fit, through quantization by integration of the residual in absolute value, remains low. The values are 3.9%, 3.0 %, 6.9 % and 4.8 % for radiation dose of 100 kGy, 150kGy, 300 kGy and 500 kGy respectively. At the same time, the Spearman's correlation rank coefficient for all considered simulations are greater than 0.99. Refining the spectroscopic parameters (such as hyperfine coupling constants, linewidth, lineshape or g-position variables) by the WinSim program[33] do not lead to any improvement, neither a lowering of the residual nor a significant increase of the correlation parameter.

Variation of each radical concentration as a function of radiation dose is presented in Figure 7. The concentration of mid-chain radicals carried by VDF units presents the same global trend than PVDF homopolymer[15] : while the concentration of polyenyl radicals (I) continuously increases with the dose, concentrations of radicals (II) and (III) increase until the threshold at 150 kGy is attained, then a sharp decrease is observed. While the concentration of end-chain radical (IV) was constant in the case of PVDF homopolymer whatever the dose,[15] the one observed for p(VDF-co-HFP) is sharply

increased between 150 kGy and 300 kGy. For HFP-based radicals, their concentration increases until the threshold in total concentration is reached, then a pseudo-plateau appears.

Regarding the polyenyl radicals (I), the only species which are not directly obtained by irradiation, their response contributes more to the overall shape of the ESR spectra, with a significant increase of the signal intensity at the field center. Polyenyl radicals are in fact known to be preferentially formed at high dose [42] at the expense of other ones.

The decrease observed for mid-chain radicals (II) and (III) is attributed to the higher crosslinking efficiency, with the increase of gel content and crosslinking density, as indirectly evidenced by sol-gel analyses through a lower solvent uptake (Figure 7 - Table 2). The latter phenomenon necessarily implies the consumption of such mid-chains species. Moreover, as radical (II) is stabilized by two highly electron-accepting fluoromethylene groups, the density of electron on the carbon bearing the radical is much lower than for radical (III), which density is highly localized on the fluoromethyne group: the latter is thus more reactive, and the decrease in terms of concentration is more pronounced. Interestingly, when looking at mid-chain radical (c) carried by a HFP unit, the profile is totally different and is related to its inner chemical stability induced by the CF_2 and CF_3 neighboring groups, associated to the steric hindrance of the rotating CF_3 group. Both these effects sharply lower the reactivity of this radical when compared to other mid-chains ones (II) and (III), and suggest that this species is not significantly taking part in the crosslinking during irradiation. Moreover, contrary to radicals (II) and (III) which generate radicals (I) by successive dehydrofluorination, radicals (c) cannot lead to polyenyl species as this reaction would imply elimination of F_2, a highly not favored reaction as it is highly endothermic.[27] As a result, the presence of HFP units well-distributed along the backbone reduces the rate of unsaturation for high dose when compared to PVDF. This was also confirmed by comparing the absorbance by UV-vis spectroscopy of films irradiated at 500 kGy (Figure 5): the absorbance of p(VDF-co-HFP) was lower at 275 nm (triene) and superior wavelength (upper-order unsaturations) than for PVDF.

Concentrations of end-chain radicals (g) slightly increase with the dose, until the plateau in concentration is reached, and then levels off. This is explained by the crosslinking efficiency which increases with dose until 300 kGy [43] and consequently reduces the end-chain mobility. Concentration of end-chain radical (V), the minor species obtained by irradiation, is very low whatever the dose, and keeps on decreasing with the dose. Indeed, this radical is highly reactive due the high localization of the electron on the fluoromethylene group.

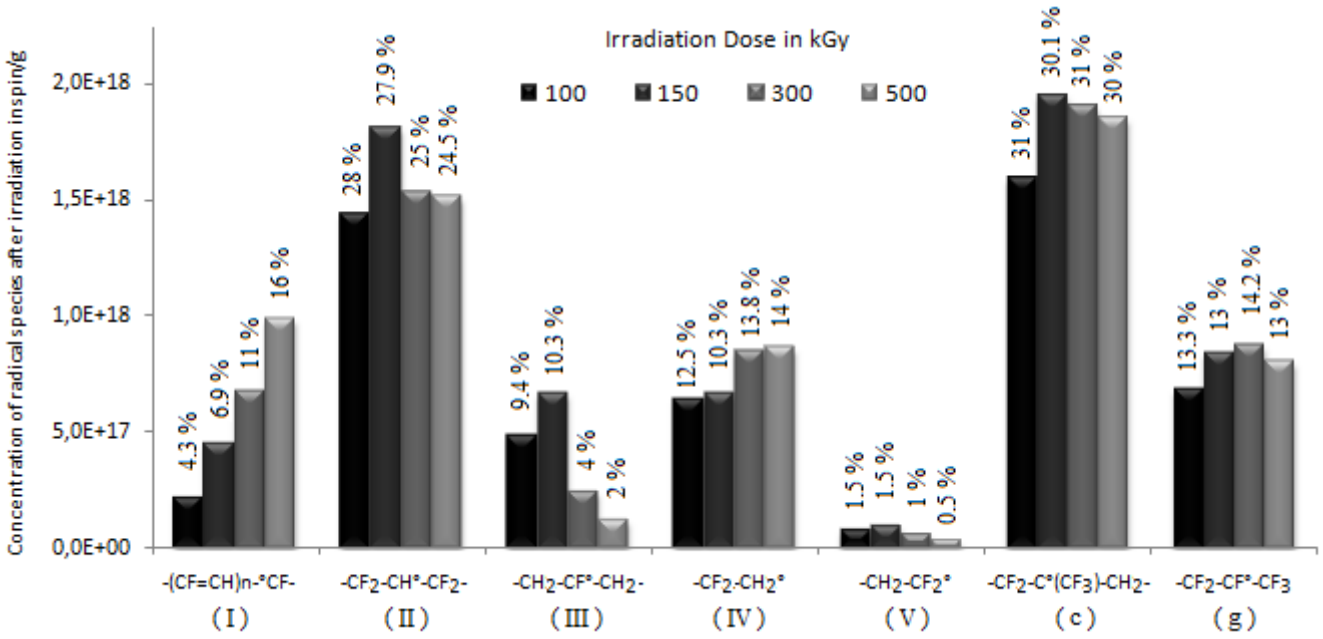

Figure 7. Detailed evolution of the concentration of each radical species with respect to radiation dose. The relative percentage of each species for a given dose is labeled.

III.2.4. Effect of annealing on radicals.

III.2.4.1. Irradiation dose of 150kGy.

The robustness of the ESR model was confirmed by first monitoring each radical concentration on p(VDF-co-HFP) samples irradiated at 150 kGy and subsequently annealed for different times at 373 K. This temperature is lower than the crystallization temperature (Tc = 388K, as determined by DSC), thus not affecting the degree of crystallinity of the polymers. The evolution of the ESR signals with the annealing time is shown in Figure 8a. The overall ESR signal is affected by the annealing time: the area globally decreases, which evidences a decrease of the overall radical concentration (Figure 8b). After 30 minutes, an apparent threshold value at around 1.10^{18} spin.g^{-1}, corresponding to ca. 16% of the initial concentration, is observed. This value is in the same order of magnitude than for PVDF annealed in the same conditions; these remaining radicals are expected to locate in the crystalline phase.[15] Moreover, the shape of the ESR signals changes along annealing, confirming a redistribution of radicals species. Simulation was performed on each experimental curve, using the ESR parameters gathered in Table 1 while only intensities were adjustment parameters. Acceptable fits were obtained, with associated Spearman's rank coefficient greater than 0.98 (Figure S5). Integration of the residual in absolute value is currently 4.83%, 5.43 % and 6.78% for annealing time of 10 min, 30 min and 60 min, respectively. These control parameters are slightly higher for annealed samples than for non-annealed samples, mainly due to the signal-to-noise ratio.

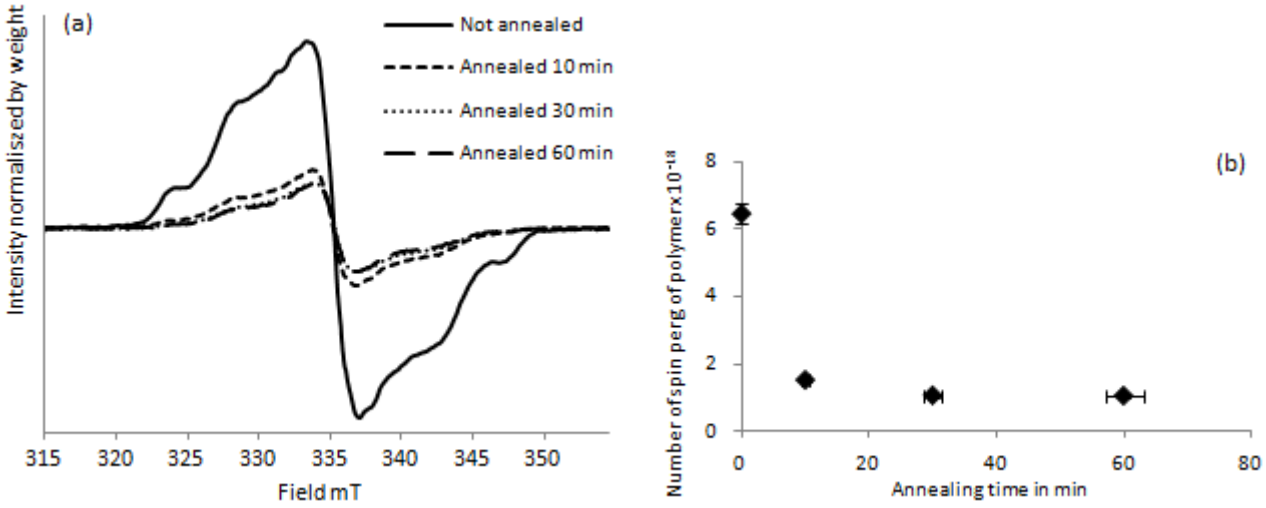

Figure 8. (a) ESR spectra obtained for p(VDF-co-HFP) irradiated at 150 kGy and annealed at 373 K for different durations. (b) Respective concentration of radicals for various annealing time.

Figure 9 presents the absolute concentration of each radical species as a function of annealing time. All concentrations decrease with annealing time, but polyenyl radicals between 30 min and 60 min of annealing, which suggests that they are formed to the expense of other radicals (mainly (II) and (III)). Species (III) and (V) almost disappeared, confirming that α-fluoro radicals based on VDF units represent the most reactive mid-chain and end-chain ones obtained by irradiation. Interestingly, decrease profile of radicals (II) resembles the one of radicals (IV), with respective concentration ratios being almost constant whatever the annealing time. This suggests that their reactivity is comparable, thus than chemical consideration (α-hydrogen radicals) prevails on mobility concern for this type of radicals. The highly stabilized tertiary radical (c) presents the slowest decay profile of all radicals directly obtained by irradiation (thus excluding polyenyl), which confirms its high stability. The decay profile of perfluorinated end-chain radical (h) is also pronounced, which evidence kind of reactivity upon annealing at high temperature, while its initial concentration suggested a relatively high stability. The gain in mobility at elevated temperature in this particular case prevails on the chemical stability afforded by the electron-acceptor character of the neighboring (CF_2) and (CF_3) groups. Moreover, its reactivity is rather more promoted by an elevation of temperature than the one of the other end-chain radical (IV); both information suggest that the relative high concentration (as determined before annealing) for radical (h) is mainly explained by the steric hindrance of the bulky CF_3 group, which limits recombination at low temperature.

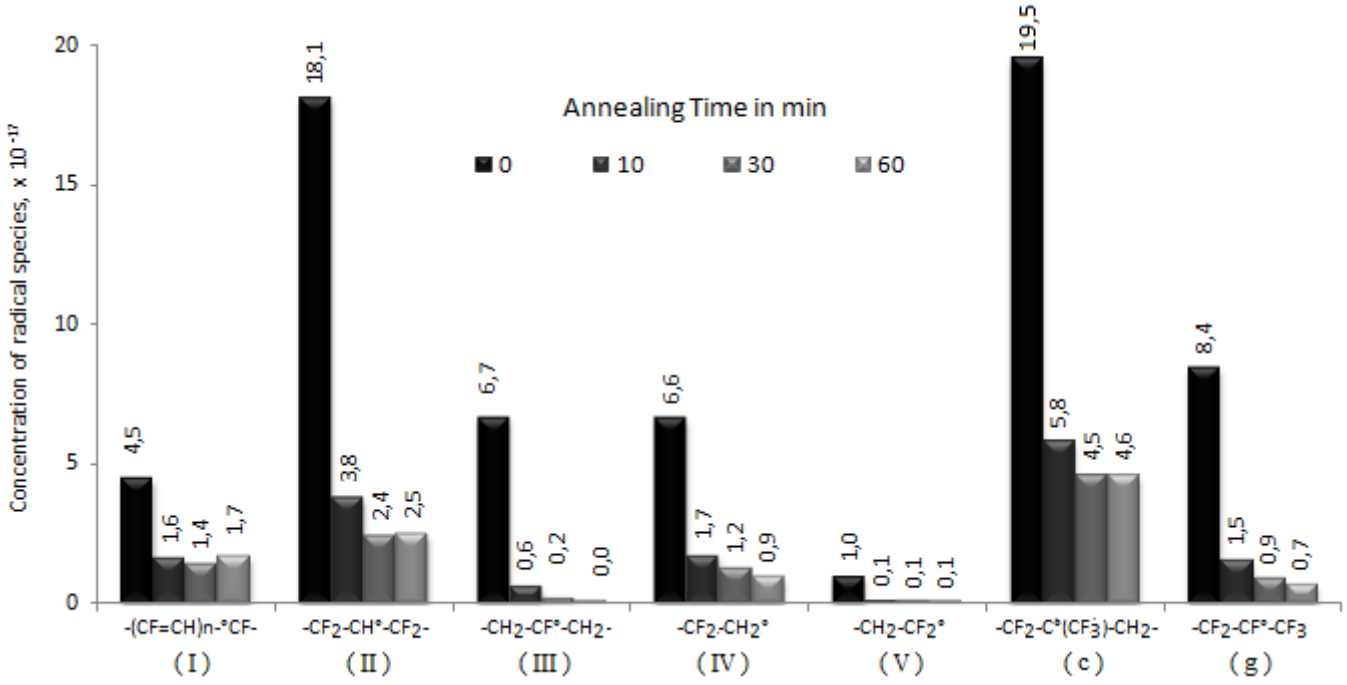

Figure 9. Evolution of the concentration of surviving radicals as a function of annealing time.

By the light of all the results above, based on the respective concentration of radicals generated by irradiation (at room temperature) on the one hand, and their remaining concentration after annealing (at elevated temperature) on the other hand, an ordering of radicals with increasing stability is proposed (scheme 4). Two important aspects, namely the chemical structure (atoms in α and β positions with respect to the radical) and the intrinsic mobility (mid-chain *vs* end-chain) including steric hindrance are taken into account.

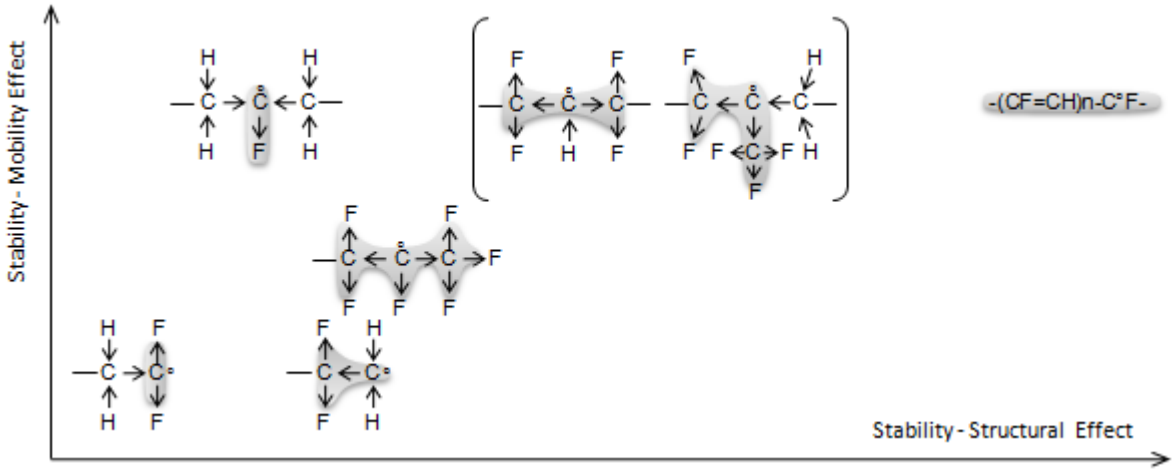

Scheme 4. Proposal of radical reactivity ranking depending on both chain motion and structural effect. Inductive effect is represented by arrow and corresponding attraction of the free electron highlighted in grey.

III.2.4.2. Combined effect of Annealing and Radiation Dose

In this last part, the effect of annealing at 373 K on samples priory irradiated at different dose is discussed. For each dose, the evolution of the ESR signals with the annealing time follows the same trend as the one reported above for 150 kGy : the concentration of radicals rapidly decreases until 30 minutes, and then stabilizes at a constant value. Moreover, the shape of the ESR signals is also affected until 30 minutes, then the spectra are superimposed. The results obtained after 60 minutes of annealing can be compared, firstly in terms of ESR shape (Figure 10a) and in terms of corresponding concentrations of radicals (Figure 10b). As can be seen, the spectra differ in both shape and area. An increase of radical concentration is first observed (until 300 kGy) before a pseudo-plateau appears, which concentration of remaining radicals represents around 25% of initial one at the given dose. The profile resembles the one previously encountered for PVDF, and was attributed to the different crosslinking density and gel content of the samples prior to annealing.[15] The results obtained with sol-gel analyses conducted in DMF (Figure 4) prove that the same reasons apply in the case of p(VDF-co-HFP): diffusion of radical [42] is hindered by crosslinked segments which consequently affect alkyl radical recombination.

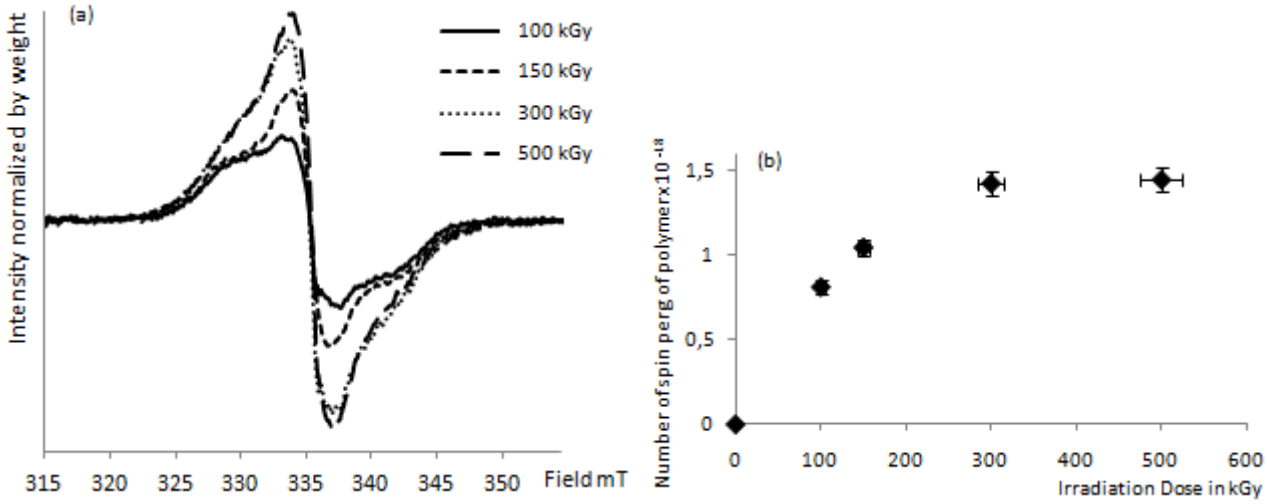

Figure 10. (a) Comparison of the first-derivative ESR spectra of p(VDF-co-HFP) γ-irradiated followed by an annealing of 60 min at 373 K for several radiation doses – Intensity normalized by sample weight. (b) Total amount of surviving radical per gram of polymer after the annealing as a function of dose.

When looking at the differences between the spectra, the signal at the center of the field scale (characteristic of polyenyl species (I)) is increased to the expense of the wings: this proves that the relative part of these radicals as well as their concentration are getting higher as the initial dose to which the sample was priory irradiated is high. This was confirmed by the concentration resolved by applying the simulation model to the experimental spectra obtained for samples annealed for 60

minutes at 373K. The simulated spectra are correctly fitting the experimental curves, as confirmed by Spearman's rank correlation average correlation parameters that are always greater than 0.98 (Figure S6). Integration of the residual in absolute value are slightly higher than for non-annealed samples, and comprised between 6.5 % and 7.5%. The comparison of each radicals concentration between the samples is presented in Figure 11. This graph confirms the significant increase of polyenyl radicals. Moreover, radicals (III) and (V) almost totally disappeared from the annealed sample. Independently of initial radiation dose, the parts of very stable end-chain radicals such as (IV) and (g) are almost constant, showing that they are not taking part of further rearrangement and crosslinking reactions occurring upon annealing.[15] This means that they are dangling chains that can no longer react. Actually, the consumption of these species necessarily implies a termination reaction through combination and not a disproportionation.

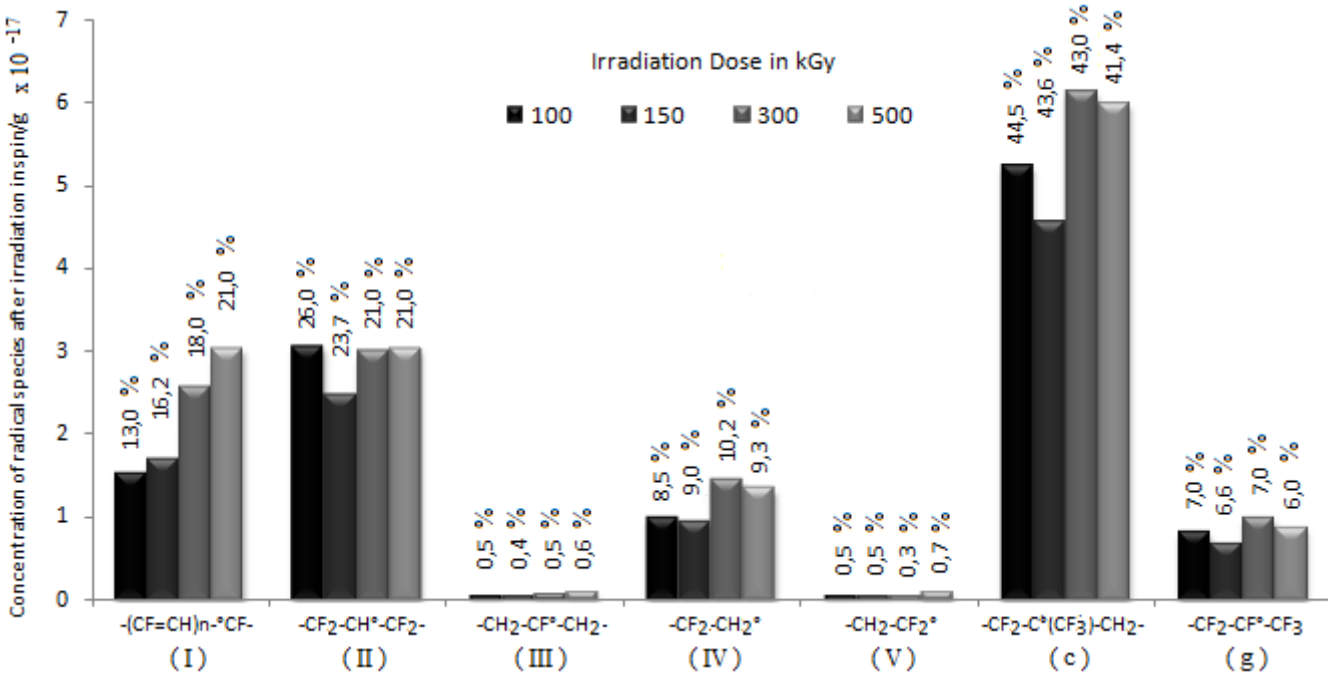

Figure 11. Evolution of the concentration of each radical remaining in p(VDF-co-HFP) irradiated at different doses and annealed at 373K during 60 min. The relative percentage of each species for a given dose is labeled.

CONCLUSION

The principal aim of this work was to study the nature of radicals formed during the γ-radiolysis of p(VDF-co-HFP). An ESR simulation model elaborated for the PVDF homopolymer has successfully been expanded to the case of this copolymer, by adding only two radical species which structure are related to HFP units. The ESR signals of each species have been isolated and have opened the possibility to probe their respective concentration upon a change of radiation dose or annealing. These studies were also used to test the robustness of the simulation. The model allows to emphasize that the stability of an entity depends on both its chemical environment and also its location, and that it can be modified during radiolysis by the formation of crosslinking. Additionally, a ranking of radical stability have been proposed depending on both these factors.

REFERENCES

1. Lovinger, A. J. Poly(vinylidene fluoride). In *Developments in crystalline polymers;* Bassett, D. C., Ed.; Elsevier Applied Science Publishers: London, 1982; Vol. 1, p 195.
2. Ameduri, B. From Vinylidene Fluoride (VDF) to the Applications of VDF-Containing Polymers and Copolymers: Recent Developments and Future Trends. *Chemical reviews* **2009,** *109* (12), 6632-6686.
3. Tournut, C. *Thermoplastic Copolymers of Vinylidene Fluoride in: Modern Fluoropolymers: High Performance Polymers for Diverse Applications;* John Wiley & Sons, Ltd. (UK): Chichester, New York, Weinheim, Brisbane, Singapore, Toronto, 1997; pp 577-597.
4. Lyons, B. J. Radiation Crosslinking of Fluoropolymers – A Review. *Radiation Physics and Chemistry* **1995,** *45* (2), 159-174.
5. Forsythe, J. S.; Hill, D. J. T. Radiation chemistry of fluoropolymers. *Progress in Polymer Science* **2000,** *25* (1), 101-136.
6. Kasser, M. J.; Silverman, J.; Al-Sheikhly, M. EPR Simulation of Polyenyl Radicals in Ultrahigh Molecular Weight Polyethylene. *Macromolecules* **2010,** *43* (21), 8862-8867.
7. Rosenberg, Y.; Siegmann, A.; Narkis, M.; Shkolnik, S. Low Dose γ-Irradiation of some Fluoropolymers: Effect of Polymer Chemical Structure. *Journal of Applied Polymer Science* **1992,** *45* (5), 783-795.
8. Makuuchi, K.; Masaharu, A.; Toshihiko, A. Effect of Evolved Hydrogen Fluoride on Radiation-Induced Crosslinking and Dehydrofluorination of Poly(vinylidene Fluoride). *Journal of Polymer Science. Polym Chemistry Edition* **1976,** *14* (3), 617-625.
9. Dumas, L.; Albela, B.; Bonneviot, L.; Portinha, D.; Fleury, E. Electron Spin Resonance Quantitative Monitoring of Five different Radicals in γ-Irradiated Polyvinylidene Fluoride. *Submitted*.
10. Helbert, J. N.; Wagner, B. E.; Poindexter, E. H.; Kevan, L. Matrix ENDOR of polyenyl radicals in polymers. *Journal of Polymer Science: Polymer Physics Edition* **1975,** *13* (14), 825–834.
11. Ohnishi, S. I.; Ikeda, Y.; Sugimoto, S. I.; Nitta, I. On the ESR Singlet Spectra Frequently Observed in Irradiated Polymers at a Large Dose. *Journal of Polymer Science* **1960,** *47* (149), 503-507.
12. Seguchi, T.; Tamura, N. Electron Spin Resonance Studies on Radiation Graft Copolymerization. I. Grafting Iniated by Alkyl Radicals Trapped in Irradiated Polyethylene. *Journal of Polymer Science : Polymer Chemistry Edition* **1974,** *12* (18), 1671-1682.
13. Goslar, J.; Hilczer, B.; Smogor, H. Radiation-Induced Modification of p(VDF/TrFe) Copolymers Studied by ESR and Vibrational Spectroscopy. *Applied Magnetic Resonance* **2008,** *34* (1-2), 37-45.
14. Goslar, J.; Hilczer, B.; Smogor, H. ESR Studies of Fast Electron Irradiated Ferroelectric Poly(Vinylidene Fluoride). *Acta Physica Polonica A* **2005,** *108* (1), 89-94.
15. Dumas, L.; Albela, B.; Bonneviot, L.; Portinha, D.; Fleury, E. Effect of dose and subsequent annealing on

radicals distribution in γ-irradiated PVDF as quantitatively monitored by ESR: correlation between network features and radical type. *Submitted*.

16. Fortin, N.; Albela, B.; Bonneviot, L.; Rouif, S.; Sanchez, J.-Y.; Portinha, D.; Fleury. E. How does γ-irradiation affect the properties of a microfiltration membrane constituted of two polymers with different radiolytic behaviour? *Radiation Physics and Chemistry* **2012,**.*81* (3), 331-338
17. Pianca, M.; Bonardelli, P.; Tato, M.; Cirillo, G.; Moggi, G. Composition and sequence distribution of vinylidene fluoride copolymer and terpolymer fluoroelastomers. Determination by 19F nuclear magnetic resonance spectroscopy and correlation with some properties. *Polymer* **1987,** *28* (2), 224-230.
18. Murasheva, Y. M.; Shashkov, A. S.; Galil-Ogly, F. A. Analysis of 19F NMR Spectra of Viinylidene Fluoride-Trifluorochloroethylene Copolymers. *Polymer Science U.S.S.R. A.* **1979,** *21* (4), 968-974.
19. Murasheva, Y. M.; Shashkov, A. S.; Dontsov, A. A. Analysis of the 19F NMR spectra of copolymers of vinylidene fluoride with tetrafluoroethylene, and of vinylidene fluoride with tetrafluoroethylene and hexafluoropropylene. The use of an empirical additive scheme and of the principle of alternation. *Polymer Science U.S.S.R. A.* **1981,** *23* (3), 711-720.
20. Isbester, P. K.; Brandt, J. L.; Kestner, T. A.; Munson, E. J. High-Resolution Variable-Temperature ^{19}F MAS NMR Spectroscopy of Vinylidene Fluoride Based Fluoropolymers. *Macromolecules* **1998,** *31* (23), 8192-8200.
21. Allayarov, S. R.; Konovalikhin, S. V.; Olkhov, Y. A.; Jackson, V. E.; Kispert, L. D.; Dixon, D. A.; Ila, D.; Lappan, U. Degradation of γ-irradiated linear perfluoroalkanes at high dosage. *Journal of Fluorine Chemistry* **2007,** *128* (6), 575-586.
22. Iwasaki, M.; Toriyama, K. Photoinduced and Thermal Radical Conversions in γ-Irradiated Copolymers of Tetrafluoroethylene and Hexafluoropropylene as Studied by Electron Spin Resonance. *The Journal of Chemical Physics* **1967,** *47* (2), 559-563.
23. Iwasaki, M.; Toriyama, K.; Sawaki, T.; Inoue, M. Electron Spin Resonance of γ-Irradiated Tetrafluoroethylene-Hexafluoropropylene Copolymers. *The Journal Of Chemical Physics* **1967,** *47* (2), 554-559.
24. Iwasaki, M.; Toriyama, K. ESR study on the photoinduced isomerization of the tert- to isobutyl radical in γ-irradiated isobutyl bromide. *The Journal of Chemical Physics* **1967,** *46* (7), 2852-2853.
25. Klimova, M.; Tino, J.; Borsig, E.; Ambrovic, P. The Effect of Crosslinking on the Reactivity of Free Radicals in Isotactic Polypropylene. *Journal of Polymer Science: Polymer Physics Edition* **1985,** *23* (1), 105-111.
26. Kuzuya, M.; Ito, H.; Kondo, S. I.; Noda, N.; Noguchi, A. Electron Spin Resonance Study of the Special Features of Plasma-Induced Radicals and Their Corresponding Peroxy Radicals in Polytetrafluoroethylene. *Macromolecules* **1991,** *24* (25), 6612-6617.
27. Allayarov, S. R.; Gordon, D. A.; Kim, I. P. Radiolysis of n-perfluoroalkanes and polytetrafluoroethylene. *Journal of Fluorine Chemistry* **1999,** *96* (1), 61-64.
28. Kispert, L. D.; Rogers, M. T. Temperature dependence of the ESR spectrum of $CO_2^-CF_2CFCO_2^-$ in irradiated sodium perfluorosuccinate. *The Journal of Chemical Physics A* **1977,** *54* (8), 3326-3335.
29. Siegel, S.; Hedgpeth, H. Chemistry of Irradiation Induced Polytetrafluoroethylene Radicals: I. Re-examination of the EPR Spectra. *The Journal of Chemical Physics* **1967,** *46* (10), 3904-3912.
30. Matsugashita, T.; Shinohara, K. Electron Spin Resonance Studies of Radicals Formed in Irradiated Polytetrafluoroethylene. *The Journal Of Chemical Physics* **1961,** *35* (5), 1652-1656.
31. Allayarov, S. R.; Mikhailov, A. I.; Barkalov, I. M. Analysis of the ESR Spectra of the ~CF_2CFCF_2~ Macroradical Trapped in a γ-Irradiated Polytetrafluoroethylene Matrix at 77 K. *High Energy Chemistry* **2000,** *34* (3), 141-144.
32. Shiotani, M.; Persson, P.; Lunell, S.; Lund, A.; Williams, F. Structures of Tetrafluorocyclopropene, Hexafluorocyclobutene, Octafluorocyclopentene and Related Perfluoroalkene Radical Anions Revealed by Electron Spin Resonance Spectroscopic and Computational Studies. *The Journal of Physical Chemistry A* **2006,** *110* (19), 6307-6323.
33. Duling, D. R. Simulation of Multiple Isotropic Spin Trap EPR Spectra. *Journal of Magnetic Resonance, Series B* **1994,** *104* (2), 105-110.
34. Gerson, F.; Huber, W. *Electron Spin Resonance Spectroscopy of Organic Radicals;* WILEY-VCH Verlag GmbH & Co. KGaA: Weinheim, 2003.

35. Komaki, Y.; Ishikawa, N.; Morishita, N.; Takamura, S. Radicals in heavy ion-irradiated polyvinylidene fluoride. *Radiation Measurements* **1996,** *26* (1), 123-129.
36. Hill, D. J. T.; Mohajerani, S.; Pomery, P. J.; Whittaker, A. K. An ESR study of the radiation chemistry of poly(tetrafluoroethylene-co-hexafluoropropylene) at 77 and 300 K. *Radiation Physics and Chemistry* **2000,** *59* (3), 295-302.
37. Waterman, D. C.; Dole, M. Ultraviolet and infrared studies of free radicals in irradiated polyethylene. *Journal of Physical Chemistry A.* **1970,** *74* (9), 1906-1912.
38. Kuzuya, M.; Niwa, J.; Noguchi, T. Electron spin resonance study on plasma-induced surface radicals of ethylene-tetrafluoroethylene copolymer. *Polymer Journal A.* **1995,** *27* (3), 251-255.
39. Mitov, S.; Hübner, G.; Brack, H. P.; Scherer, G. G.; Roduner, E. In situ Electron Spin Resonance Study of Styrene Grafting of Electron Irradiated Fluoropolymer Films for Fuel Cell Membranes. *Journal of Polymer Science: Part B: Polymer Physics* **2006,** *44*, 3323-3336.
40. Palacio, O.; Aliev, R.; Burillo, G. Radiation Graft Copolymerization of Acrylic Acid and N-Isopropylacrylamide from binary mixtures onto Polytetrafluoroethylene. *Polymer Bulletin A.* **2003,** *51* (3), 191-197.
41. Li, J.; Sato, K.; Ichiduri, S.; Asano, S.; Ikeda, S.; Iida, M.; Oshima, A.; Tabata, Y.; Washio, M. Pre-irradiation induced grafting of styrene into crosslinked and non-crosslinked polytetrafluoroethylene films for polymer electrolyte fuel cell applications. I: Influence of styrene grafting conditions. *European polymer journal A.* **2004,** *40* (4), 775-783.
42. Aymes-Chodur, C.; Esnouf, S.; Le Moël, A. ESR STudies in γ-irradiated and PS-Radiation-Grafted Poly(vinyldene fluoride). *Journal of Polymer Science: Part B: Polymer Physics* **2001,** *39*, 1437-1448.
43. Dargaville, T. R.; Celina, M.; Clough, R. L. Evaluation of vinylidene fluoride polymers for use in space environments : Comparison of radiation sensitivities. *Radiation Physics and Chemistry* **2006,** *75* (3), 432-442.

SUPPORTING INFORMATION

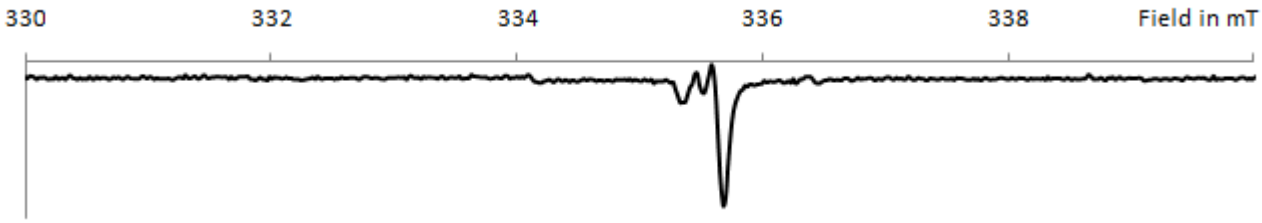

Figure S1. ESR signal of irradiated tube in quartz.

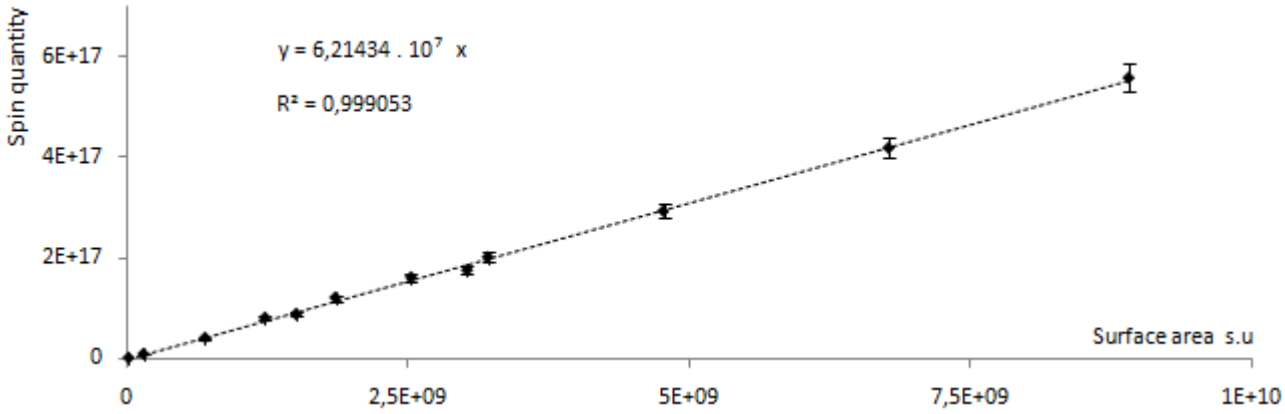

Figure S2. Calibration curve determined using DPPH as a standard showing correspondence of spin quantity with surface area determined after the double integration process.

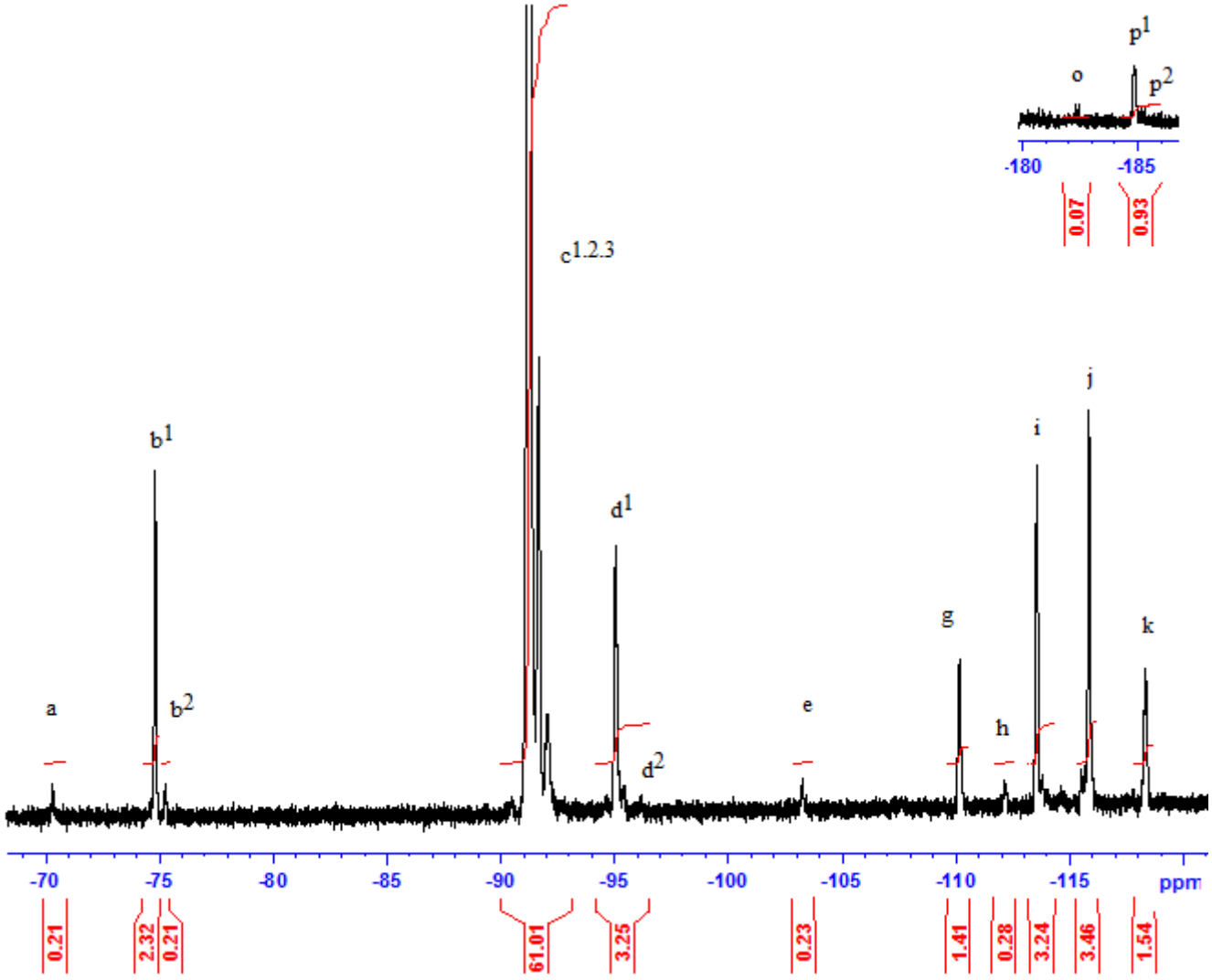

Figure S3. ^{19}F NMR spectrum of the unirradiated p(VDF-co-HFP).

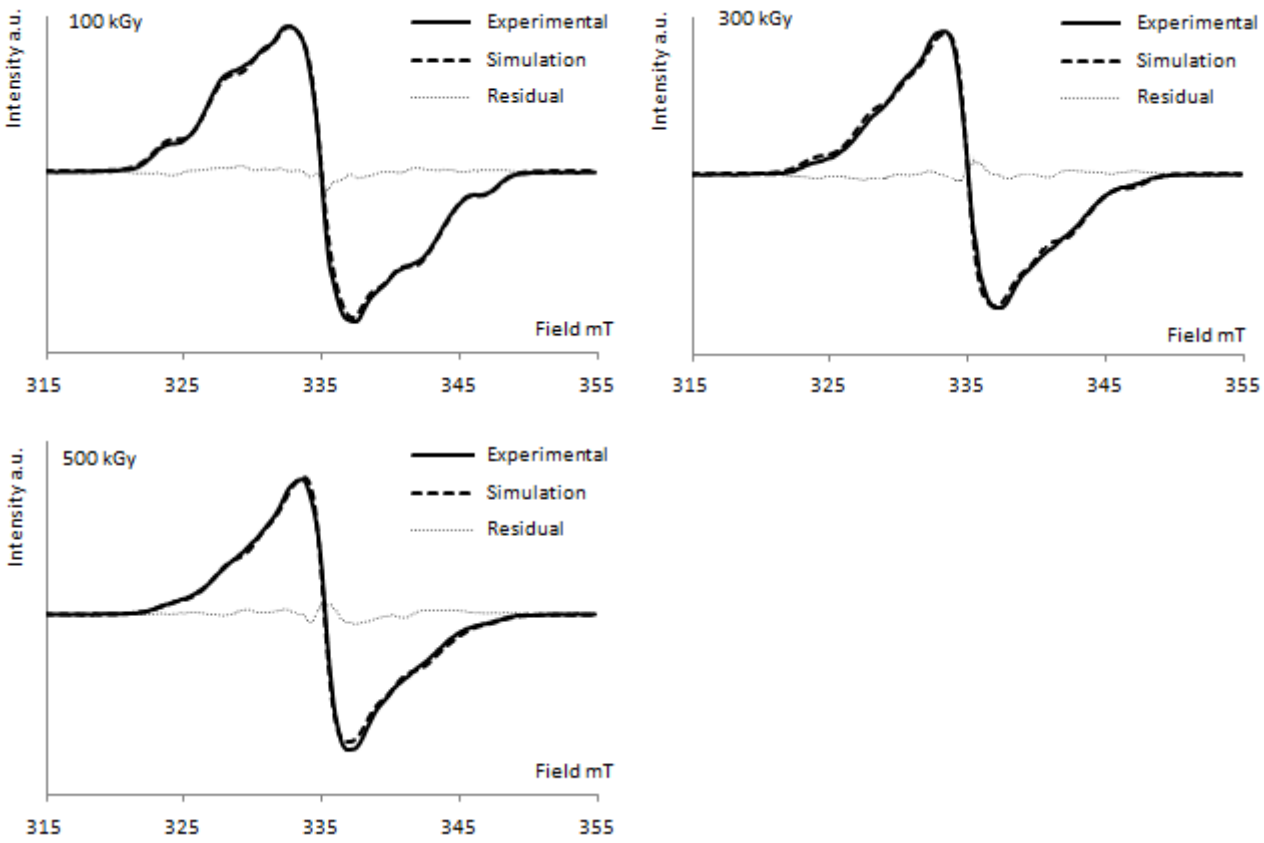

Figure S4. Experimental and simulated spectra of γ-irradiated p(VDF-co-HFP) at 100 kGy, 300 kGy, 500 kGy and their corresponding residual

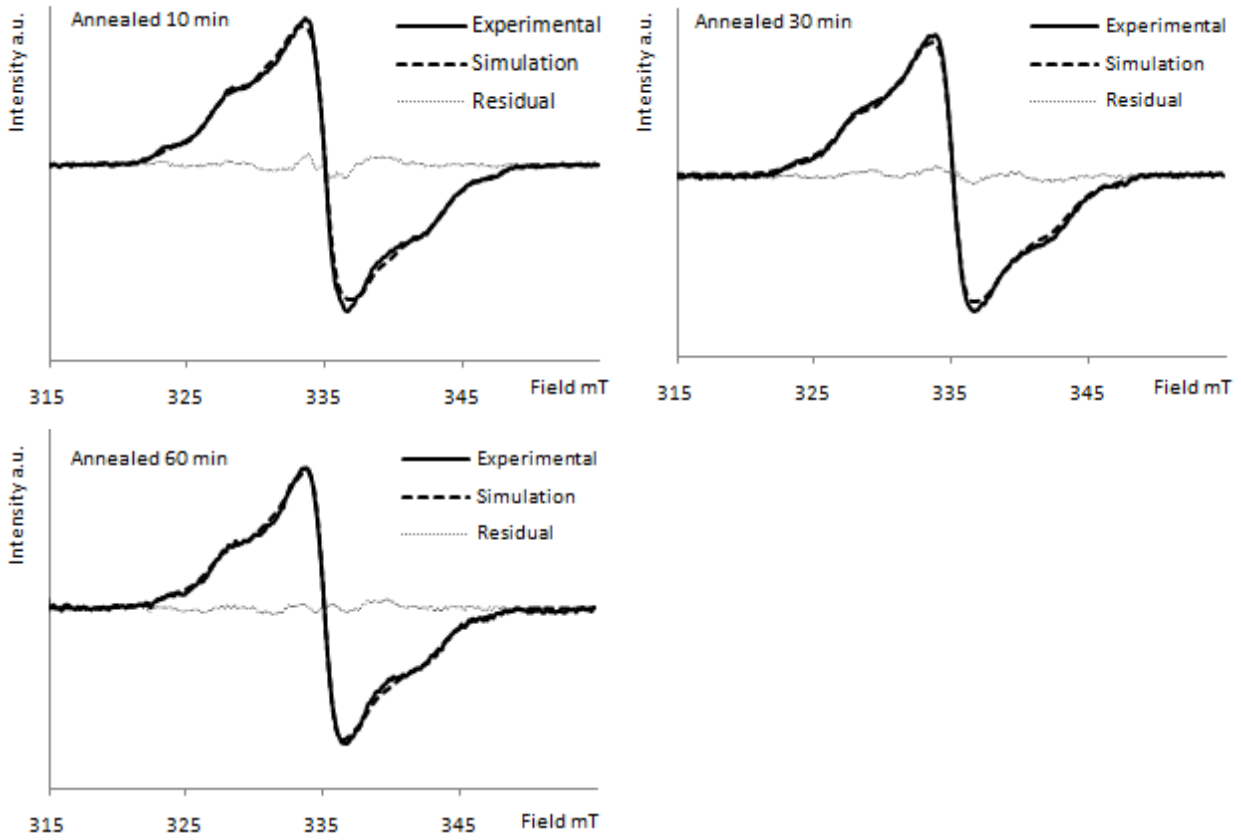

Figure S5. Experimental and simulated spectra of γ-irradiated p(VDF-co-HFP) at 150 kGy annealed at 373 K during 10, 30 and 60 min.

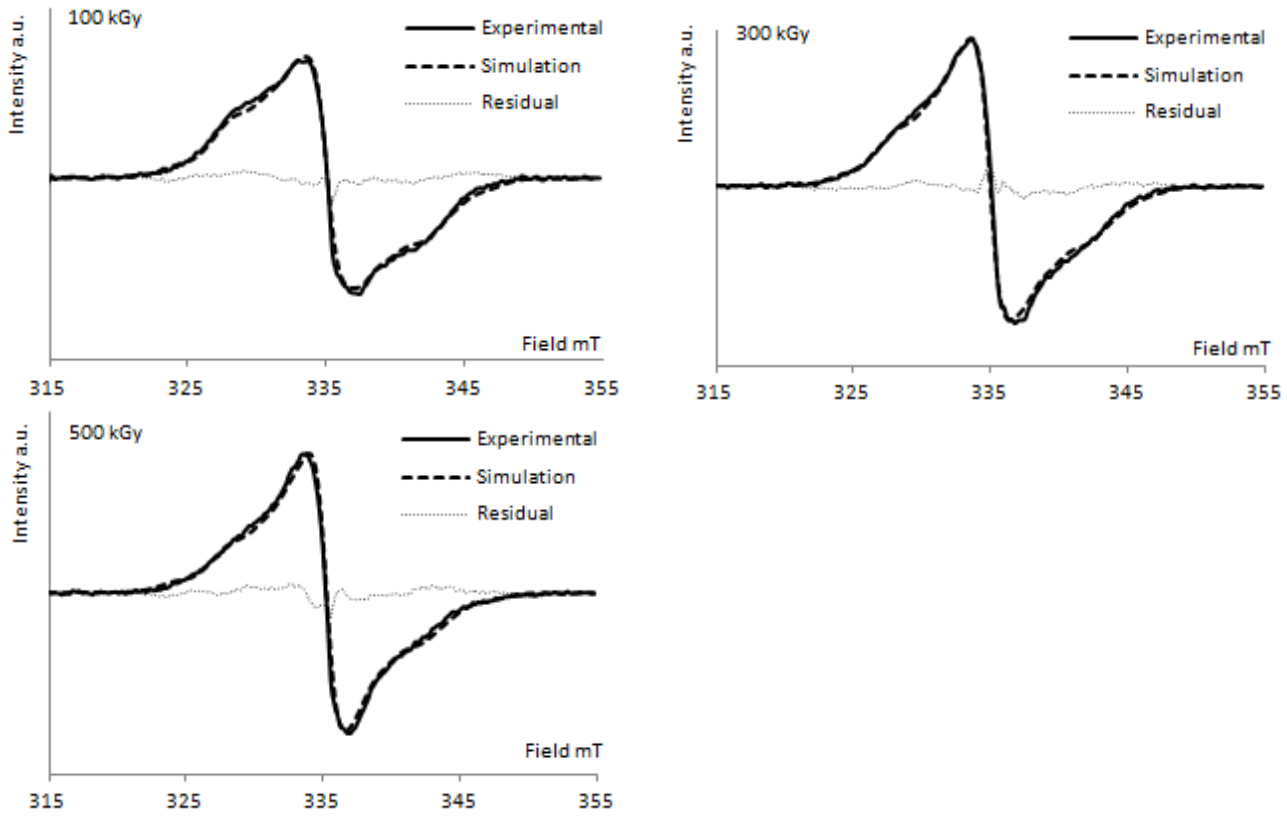

Figure S6. Experimental and simulated spectra of γ-irradiated p(VDF-co-HFP) at several doses and annealed at 373 K during 60 min

Table S1. Assignement of ^{19}F NMR resonances of p(VDF-co-HFP)

Signal	δ (ppm vs $CFCl_3$)	Assignement
a	70.3	CH_2-CF_2-CF($C\underline{F}_3$)-CF_2-CH_2-CF_2 CH_2-CF_2-CF_2-CF($C\underline{F}_3$)-CF_2-CH_2
b^1	74.8	CH_2-CF_2-CF_2-CF($C\underline{F}_3$)-CH_2-CF_2- CF_2-CH_2-CF_2-CF($C\underline{F}_3$)-CH_2-CF_2-
b^2	75.2	CH_2-CF_2-CF_2-CF($C\underline{F}_3$)-CH_2-CF_2- CF_2-CF(CF_3)
c^1	91.3	CH_2-CF_2-CH_2-$C\underline{F}_2$-CH_2-CF_2-CH_2
c^2	91.5	CH_2-CF_2-CH_2-$C\underline{F}_2$-CH_2-CF_2-CF(CF_3)-
c^3	92.0	CF_2-CF(CF_3)-CH_2-$C\underline{F}_2$-CH_2-CF_2-CH_2
d^1	95.0	CF_2-CH_2-CH_2-$C\underline{F}_2$-CH_2-CF_2-CH_2 CF_2-CH_2-CH_2-$C\underline{F}_2$-CH_2-CF_2-CF_2-CH_2
d^2	96.2	CF_2-CH_2-CH_2-$C\underline{F}_2$-CH_2-CF_2-CF(CF_3)
e	101.4 102.6 103.2	CF_2-CH_2-$C\underline{F}_2$-CF(CF_3)-CH_2-CF_2- CF_2-CF(CF_3)-$C\underline{F}_2$-CH_2-CH_2-CF_2- CF_2-CF(CF_3)-CH_2-$C\underline{F}_2$-CF(CF_3)-CF_2 CH_2-CF_2-CF(CF_3)-$C\underline{F}_2$-CH_2-CF_2 CF_2-CF(CF_3)-$C\underline{F}_2$-CF_2-CH_2-CF_2-CF(CF_3)
f^1	108.6	CF_2-CF(CF_3)-CH_2-$C\underline{F}_2$-CF_2-CF(CF_3)
f^2	109.6	CF(CF_3)-CF_2-CH_2-$C\underline{F}_2$-CF_2-CF(CF_3)
g	110.0	CH_2-CF_2-CH_2-$C\underline{F}_2$-CF_2-CF(CF_3)
h	112.1	CF_2-CF(CF_3)-CH_2-$C\underline{F}_2$-CF_2-CH_2 CF_2-CH_2-CH_2-$C\underline{F}_2$-CF_2-CF(CF_3) CH_2-CF_2-$C\underline{F}_2$-CH_2-CF_2-CF(CF_3)
i	113.5	CH_2-CF_2-CH_2-$C\underline{F}_2$-CF_2-CH_2
j	115.9	CH_2-CF_2-$C\underline{F}_2$-CH_2-CH_2-CF_2
k	115.3 119.5	CH_2-CF_2-$C\underline{F}_2$-CF(CF_3)-CH_2-CF_2 CH_2-CF_2-$C\underline{F}_2$-CF(CF_3)-CF_2-CH_2
o	182.3	CH_2-CF_2-$C\underline{F}$(CF_3)-CF_2-CH_2-CF_2 CH_2-CF_2-CF_2-$C\underline{F}$(CF_3)-CF_2-CH_2
p^1	185.0	CH_2-CF_2-CF_2-$C\underline{F}$(CF_3)-CH_2-CF_2-CH_2-CF_2 CF_2-CH_2-CF_2-$C\underline{F}$(CF_3)-CH_2-CF_2
p^{12}	185.2	CH_2-CF_2-CF_2-$C\underline{F}$(CF_3)-CH_2-CF_2-CF_2-CF(CF_3)

CONCLUSION DU CHAPITRE

Le travail principal développé dans cette partie consistait en l'élaboration d'un modèle de simulation de spectre RPE permettant de déterminer la nature et la proportion de chaque radical formé lors de l'irradiation, sous atmosphère inerte, d'une matrice de PVDF. Bien que la littérature faisait état de cinq espèces radicalaires, la simulation de leurs réponses RPE n'étaient connus que pour certains radicaux, et pour les autres manquaient notamment les valeurs des constantes de couplage hyperfins. L'estimation de ces paramètres de simulation à été proposé en se basant sur les valeurs déterminées pour des espèces radicalaires de structure chimique proche, comme les radicaux perfluorés. Les valeurs des paramètres ont ensuite été affinées afin d'obtenir la meilleure recouvrance du spectre simulé et expérimental. La signification physique des valeurs des constantes de couplages hyperfins, de largeurs de raies et de *g* a été discutée. La concentration de chacun des radicaux à ainsi pu être déterminée et traduit leur stabilité relative, qui dépend de deux facteurs : la mobilité de la chaine et l'environnement chimique. Ainsi, les radicaux de milieu de chaîne sont plus stables (car moins mobiles) que ceux localisés en bout de chaîne, ce qui diminue la probabilité de réaction de terminaison irréversible. De même, les radicaux dont l'électron célibataire est délocalisé par effet mésomère ou inductif sont plus stables que les radicaux dont l'électron est fortement localisé sur le carbone en position α.

La seconde publication a été l'occasion de mettre en application le modèle établi. L'évolution de la forme des signaux RPE en fonction de la dose d'irradiation et du temps de recuit à 373 K a pu être reliée à la redistribution de la proportion de chaque espèce. Les variations de leur concentration, fonction de leur réactivité, ont aussi pu être mises en relation avec la formation d'un réseau. Ainsi, une diminution des espèces de milieu de chaine coïncide avec une augmentation de la densité du réseau, déterminée par des mesures sol-gel. De plus, les études de l'influence de la durée de recuit ont montré que la densification du réseau augmentait la stabilité des espèces en réduisant la mobilité moléculaires des chaînes.

L'objectif principal de la troisième publication concernait la détermination de la nature des radicaux formés lors de l'irradiation du copolymère p(VDF-co-HFP) présentant 2,65 % en mole de motif HFP à partir de spectre RPE expérimentaux. La difficulté principale résidait en l'identification des radicaux issus de la présence de l'HFP, ainsi que la détermination de leurs paramètres de simulation. Basé sur une étude de la microstructure des chaînes polymères, deux nouvelles espèces radicalaires relatives à l'unité HFP ont été intégrées au modèle de simulation établi pour l'homopolymère PVDF. Un modèle a été proposé et a permis d'étudier l'influence des paramètres expérimentaux (dose d'irradiation, temps de recuit). Les concentrations de chacune des espèces ont

été discutées et comparées au cas de l'homopolymère, et sont en bonne adéquation avec la meilleure propension du copolymère à réticuler comparativement à l'homopolymère PVDF.

Cette partie, consacrée principalement à l'étude RPE des polymères irradiés, montre toutes les possibilités qu'offre cette technique pour étudier la radiolyse des matériaux polymères. Néanmoins, le nombre d'espèces radicalaires et la complexité de leurs interactions n'ont pas permis de déterminer les mécanismes de réaction aboutissant à leur consommation. Les tendances observées peuvent cependant constituer de précieux indices lorsqu'elles sont comparées aux évolutions d'autres propriétés. De plus, la simulation des spectres RPE est complexe et la multiplication des espèces à simuler rend l'exercice périlleux ; en effet, la corrélation entre la simulation et le spectre expérimental peut être améliorée en intégrant et/ou utilisant des paramètres dont la signification physique peut être altérée. La connaissance partielle des espèces générées lors de l'irradiation et de leurs constantes de simulation associées constitue une des limites de la démarche Afin d'illustrer ceci, la discussion autour d'un autre copolymère intégrant des unités CTFE p(VDF-co-CTFE) comprenant 4,56 % en mole d'unités CTFE est présentée en Annexe 1. Trop d'incertitudes et de doutes subsistaient quant à la sélection des espèces à simuler et à la détermination de leurs constantes de couplage hyperfins, ce qui a rendu impossible l'établissement d'un modèle de simulation pour ce type de copolymère.

Enfin, une étude supplémentaire a été réalisée afin de déterminer la quantité et le devenir des radicaux libres exposés au contact de l'air. Cette étude est présentée en Annexe 2.